OPTIMAL MANAGEMENT OF VOLTAGE CONDITIONS IN POWER DISTRIBUTION SYSTEMS

By

WALEED ALABRI

A thesis submitted to the University of Birmingham for the degree of

DOCTOR OF PHILOSOPHY

Department of Electronic, Electrical and Systems Engineering

College of Engineering and Physical Sciences

University of Birmingham

April 2022

Dedication

I wish to dedicate this thesis to my beloved parents

Acknowledgements

My special thanks go to my supervisor, Dr. Dilan Jayaweera, for all his timely and invaluable advice, continuous support, and guidance over the past four years. His patience, technical ideas, motivation, and contributions throughout all phases of my PhD study are deeply appreciated.

I acknowledge the Ministry of Higher Education, Research and Innovation and the University of Technology and Applied Science, Sultanate of Oman, for providing financial support during my PhD study and the Oman Cultural Attaché, Embassy of Oman in London, for looking after my education and welfare.

I would like to extend my thanks to my colleagues at the Electrical Power and Control Systems Group at the University of Birmingham for their supportive effort and constructive feedback, sharing their experience and knowledge with me and encouragement throughout my PhD study. I am particularly grateful to Dr. Zafar A. Khan, Dr. Hasan Gunduz, Dr. Manuel Alvarez-Alvarado, Dr. Abdullah Altamimi, Dr. Peju Oyewole, Bader Alharbi, Daniel Donaldson, and Wilson Vasquez.

I also wish to express my deepest gratitude to my beloved wife, Jalila and my children Khalid, Alaa, and Osama for their enduring support, endless belief in me, and being with me during my PhD journey. Their prayers, understanding, and motivation have made this journey much easier. I cannot express how grateful I am for all the countless sacrifices they have made for me.

Finally, yet importantly, I would like to extend my appreciation to my parents, brothers, and sisters for their prayer, unconditional love, and encouragement, who have also supported me emotionally, trusted me, and had faith in me, that all have helped me through the entire PhD study.

Abstract

Power distribution systems are currently experiencing an increased connection of Renewable Energy Technologies (RETs) such as Photovoltaics (PVs) and Electric Vehicles (EVs), mainly due to the widespread awareness of global warming. The massive diffusion and intermittent nature of these technologies can exacerbate the voltage unbalance level and pose additional operational stresses to the existing voltage regulation devices, such as power transformers. These conditions can introduce components failure, capacity waste, energy losses and restrict further integration of RETs. To address these obstacles, novel and effective control techniques and management strategies of various power distribution assets are required. However, developing adequate and practical approaches can be challenging due to the size, unbalance, and complexity of typical power distribution systems. Therefore, this thesis proposes a novel methodology for optimal unbalanced voltage management in modern power distribution systems integrated with the expanded penetration of RETs.

The thesis presents an innovative Three-phase Power and Current Injection Mismatch (TPCIM) method as an alternative and more robust unbalanced load flow calculation method by implementing a new voltage-controlled bus model. This involves guaranteed convergence modelling of modern power distribution system assets, particularly Static Var Compensator (SVC) and STATic synchronous COMpensator (STATCOM). The developed models and mathematical formulation of load flow calculation improve the convergence characteristics and are computationally efficient, providing a superior method that can be better suited for the applications of real-time control and management in a power distribution system. The proposed load flow calculation methodology is utilised to establish a comprehensive and accurate assessment of RET integration impacts on power distribution systems. The investigation underlines that the unbalanced voltage level can be significantly high in a power distribution system, and with ordinary control and spread of RETs, it can be further intensified due to the inter-phase coupling of distribution lines. The thesis then presents an effective approach to limit voltage unbalance and prevent overvoltage problems by proposing an innovative reactive power control of PV inverters, which could also limit the ageing of PV inverters.

In order to facilitate the massive deployment of RETs and obtain an effective unbalanced voltage regulation, this thesis also proposes an advanced mathematical framework for the optimal coordination of RETs under modern power distribution system operating conditions. The advanced framework has been innovated with an Advanced Hybrid Particle Swarm Optimization (AHPSO) algorithm to further enhance the accuracy, convergence, and effectiveness of the multi-objective optimisation solution. The development of the coordination scheme and AHPSO provides a key tool for real-time voltage management that requires highly accurate solutions with a fast and scalable formulation. Thus, the thesis offers a significant knowledge advancement for the formation of mathematical frameworks of voltage management in modern power distribution systems.

List of Publications

Parts of the thesis outcomes were published in peer-reviewed journal articles and conferences. The list of the publication are as follows:

1- **W. Alabri** and D. Jayaweera, "Optimal Coordination of Unbalanced Power Distribution Systems with Integrated Photovoltaic Systems and Semi-Fast Electric Vehicles Charging Stations", IET Generation, Transmission & Distribution, 2022, (Published journal paper).

2- **W. Alabri** and D. Jayaweera, "Impact of Semi-fast Charging Stations on Unbalanced Power Distribution Systems Integrated with PV Systems," in 2021 IEEE PES Innovative Smart Grid Technologies Europe (ISGT-Europe), 2021, pp. 1–5, (Published conference paper).

3- **W. Alabri** and D. Jayaweera, "Voltage regulation in unbalanced power distribution systems with residential PV systems," International Journal of Electrical Power and Energy Systems, vol. 131, p. 107036, 2021, (Published journal paper).

4- **W. Alabri** and D. Jayaweera, "Unbalanced Modelling of STATCOM and SVC in Hybrid Load Flow Method," in 2019 IEEE PES Innovative Smart Grid Technologies Europe (ISGT-Europe), 2019, pp. 1–5, (Published conference paper).

5- **W. Alabri** and D. Jayaweera, "Unbalanced Three-Phase Power Flow Calculation in a Smart Distribution System using Power and Current Injection Hybrid Method," 8th Saudi Arab. Smart Grid Conf. (SASG 2018), IEEE, 2018, (Published conference paper).

Table of Contents

List of Figures

List of Tables

List of Abbreviations

AHPSO	Advanced Hybrid Particle Swarm Optimisation
DG	Distributed Generation
EV	Electric Vehicle
FACTS	Flexible AC Transmission Systems
GA	Genetic Algorithm
NC	No Convergence
NS	Natural Selection
OLTC	On-Load Tap Changer
OPF	Optimal Power Flow
PCC	Point of Common Coupling
PF	Power Factor
P-Q Bus	Load Bus
P-V Bus	Generator Bus
PSO	Particle Swarm Optimisation
PSO-GA	hybrid PSO and Genetic Algorithm
PSO-NS	PSO based on Natural Selection
PV	PhotoVoltaics
RET	Renewable Energy Technology
RSD	Rational Standard Deviation
SD	Standard Deviation
STATCOM	STATic synchronous COMpensator
SVC	Static Var Compensator
TCR	Thyristor Controlled Reactor
TCSC	Thyristor Controlled Series Compensator
TCIM	Three-phase Current Injection Mismatch
TPCIM	Three-phase Power and Current Injection Mismatch
TPIM	Three-phase Power Injection Mismatch
UTLFC	Unbalanced Three-phase Load Flow Calculation
VU%	Voltage Unbalance Percentage

Chapter 1: Introduction

This introductory chapter first presents the research background of the thesis and its relevance to the challenges confronting unbalanced voltage regulation in power distribution systems integrated with Renewable Energy Technologies (RETs). Then it presents the motivation of the thesis, followed by the aim, objectives, and main contributions of the thesis. The last section of the chapter provides the organisation of the thesis.

1.1 Research Background

Power distribution systems are one of the major components of a power system. Their primary function is to deliver efficient, secure, and reliable electric power to individual customers after being transferred from generation centres through a high voltage transmission system [1]. Conventional power distribution systems are generally operated as passive networks with the philosophy of unidirectional power flows, which were mainly designed to serve loads through feeders from a centralised generation without the presence of distributed generation, including renewable energy resources. Maintaining the acceptable voltage magnitude at the connection nodes of the end-users and the thermal limits of network assets such as distribution lines and transformers are two of the main technical issues that concern the daily operation of a passive power distribution system. However, some other power quality problems, particularly unbalanced voltage, were disregarded due to the absence of observation and control platform in the passive power distribution systems [2]. The unbalanced voltage issue has recently gained significant attention due to its increase to extreme levels, adversely impacting power distribution system's security and efficiency [3].

During the past few years, the intention to reduce reliance on fossil fuel and introducing new environmental measures have driven the transport and electricity sector to

shift network development direction toward RETs, particularly grid-tied PhotoVoltaics (PVs) and Electric Vehicles (EVs) [4], [5]. This has led to the non-dispatchable power generation and charging station's infrastructure being part of the power distribution system topology. The connection of RETs into power distribution systems can bring many opportunities, but with the large-scale integration of these technologies, the challenges that are confronted by power distribution systems operation have increased [6]. For example, high penetration and uncertainty of PV systems and EV load connections can cause several operational issues for power distribution systems, particularly voltage regulation problems and power components overloading [7]. In addition, the sizeable power ratings of single-phase EVs during the charging process and the connection of PV systems can exacerbate the level of voltage unbalance [8]. All these consequences cannot be effectively alleviated through conventional voltage regulation such as On-Load Tap Changer (OLTC) and autotransformers, [9] or network augmentation. Therefore, a traditional power distribution system may face challenges when dealing with voltage management, and it can become one of the main obstacles to further increasing the hosting capacity of RETs [10].

With the high deployment of PV systems and EV charging stations, it is clear that the capabilities of the present power distribution systems are unable to address these sorts of challenging issues. Therefore, the transition of the conventional power system into an active power system intervention is becoming a vital paradigm shift in the modern topology of power distribution systems. This has led to propose new voltage management approaches and installing novel power electronic-based devices, such as Flexible AC Transmission Systems (FACTS) devices and allowing PV inverters to participate in voltage management to cope with the new challenges [11]. Furthermore, the tremendous transformation in the power distribution systems promote the rapid advancement in smart technology and reveal the necessity of real-time management and control of network assets to strengthen system

reliability and resiliency. Therefore, there is a need for advanced coordination schemes that can promote better utilisation of existing network assets by fully exploiting the connection of RETs [12]. This can help achieve better voltage regulation, minimise voltage unbalance levels, and increase the uptake of renewable energy resources without the need for costly network augmentation.

1.2 Research Motivation

Modern power distribution systems are currently experiencing unconventional technical challenges, particularly overvoltage and voltage unbalance problems, mainly due to the increased connection of PVs and EVs. The stochastic nature of PV power generation and real power injection in excess of demand can lead to raise the voltage beyond the operating criteria. Moreover, the increased connection of single-phase PV systems and EVs are likely to aggravate voltage unbalance levels. Overvoltage can be the leading cause of equipment failure and sometimes is considered as the major obstacle for further PV system integration. High unbalance in voltage levels can reduce the actual operating capacity of electrical power equipment and increase network energy losses [13]. The intermittent nature and increased connection of RETs made traditional voltage regulation approaches inadequate to address these operational challenges in modern power distribution systems. Besides that, integration of these technologies may impose a threat on operating characteristics of power system components such as violating thermal limit and frequent operation action that may derate and increase degradation process of the power system equipment (e.g., power transformer, capacitor banks, distribution lines, etc.) [14]. Therefore, if no innovative approaches are established and adopted, redundant distribution grid reinforcements would be required to ensure the continuous operation of power distribution systems. This would lead to substantial network investment and reduce the leverage of RETs connection. Developing a well performing coordination approach of RETs with existing

network facilities would ensure high-efficiency operation of power distribution systems while operating within the corresponding technical and physical constraints.

Developing such a coordination approach requires a robust and fast optimisation-based technique and load flow calculation that are used as decision-making tools for optimal voltage management [15], [16]. Given the increase in the number of components of power distribution systems with increased intricacies, new voltage management approaches are required, which are more efficient at undertaking complex and larger system load flow and optimisation studies. With the existing load flow and optimisation approaches, the accuracy will need to be compromised to reduce the computational time so that they can satisfy the requirement of real-time management and control [17], [18]. For example, most of the proposed approaches ignore the practical operation of some voltage regulating devices (e.g., OLTC) by assuming a continuous tap operation and neglecting the inter-phase coupling of distribution lines. These inaccuracies may not reflect the realistic outcome and can create an off-target control signal that can inadvertently deteriorate the unbalanced voltage level and power distribution operation performance. Therefore, before proposing any coordination schemes and power quality enhancement approaches, it is crucial to develop network-ready power flow calculation and optimisation models that can fit into modern power distribution systems. They should handle the inherent large degree of unbalance operation and be capable of accommodating multi-phase models of modern power distribution systems topologies and components with fast and accurate solutions.

1.3 Research Aim and Objectives

The power distribution systems are experiencing dramatic changes, and they are with more operational challenges. As a result, advanced control of modern power distribution components should be further developed to cope with these challenges and to promote higher network performances. To address some of these challenges, this thesis aims to

facilitate the widespread connection of PV systems and EVs in an unbalanced power distribution system and then to remedy the issues related to their integrations through adequate control supported by optimisation techniques. Therefore, the primary focus of this thesis is to propose an advanced and effective framework to manage and limit the unbalanced voltage problems in modern power distribution systems considering the higher penetration of PVs and EVs. The proposed optimal control framework limits constraints in the uptake of RETs, limits the need for future network upgrades, and maintains a healthy operation of power distribution system assets. An essential step to enable the optimal operation is to establish an adequate formulation that can be implemented to handle the size and complexity of a realistic and unbalanced power distribution system. In addition, the solution time must be shorter for operational effectiveness where control decisions are needed instantly. To fulfil the aim, the following research objectives have been set:

- Develop an advanced, computationally efficient, and accurate unbalanced load flow calculation method that could be utilised for real-time management and control of power distribution systems.
- Develop a novel, accurate, and robust steady-state model for unbalanced load flow calculation of modern three-phase power distribution system components, including SVC, STATCOM and EVs loads.
- Develop a new control strategy for PV inverters that can provide adequate voltage regulation and voltage unbalance improvement in the network.
- Develop a mathematical model for an optimal coordination control scheme that could solve the unbalanced voltage problem and reduce the total power losses while complying with other network operation criteria.
- Enhance Particle Swarm Optimisation (PSO) technique and demonstrate its efficacy over other optimisation techniques.

1.4 Research Contributions

The main contributions of the research presented in this thesis are as follows:

1. **A novel mathematical framework for calculating the unbalanced three-phase load flow in modern power distribution systems is presented.** The thesis (Chapter 3) provides a novel mathematical formulation of the Three-phase Power and Current Injection Mismatch (TPCIM) method as an alternative and more robust unbalanced load flow calculation method. The computation time and convergence characteristics of the developed method are compared with other well-known Newton Raphson methods. The developed TPCIM method offers a reduction in load flow calculation complexity, improves the computing time, and reduces the number of iterations. As a result, the new developed three-phase load flow calculation method can be the best option for online voltage management applications in an unbalanced power distribution system.
2. **A novel three-phase model of SVC and STATCOM for unbalanced load flow calculation is developed**. A robust model of the three-phase SVC and STATCOM is proposed in the thesis (Chapter 4) to improve the computation time and reduce the number of unbalanced three-phase load flow calculation iterations while keeping the high accuracy of the solution. The power mismatch equations are used to represent SVC and STATCOM connected buses as voltage-controlled buses while maintaining the original Jacobian matrix unchanged. The parameter of voltage control devices can be calculated during the iteration process using simple equations, avoiding divergence of load flow calculation. Such advantages are considered added values for modern power distribution systems requiring rapid monitoring and control platforms.
3. **An accurate assessment is presented to study the influence of RETs connection on unbalanced three-phase power distribution systems**. The thesis (Chapter 4) provides accurate modelling and assessment of various modern power distribution system

components. The study investigates the impact of unbalanced EV connections on an unbalanced power distribution system considering semi-fast charging stations and the autonomous control of PV inverters for reactive power support. This assessment identifies the limitation of uncoordinated voltage control schemes and highlights the necessity of centralised control in modern power distribution systems.

4. **A novel reactive power control scheme for PV inverters is developed.** The newly developed control in the thesis (Chapter 5) is based on step-droop reactive power control using local voltage measurement. The step control purposes are to keep the unbalanced voltage level under the permissible limit and voltage magnitude within the specified boundary while restricting the PV inverter from derating. The performance of the proposed voltage unbalance mitigation approach is verified through different case studies implemented on a typical unbalanced power distribution system using actual recorded PVs and loads data. The newly developed PV inverter control could be considered the preferable approach for unbalanced voltage regulation requiring minor modification, fast response, and allowing higher PV system connection.
5. **A mathematical framework is developed for the optimal coordination of various modern power distribution system components**. A methodology for optimal operation of different voltage control devices in power distribution systems with high penetration of PVs and EVs is proposed in this thesis (Chapter 6). The approach coordinates four different types of voltage management devices: transformer OLTC, STATCOM, PVs and EVs, considering the natural intermittency operation of unbalanced power distribution systems and the inter-phase coupling between distribution lines through real-world data. The main objectives of optimal coordination are to enhance the network voltage profile, restrain voltage unbalance level, minimise the total active power losses, and reduce the frequent switching operation of OLTC on the power distribution system.

This mathematical framework will help utilities and other stakeholders to develop a coordination scheme that enhances the reliability, security, and efficiency of delivered electric power to the end-users.

6. **A new advanced Hybrid Particle Swarm Optimisation (AHPSO) technique is developed to solve the optimisation problem.** The thesis (Chapter 6) provides a new enhanced optimisation method based on combining two modified Particle Swarm Optimisation (PSO) methods. The new advanced method improves the accuracy, convergence, and effectiveness of the optimisation solution. Such improvement makes AHPSO a potential option for power system operators to solve different complex optimisation problems with better robustness and accuracy.

1.5 Thesis Outline

The thesis comprises of seven chapters, including this introductory chapter, as described in Figure 1.1. The remaining six chapters are outlined as follows:

Chapter 2 presents a literature review surrounding the basic principles and related research work. The relevant literature is reviewed from the perspective of voltage regulation issues in unbalanced power distribution systems to give a context for the research problems. First chapter 2 highlights the challenge associated with modern power distribution system operation integrated with RETs. This includes the associated voltage unbalance problem and its significance. Then, this chapter presents different techniques employed to regulate the unbalanced voltage in modern power distribution systems by either autonomously or a centralised control approach. Finally, this chapter reviews the existing modelling and optimisation techniques used for the application of unbalanced voltage regulation in modern power distribution systems, where the research direction is pointed out.

Chapter 3 proposes a new fast, accurate, and robust unbalanced load flow calculation (TPCIM) method, which is based on combing the three-phase power and current

injection mismatch equations. In addition, this chapter introduces mathematical modelling of some basic components in power distribution systems, including distribution lines and three-phase transformers. Different case studies are performed in this chapter to validate the proposed TPCIM method result and check its performance. The case studies are demonstrated on IEEE 13-node, IEEE 37-node, and IEEE 132-node test feeders to confirm the superior performance of the developed TPCIM method compared with other well-knowing methods with regard to convergence characteristics and computing time. The TPCIM method developed in this chapter is used as the basis tool for all subsequent chapters.

Chapter 4 presents the mathematical representation of various modern power distribution system components for load flow calculation. This includes a robust model of three-phase SVC and STATCOM. These models are validated, and their performance is compared with other models from convergence characteristics of the load flow calculation perspective through several case studies conducted on IEEE 13-node, IEEE 37-node, and IEEE 132-node test feeders. Furthermore, this chapter studies the influence of EVs and PVs system connection on unbalanced power distribution system operation after their accurate models have been developed. This chapter also explores the application of some FACTS devices and PV inverters in mitigating the unbalanced voltage and highlight their limitations.

Chapter 5 develops an innovative reactive power control approach for the PV inverters to decrease the severity of voltage unbalance levels in a power distribution system merged with spread connection of PV systems. This chapter first describes the problem associated with the increased connection of PV systems. Then, the proposed step-droop control approach of the PV inverter is discussed in detail, including their reactive power capability. Finally, several case studies are performed in this chapter on the selected IEEE 37-node test feeder under various PV penetration levels and meteorological conditions to examine the effectiveness and the performance of the developed reactive power control.

Chapter 6 describes a methodology for optimal controlling of various voltage control devices in the power distribution systems integrated with the massive number of PV systems and EVs. This includes the mathematical formulation of optimisation problems taking into consideration various operational constraints and objectives. In addition, this chapter describes the new advanced hybrid particle swarm optimisation (AHPSO) technique that is employed to solve the optimisation problem, and its superior performance is compared with other techniques. Finally, analysis of three operation scenarios on selected IEEE 37-node and IEEE 132-node test feeders is carried out in this chapter throughout a number of case studies to demonstrate the significance of coordination schemes in maintaining the voltage unbalance within the permissible level and power losses reduction.

Chapter 7 concludes the key outcomes of this thesis and presents the potential future works that are relevant to the modelling and unbalanced voltage regulation of modern power distribution systems integrated with increased RETs.

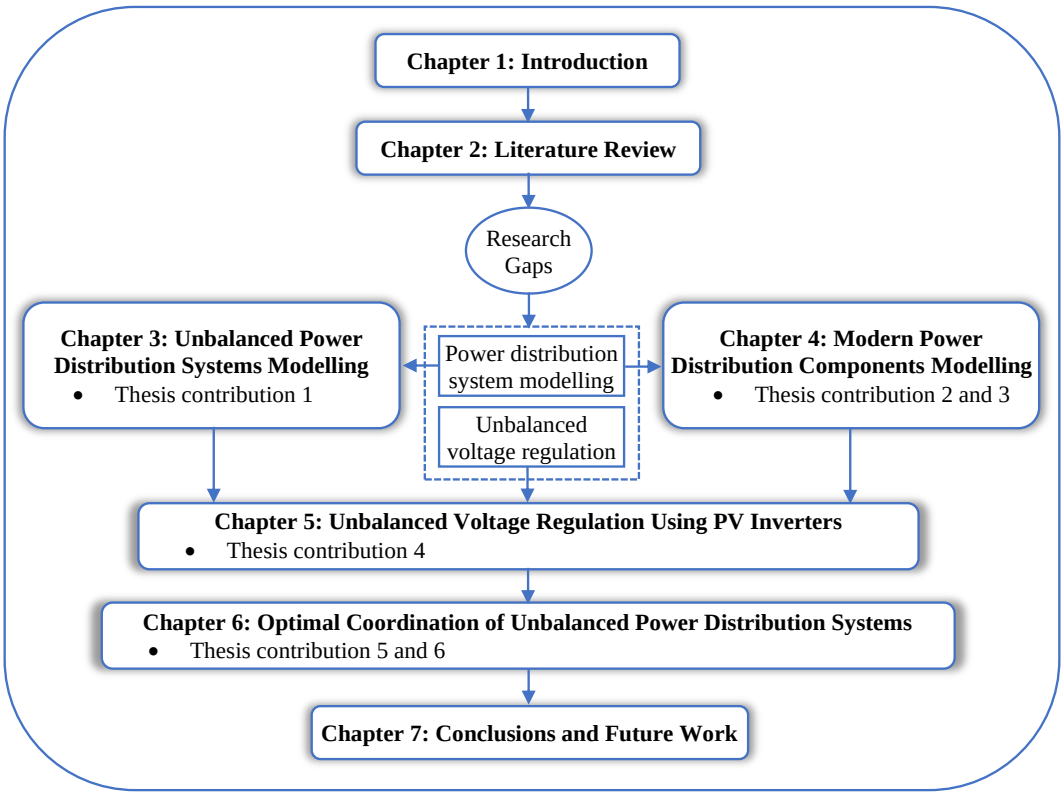

Figure 1.1. Overview of the thesis structure

Chapter 2: Literature Review

2.1 Introduction

The integration of RETs such as PVs and EVs is projected to rise significantly in the coming years as a result of various measures being rolled out by most governments due to environmental and other concerns [19]. Integration of PVs and EVs can bring many opportunities, but it can introduce some operational challenges on conventional control devices and negatively impact network performance, forcing power distribution operators to limit their penetration level. The severity of voltage unbalance level is among the critical issues arising from the increased integration of RET, which has been regarded as one of the metrics to evaluate the efficient operation of the power distribution systems [20].

As a result, different approaches have been introduced in the last few years to address the challenges associated with the RETs connection. These approaches are essential to the idea of an active power distribution system, which involves real-time monitoring and management of different network assets. Nevertheless, due to power distribution systems' complex structure and operation, many practical difficulties must be resolved before monitoring and control can be practically integrated into power distribution systems.

Thus, this chapter provides a literature review in the context of the challenging confronting the operation of modern power distribution systems integrated with increased RETs and the corresponding approaches used to address these challenges. This chapter first presents an overview of the modern power distribution systems challenges in section 2.2, including the impact of RET integration and the voltage unbalance. Section 2.3 provides the various approaches and recent related work used to mitigate the impact of RET, especially voltage unbalance issue. In sections 2.4-2.6, the various approaches and limitations associated with the unbalanced modelling and optimisation techniques for power

distribution systems are presented. Finally, section 2.7 summarises the content of this chapter and highlights the potential research gaps.

2.2 Modern Power Distribution Systems challenges

The power distribution system is the most complex power system structure because of the massive number of feeders, nodes, and loads [1]. Medium voltage and low voltage are the two different voltage levels used in a power distribution system, where the specific voltages used worldwide may vary. Standard voltages used in medium voltage networks can vary from several kV to tens of kV; for example, the most typical voltages used in Europe are 6.6 kV, 11 kV and 32 kV. Conversely, low voltage feeders are interfaced with the customer directly through low voltage distribution transformers. The nominal line voltage is 400 V for three-phase connections, and the phase voltage is 230 V for single-phase connections [21]. However, these medium and low-voltage distribution networks can be operated as passive networks or active networks, depending on the designed topology, availability of voltage regulation devices, and the level of RETs integration.

2.2.1 Active Distribution Network

The characteristics operation of renewable energy sources (e.g., PV and wind energy) and EVs pose new challenges to the power distribution system. Their rapid growth constrains a paradigm change in the way power distribution systems are managed and designed, shifting from a convention power distribution system towards active distribution networks. It involves utilising intelligent observation and control, which can accomplish the purpose of maintaining the efficient and economical operation of the network and leverage the use of RETs. Active distribution networks can suppress any violation constraints such as overvoltage and voltage unbalance during the operational period through real-time management of network assets. It also plays a pivotal factor to accommodate extensively

higher penetrations of RET. Furthermore, the invitation on power electronics-based devices recently, particularly SVC and STATCOM, has enabled easy power flow and voltage management to attain better system performance.

For this purpose, transformation to an active power distribution system is becoming a more practical and reliable option nowadays, which is also one of several countries' key measures to comply with the environmental requirement by optimising the electrical power system operation [22]. A significant obstacle to the transaction toward an active power distribution system regards the cost associated with upgrading the overall infrastructure. However, by taking advantage of existing large scale installed smart meters and the availability of communications infrastructure, the necessity of expensive network upgrading can be reduced. Furthermore, achieving a higher operational efficiency level resulting from minimising the power losses and maintaining the healthy operation of distribution components can bring substantial money-saving [7], [23].

A concept of an active power distribution system is illustrated in Figure 2.1. Various types and sizes of renewable energy sources can be seen as part of an active network. Although not explicitly shown, novel technologies such as distribution STATCOM [24], storage energy system [25], and demand-side management [26] can also provide a further advantage to manage the power flows. The central unit is the core of the active power distribution system, where the required network measurement and controllable devices' current setpoints are received and processed at each control cycle. It can adopt minute-scale control cycles to routinely evaluate the performance and dispatch setpoints for the controllable devices (e.g., OLTC, PV inverters, STATCOM, etc.) in an active distribution network if necessary. This process involves load flow calculation to check for potential issues, such as thermal and voltages magnitude violation, and then perform the optimisation model to generate adequate control signal to the controllable devices [27].

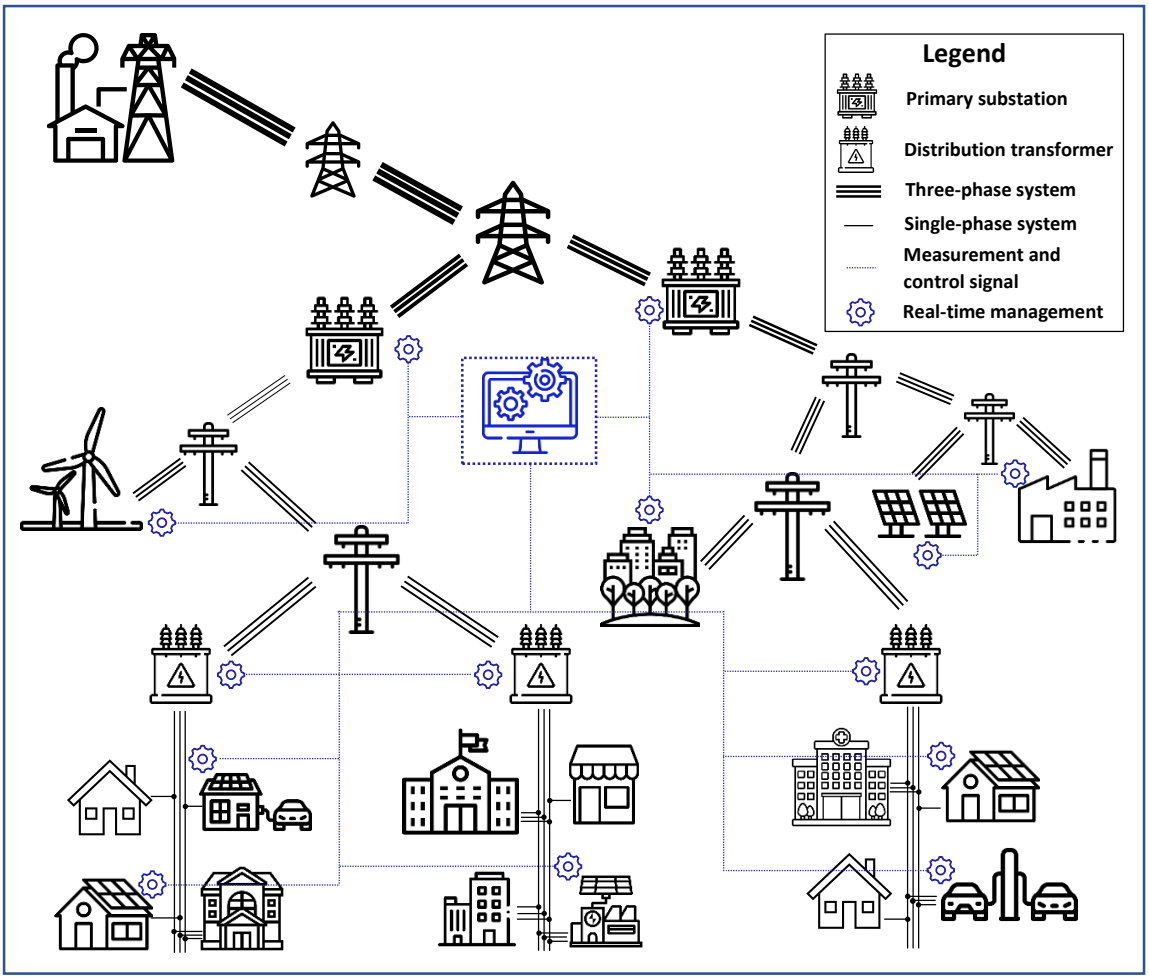

Figure 2.1. The concept of the active power distribution system

It is clear that the revolution in communication systems and intelligent electronic devices will unlock the transition toward active distribution networks and allow new avenues to facilitate the flexibility of power flows via centralised control of power distribution components [28]. Power flow calculation and optimal power flow are the two most essential tools that are required for centralised control [29]. Using these tools will facilitate network operation observation and determine feasible steady-state control action to achieve various objectives while respecting the corresponding constraints [12]. However, there are several limitations on utilising these tools in monitoring and controlling the power distribution systems, and these limitations must be addressed before adopting centralised control on readily power distribution systems.

The scalability and speed of centralised control are also some of the major obstacles to the transition toward active distribution networks. The active power distribution system's control scheme should act instantly to cope with rapid changes in load demand and solar ramps. Furthermore, due to the nature of discrete operation of some voltage regulation devices, particularly OLTC and capacitor banks, there will be a necessity for solving a mixed-integer problem, which often requires an extensive search to reach the optimal control variable [30]. For this reason, the non-convex and mix-integer nature of optimisation formulations usually make the execution timing for each setpoint control signal extremely slow. Simple representation of power distribution system operation and employing linear programming for solving optimisation problems were used to solve computation time problems [18], [31]. However, sacrificing accuracy can result in off-target control signals and might consequently deteriorate the performance of power distribution systems operation. Therefore, this requires the proposal of a suitable power flow calculation and optimal power flow techniques, reassembling the unbalanced real-time operation of power distribution systems with accurate modelling of various existing and modern power distribution system components.

2.2.2 Integration of Renewable Energy Technology (RET)

PV systems and EVs play a primary part in decarbonising the electricity and transportation sectors. However, the existing power distribution system faces new challenging tasks due to the enormous size integration of these technologies [8]. Many research studies have been performed to assess the problematic implication of PV and EV integration in power distribution systems [13], [32]–[35], considering uncertainties and various penetration levels. Most of these research studies target the implications of the PVs and EVs integration individually. However, the power distribution system is currently experiencing combined integration, which may increase operation severity. Moreover, the

multifunction of PV inverter (e.g., reactive power compensation) and introducing various new charging stations will be the new features attached to the future power distribution system that need to be considered.

A comprehensive analysis of the impact and challenges associated with the PV connections into power distribution systems is presented in [13], [32], [34]. The major technical challenges caused by PVs integration could be recognised as power quality problems and stress on voltage regulator devices. The massive connection of non-dispatchable PV systems can lead to reverse power flow, especially during periods of excess generation, causing several technical issues such as overvoltage and thermal limits violation. The severity of PVs' impact is subjected to penetration level, PV system location, and the control scheme adopted in the PV inverter. Besides potential voltage and thermal limit violations, high penetration may lead to excessive voltage regulation devices operation due to the frequent solar power output change resulting from rapid clouds moving [36]. Moreover, disconnection of PVs is another issue that has been seen at some nodes because of overvoltage protection, which will considerably prevent PVs deployment in the future if mitigation measures are not in place. In general, voltage and thermal limits are only the two main issues that were considered to evaluate the technical viability of PV systems integration [13]. Nevertheless, the recent advance control employment on the PV inverters leverages the PV system's integration and increase their hosting capacity.

Similarly, EV integration is uncertain and represent a heavy load connection, which can cause significant sequences, especially when fast charging is used. Growing EVs market results in many EV charging stations that are mostly connected to a power distribution system. Among the most problematic features regarding EVs' connection to the power distribution systems is to predict when and where EVs owners decide to schedule charge events and for how long. Consequently, the power distribution systems will suffer from

unpredicted additional EVs charging demand that may ultimately cause the declination of power quality and increase the power losses. Furthermore, in an extreme scenario, the power supply may be insufficient to meet the additional EV charging demand. On the other hand, EVs can contribute to power quality improvement through coordination control and demand management since they can be treated as flexible loads [37], [38].

Detailed impacts of EVs are investigated in [33], [35], [39], where the authors either consider slow residential charging [39] or fast charging [35]. Normally, the car owner charges his car at home during the night to be ready for the next day. This kind of charging habit has less impact on the power distribution systems operation because most of the time, the EVs are charged during the light loads demand. On the other hand, fast charging is demanded during the day, which may add extra stress to the power distribution system. However, as the number of EVs is rapidly increasing, there will be demands for more charging stations, especially for those travelling long distances for work or pleasure purposes. This can be seen in every public and workplace car parking, which are typically equipped with semi-fast charging speed, and they represent the high portion of the overall charging stations [40]. The demand for these types of charging is different such that they are mostly used during the day where the loads demand might be at its peak.

Nevertheless, there are other technical issues that have been neglected, which are becoming more severe, such as voltage unbalance. EVs and single-phase PV systems' connection is considered among the major causes of the severe voltage unbalance level in power distribution systems [41]. Some research authors study the detailed impact of PVs [42], and EVs [39] on voltage unbalance; however, they did not consider mutual line coupling. Inert-phase coupling may consequently affect their analysis and the effectiveness of any proposed approaches to mitigate RET integration's detrimental impact [43]. Moreover, the battery of EVs is currently represented in load flow formulation as a constant

power load model, such as in [39], without considering the EV charging system's voltage dependence. Modelling EVs load as a constant load can lead to inaccurate information about the charging system's behaviour during the charging process.

Therefore, the implications of combined integration of PVs and EVs, accurate load modelling of EV with various charging speed stations, consideration of multiple functions of PV inverters, and inter-phase coupling are all essential for realistic and objective analysis. The work in chapter 4 fills the gaps mentioned above by quantifying the impact of both EVs and PVs, especially on the voltage unbalance level in the power distribution system. Based on the above exploration, voltage unbalance is one of the implications that resulted from the integration of EV and PV that have been ignored in most of the studies. The following subsection discusses the other causes of voltage unbalance and its consequences.

2.2.3 Voltage Unbalance

Three-phase power systems are known as balanced or symmetrical three-phase systems when they have identical voltage and current magnitude in all phases and the phase angle are shifted by 120° with respect to each other. Voltage unbalance is referred to the magnitudes of three-phase voltage when they are not equal and/, or the phase displacement between them is not exactly 120º [20]. At medium voltage levels (11 kV and 33 kV) in the UK, the assumption of balanced three phases is not necessarily true, but it can be considered as an acceptable approximation. However, phase unbalances or voltage unbalances can be significant in low voltage feeders [44]. It was found that more than 70% of LV networks [45] experience serious phase power imbalances, primarily due to the unsymmetrical load connection and arbitrary load behaviours [46]. With the increased RET integration, the voltage unbalance can be one of the significant issues facing modern power distribution systems that received serious attention recently, which has usually been disregarded because of supervision data absence in power distribution systems.

One of the main causes of voltage unbalance is the asymmetry of the residential load connection between the three-phase systems [47]. Imbalance distribution of household single-phase loads and unsymmetrical impedance of three-phase power equipment can produce unbalanced currents, which consequently cause voltage unbalance. Uncertainty of load demand and connection makes loads balancing across three phases in the typical power distribution systems unattainable. Various rating and random locations of single-phase PV mounted by the customers can be accountable for the severity of unbalanced operation [44]. The asymmetries in the network impedances caused by un-transposed overhead lines and unbalanced transformer impedances can also promote unbalanced voltages at receiving end nodes even with completely balanced voltage sources and load connection between the three phases [3]. The perfect transposition of overhead lines can theoretically restrain the voltage unbalance, but practically, it is hard to implement transposition entirely since it is not economically justified. Moreover, the large number of EV connections has recently raised the voltage unbalance level, especially when utilising high speed charging facilities [19].

The adverse impacts and consequences of voltage unbalance on power distribution systems and equipment, in particular three-phase induction motors, some power electronics-based devices, and power transformers were discussed in [34], [41], [47]. According to the aforementioned literature, it is clear that the majority of the power distribution components, particularly on the low voltage side, are highly affected by voltage unbalance conditions. It is noticeable that a slight deviation of voltage magnitude between the three phases can contribute to a severe current unbalance due to low negative sequence impedance. This unbalanced current can cause additional heating to the stator winding of the three-phase motor, which weakens the insulation, reduces the life span of the motor, and lowers its efficiency [48]–[50]. Besides that, the voltage unbalance can overheat the transformer and end-users devices [51]. Furthermore, current unbalance increases active power losses,

including power losses in distribution lines, power transformers, and the losses resulting from current flows in the neutral wire, and accordingly lowers the overall power distribution system efficiency. In addition, the actual rating of power transformers and conductors cannot be attained during the unbalanced operating conditions, restricting the power system's components to reach their full operating capacity. For instance, one phase of transformer can be excessively loaded while the other two phases remain lightly loaded, which leads to investment made in power distribution assets is never entirely achieved.

Another major issue caused by voltage unbalance is adding complexity to voltage regulation. Due to inter-phase coupling and significant voltage differences between the phases, reducing the voltage magnitude in one phase may increase the voltage magnitude of other phases [43]. For example, changing the conventional transformer tap position, which is usually operated off-load, may improve some phases voltage but worsen the other phases. Therefore, unintended voltage regulation response across phases could pose substantial challenges to the voltage regulation device's performance when it comes to alleviate the overvoltage and undervoltage problem simultaneously in unbalanced conditions.

Based on the above investigation, voltage unbalance can be significant with the increased PV and EV connection, and it should not be disregarded. Several studies have been conducted to mitigate the voltage unbalance problem and reduce RET integration's adverse impact, considering different tools and approaches. The following section explores the most relevant of these approaches and their limitation.

2.3 Unbalanced Voltage Regulation

Since end-user customers are directly connected to the power distribution system, maintaining voltages magnitude within regulatory levels is crucial. Undervoltage can activate the operation of undervoltage relays, causing a complete disconnection of loads, and hence negatively influencing consumers and power system operator revenue. At the

same time, overvoltage increases the likelihood of equipment failures because of insulation breakdown and cause disconnection of the PV systems. Therefore, voltage magnitude across the feeder nodes should not vary considerably from its nominal value while a secure and efficient operation of the power distribution system is to be accomplished. As a result, various voltage regulation standards have been adopted. For example, EN 50160 and ANSI C84.1-2011standards specified the voltage deviation boundary to be ±10% and ±5%, respectively [34]. However, with the increase of RETs connection and voltage unbalance level, the voltage regulation has become more challenging, demanding new practical approaches to address these challenges. Consequently, there are several studies carried out on improving the unbalanced voltage regulation, which are either based on autonomous or coordinated voltage regulation.

2.3.1 Autonomous Voltage Regulation

Traditional voltage regulation measures on the power distribution systems were depended on adjusting the OLTC and switching shunt capacitors [52]. Simple autonomous control of these devices can potentially maintain the operational voltages range. However, a high portion of RET's appearance on the power distribution system made the conventional voltage regulation devices incapable of addressing the voltage regulation problem. This is because their operation needs too much time to respond to the voltage variation, and their lifespan is affected by the fluctuation of the PV systems [53]. Besides that, their application in mitigating the problem of voltage unbalance is very limited [9].

Feeder reconfiguration and phase swapping in power distribution systems are among several other methods that have been proposed to maximise the PV penetration, alleviate the voltage violation limit, and obtain acceptable voltage unbalance levels [54]–[58]. Reinforcement of power distribution is basically changing the structure of the distribution feeder, which can be accomplished either by replacing the conductor size with a higher

cross-section or placing a new parallel line to reduce the feeder's resistance. Although it was considered the most effective method to solve overvoltage, it is the most expensive and complex approach and has less impact on voltage unbalance. On the other hand, phase switching (also defined as phase swapping) primarily relies on determining the phase where the load should be connected. It involved altering the phases connection of several delicate distribution points to a particular feeder or varying the phase connection for a number of loads following the adoption of field measurement and load flow analysis. This method could be enhanced with the smart grid components, but as a result of the load deviation and PVs energy uncertainty, it is time-consuming, impose service interruption and sometimes fail to address the unbalanced voltage problem [59].

The development in power electronics and digital technology allows efficient integration of inverter-based Distributed Generation (DG), especially PV systems [60] and some other custom power devices (e.g., FACTS devices and energy storage systems) [61] into power distribution systems. Energy storage systems were utilised to store the surplus power generated by PV systems and control the real and reactive power supplied into the network, which they can play a part in regulating the network voltage. Although the energy storage systems have high operation costs, they are considered the most attractive solution for voltage regulation, especially for medium voltage applications. At the same time, reactive power compensator, in particular STATCOM and SVC, is regarded as one of the cost-effective approaches to regulate the unbalanced voltage and improve other power quality problems such as power factor correction [62], [63].

The high integration of PV system recently has imposed the power system operator to change the grid codes and regulations such as grid code IEEE 1547-2018 [64], allowing PV systems to contribute to the voltage regulation locally with fast response. Furthermore, with the enormous employment of PV energy generation as an alternative to the

conventional DGs, it becomes essential to place effective control measures to mitigate both voltage unbalance and voltage rise issues. For these reasons, various control options were proposed to adjust the node voltage by controlling the injection of real power [65], [66] and reactive power of the PV inverter [67]–[70]. In [9], a comparison has been made between these control approaches. It concludes that active power curtailment can be more effective in controlling voltage magnitude than reactive power control because of the large R/X ratio in power distribution systems. Yet, active power control is ineffective for voltage unbalance reduction, especially when the power distribution system is experiencing under-voltage. Moreover, curtailment of PV generation is also unlikely to be an acceptable societal solution since society looks to increase reliance on renewable energy due to the environmental and monetary benefits. On the other hand, reactive power control can be a practical solution to alleviate both voltage rise and voltage unbalance if an adequate control strategy is in place. A potential solution to address both voltage unbalances and undervoltage problems can be by utilising the extra capacity (i.e., PV inverter oversizing) available in the PV inverters to supply or absorb reactive power without curtailing the generated active power [71].

PV systems at a residential level can be single-phase or three-phase, depending on the demand and availability of other facilities, including three-phase lines. Normally, a three-phase PV inverter is designed as a compact three-phase unit [72], where the total active power is split equally between the three phases and the available reactive power is divided between the inverter phases according to the measured voltage. However, several studies, including [73], confirmed that additional operational functions of PV inverters (including reactive power control function) could potentially cause a higher level of electro-thermal mechanical stress on the inverter components. This can eventually reduce the likelihood of component availability and subsequent impacts on the system's reliability performance. The reason behind it is that additional operational functions increase conduction losses,

switching losses, and gate driver losses, which on the other hand, depending on the control scheme adopted in the inverting system. Typically, the Point of Common Coupling (PCC) voltage is controlled using a linear droop control in the traditional voltage-dependent reactive power control approach [55]. The droop characteristic is a piecewise linear function of the voltage, where the PV inverter absorbs or provides the reactive power according to the linear relation with the measured voltage. Linear droop control was only aimed to alleviate the overvoltage problem and has less influence on mitigating the voltage unbalance problem. Moreover, droop control's linear characteristic keeps the inverter operation continuous (i.e., only one deadband interval) even if there is a slight change in PCC voltage, which could place additional stress on the inverter.

An alternative approach is attempted in [74] for a PV inverter to mitigate only voltage unbalance by generating a negative sequence reference current. In [72], both voltage magnitude and voltage unbalance improvement techniques are suggested by operating three single-phase inverters under various values and types of power factor. Nevertheless, authors in [72] did not take into consideration the penetration level of PV, and the suggested scheme can only work effectively in particular operating conditions where all three inverters should operate at a different type of power factor. Another possible solution was recently proposed in [75] using a voltage-based droop controller and a three-phase PV inverter's damping control strategy. Although the proposed control offers promising results, active power curtailment is applied to alleviate the overvoltage issues, and the effect of the damping control strategy on voltage unbalance is limited only to the use of a three-phase inverter. In addition, authors in [75] also ignore the PV power generation and load variability, which might not reflect a realistic outcome.

Limited research is dedicated to address the challenges of overvoltage and voltage unbalance mitigation in an unbalanced power distribution systems operation. For example,

[68], [76], [77] presented approaches to limit the voltage rise on a balanced network model. However, the application of such a model does not represent reality since actual power distribution systems are naturally unbalanced. Other studies consider the unbalanced operation of power distribution systems [24], [78], but the inter-phase coupling of distribution lines was disregarded in these studies. Failure to consider unbalanced line coupling can unintentionally increase the voltage unbalance when traditional voltage control is applied [28]. Therefore, the above literature review reveals that the autonomous control of PV inverters can be the best option for comprehensive autonomous unbalanced voltage regulation in an unbalanced power distribution system if an adequate control scheme is in place. The work in chapter 5 fills the gaps mentioned above by proposing a new control scheme for PV inverters. Nevertheless, autonomously voltage control can be sometimes harmful to the power system operation at some RETs penetration level, and therefore, coordinated voltage regulation approaches might be required.

2.3.2 Coordinated Voltage Regulation

Although local control approaches of voltage regulation devices respond much faster at minimum additional cost required, it can increase the system power losses due to lack of coordination between these devices [79]. Moreover, voltage regulation devices' influence on unbalanced voltage cannot be readily determined due to the unbalanced line coupling, which may deteriorate the voltage unbalance level [80]. Therefore, high RET's integration imposes transforming the current systems into coordinated based supervisory control systems. The centralised control strategies allow effective control and operation of the network assets to mitigate voltage unbalance problems and achieve various objective functions such as minimising power losses and maximising RETs penetration.

In the last few years, many centralised control approaches have been suggested for modern power distribution systems to minimise voltage rise and power losses while

reducing voltage control devices' wear and tear resulting from PV fluctuations. In [81], an optimal operating of OLTC based on PV generation forecasts is proposed. A distribution STATCOM is coordinated with OLTC and distributed generation in [82] to control the voltage and minimise the power losses. A multi-objective technique for coordinating PVs, OLTC, and energy storage systems is developed in [25] based on forecasting data. Implementing these proposed optimisation problems is based on balanced power distribution system operation assumption and forecasts PV generation and load data. This can lead to an inaccurate representation of the power distribution system operation, which is inherently unbalanced. Besides that, the penetration of RETs is uncertain, and their output cannot be projected precisely, and there may be deviations between the predicted and realised values [15].

Several techniques are considered the unbalanced operation of the power distribution system by some authors [83], [84]; still, they did not consider minimising voltage unbalance in the optimisation problem. A coordinated control method of PVs, batteries and OLTC is suggested in [85] to reduce the severity of voltage rise and unbalancing in modern power distribution systems. Voltage unbalance reduction during the daytime is suggested in [86] by optimally re-phasing grid-tied PV systems, but this approach is limited to only use single-phase PV systems. Other methods were suggested to dynamically switch the single-phase load across the three-phase system [87] and feeder reconfiguration [88]. The main problems involved in phase switching and feeder reconfiguration in three-phase power distribution systems are the additional switching transients, operating costs, and require considerable computational time [89].

EVs' potential to suppress the voltage rise resulting from high PV penetrations has recently attracted attention, and only a few studies have paid attention to the role of EVs on voltage unbalance reduction. In [90], [91] EVs are used as one of the control variables in the

optimisation problem to limit the voltage unbalance by optimally determining the state of EV, EV point of connection, and charging/discharging rating power. However, these methods affect customers' comfort and demand monitoring and control infrastructure that outstripping the capability of the coordination scheme to reach hundreds to thousands of EVs in a given power distribution system. Moreover, either a residential-based charging station or a fast-charging station was only considered for most proposed coordination schemes. As previously mentioned, semi-fast charging stations are a new growth infrastructure in power distribution systems where their charging characteristics varies from slow and fast charging station, and therefore should be considered.

A review of the existing literature reveals that the awareness of climate change and advanced technology will undoubtedly introduce a large volume of PVs and EVs connections in the power distribution system. Their integration brings new challenges, and consequently, there is a demand for more advanced schemes to manage the various power distribution components in coordination with the new RETs, considering the unbalanced nature of the power distribution system. The work in chapter 6 fills the gaps mentioned above by proposing comprehensive coordination control schemes. However, before such schemes can be integrated into a typical power distribution system, a suitable unbalanced load flow calculation, modern voltage control device modelling, and optimisation method should be developed. The following sections explore these methods and their limitation.

2.4 Unbalanced Load Flow Calculation

Since the structure and operation of the power system are becoming more complex because of the increased connection of intelligent and regulator devices, adequate power flow calculation methods have become essential. At first, a balanced three-phase power flow or single-phase power flow was employed especially for the power transmission system. The power transmission system was assumed to be operated under balanced conditions, and

it was represented by a single-phase model through positive sequence system parameters. Nevertheless, this assumption is invalid for the power distribution system because the operation and unique structure are much more complex than power transmission systems. For example, power distribution systems are typically radial or weakly meshed, categorised by high R/X ratios, and operated with various number of phases. Moreover, they contain an increased number of distributed loads and generation, causing unbalanced operation [92].

All these elements make conventional power flow methods (e.g., based on single-phase representation) inadequate for the application of power distribution systems, leading to poor accuracy in load flow results. Besides that, the single-phase representation of modern power distribution systems components is no longer valid. Therefore, different load flow (power flow) methods have been developed in the past few years. These load flow methods can principally be grouped into two categories; Backward–Forward Sweep based techniques and modified Newton-Raphson techniques. The Backward–Forward Sweep algorithm is basically based on Kirchhoff's Current Law & Kirchhoff's Voltage Law, where the line currents are determined in the backward sweep while the voltage at buses are found using the forward sweep. The original mathematical formulation of Backward–forward sweep method was first developed in [93], and was modified to handle a weakly meshed system, voltage-controlled nodes and unbalance in [94], [95].

The Backward–Forward Sweep algorithm requires no matrix-based formulation compared to other algorithms, which leads to a simple mathematical formulation and less computation time, specifically for the purely radial power distribution systems. During a particular period of time, the Backward–Forward Sweep-based method was considered the preferable method for analysing the radial distribution network. At the same time, some authors [96], [97] argue that as the power distribution system becomes highly meshed, having many voltage control devices, DGs, and heavy-load conditions, the Backward–

Forward Sweep method will experience an increased number of iterations, and it will be at greater risk of divergence. In spite of the fact that new mathematical modification has been made in the Backward–Forward Sweep algorithm to address the divergence issue, the computational time has risen considerably, and the convergence is not achieved at some ill-conditioned operations [98].

Amongst all traditional load flow techniques, the Newton-Raphson technique is regarded as the best method of solving the load flow problem due to its robust convergence characteristics in a well-conditioned transmission system [99]. Six various versions of the Newton-Raphson formulations are available for load flow calculation. These six versions resulted from power and current mismatch equations that are written in three different coordinates, namely complex, polar, and rectangular coordinates. The load flow formulation details and the performance evaluation of all these different six versions of the Newton-Raphson method are presented in [100]. The evaluation concludes that the most two robust methods for both balanced and unbalanced power distribution system application are current mismatch functions written in polar and rectangular coordinates. In the current injection mismatch formulation, the current injected equations presented in rectangular forms are used for each network nodes in load flow calculation, which was originally proposed in [101]. Two sets of current injection mismatch equations written in rectangular coordinates were used for both generator buses and load buses. In such an approach, the Jacobian matrix updates much faster compared with the Jacobian in other Newton-Raphson load flow methods, particularly for a network with only load buses. This is because most of the components in the Jacobian matrix are equal to the admittances and do not necessarily need to be updated through the iteration process. This developed technique was expanded to the Three-phase Current Injection Mismatch (TCIM) method for an unbalanced three-phase network in [102]. TCIM method was further enhanced by developing control devices models

such as voltage control devices [103] and a new mathematical formulation for generator (i.e., voltage-controlled or P-V) buses [104].

Performance comparisons study has been conducted between Backward–Forward Sweep and TCIM method in [97]. The study concludes that the TCIM method provides superior performance in large-scale meshed power distribution systems with the presence of control devices and DGs. This is because the number of iterations for the TCIM method increases slightly, whereas in Backward–Forward Sweep increases significantly, and the convergence may not necessarily be achieved. Although the computational time of Backward–Forward Sweep is relatively lower, TCIM has proven to be numerically robust and accurate and can be applicable for meshed or radial power distribution systems [98].

However, the representation of voltage-controlled buses was the main concern in the current injection mismatch method, which has either reduced the accuracy of load flow calculation or increased its complexity. In [105], the authors assumed that the voltage mismatch is equal to zero from the first iteration at a voltage-controlled bus. Nevertheless, this assumption is only valid after the convergence of the load flow calculation has been achieved. Apart from that, some divergence concerns were reported when the same voltage-controlled representation was applied in the unbalanced load flow formulation considering a heavily loaded network integrated with voltage control devices. The drawback of this voltage-controlled buses representation was addressed in [106]. Yet, the revised representation of voltage-controlled buses raises the computation time since the number of needed equations to represent at each voltage-controlled bus rises to three [107].

A novel mathematical representation of voltage-controlled buses has been developed in [107] for the current injection mismatch method that is used for balanced load flow calculation. In the newly developed method, a power injection mismatch equation was applied to represent the voltage-controlled buses where the number of required equations

decreases from three to one for each voltage-controlled type bus, leading to fewer iterations and reduced computation time. Therefore, the new development of voltage-controlled bus representation needed to be extended to the unbalanced three-phase load flow calculation. The work in Chapter 3 fills the gaps mentioned above by developing advanced an unbalanced load flow calculation method that offers a reduced computation time with robust mathematical modelling of modern power distribution components.

2.5 Modelling of SVC and STATCOM

For electrical power systems equipped with SVC and STATCOM, accurate modelling of these devices is necessary for the power flow calculation. Accurate models can be used to identify the best location and the required ratings of these devices and to investigate their impacts on the power systems, including power quality under normal, abnormal, and contingency conditions. Moreover, the load flow result incorporated with the connection of SVC and STATCOM devices provides the initial conditions for adopting centralised control, which involves optimal power flow calculation. However, the balanced or single-phase equivalent representation of these devices is no longer valid for the unbalanced power distribution system application. Moreover, achieving only accurate modelling of these devices alone is not good enough for online monitoring and control applications. Their representation in load flow calculation should offer reduced computation time, high convergence performance, and capability to cope with any operating conditions.

In most Newton-Raphson load flow formulations, the control variables of SVC and STATCOM were used as independent variables, and their values were determined during the load flow iterative procedures. This attempt requires some adjustments to the existing load flow algorithm. It increases the Jacobian and admittance matrices' size to accommodate the extra independent variables, and consequently raise the execution time. Furthermore, the convergence of this approach is affected by the initial values of control variables [108].

Besides that, the existing three-phase mathematical models of these devices were formulated for the Three-phase Power Injection Mismatch (TPIM) method, which is considered less performance with other recently developed, such as TCIM method.

In [109]–[111], the SVC and STATCOM devices were modelled for the three-phase load flow calculation based on the conventional TPIM method. An extra two mismatch equations were used for the STATCOM model to determine the two state variables of the controllable voltage source ($V_{sh}\angle\delta_{sh}$), and one extra mismatch equation was used for the SVC control variable to determine either the total susceptance B_{svc} or firing angle α_{svc}. This formulation made the algorithm more complex, computationally heavy, and may lead to poor convergence. A simplified model of SVC and STATCOM in the balanced Newton-Raphson load flow method has been suggested in [112], [113] to decrease the computing time and improve the accuracy of the load flow solution. The power mismatch equation was used to represent SVC and STATCOM as voltage-controlled buses with predefined voltage and zero generated active power, which kept the original Jacobian matrix unchanged. Then, the variables of voltage control devices can be computed during the iteration process using simple equations. The work in Chapter 4 extends this modelling framework of SVC and STATCOM to represent an unbalanced power distribution system.

2.6 Optimal Power Flow

The Optimal Power Flow (OPF) model is one of the core tools for real-time monitoring and management of active power distribution systems [15]. It aims to optimise power system control assets while satisfying equality and inequality constraints for secure, reliable, and optimal power system operations. The optimisation problem can be solved using some available techniques that might be classified as mathematical-based techniques and heuristic-based techniques. Mathematical-based techniques such as linear programming and nonlinear programming have achieved reasonable success in solving optimisation

problems [114]–[116]. The major strengths of these methods are numerical stability and reliable convergence, but they are hard to handle discrete variables, exposed to get trapped in local minima solution, and highly sensitive to initial values [115].

To satisfy the requirement of real-time power distribution system operation, some authors choose to sacrifice accuracy to increase the optimisation algorithm's computational performance. For example, in [17], [18], the authors ignore the discrete variables in the formulation like OLTC and voltage regulator. They assumed a continuous tap of voltage regulation devices, and they had to round the optimal value to the closest integer number. There is no assurance that the rounded number is the correct optimal solution, especially if there is a very large step. A simplification is also adopted in [31], [117] to use a mixed-integer linear programming to solve optimisation problems for the unbalanced power distribution system. One of the assumptions made is to ignore the inter-phase coupling between the conductors to linearised the power flow equations. However, these simplifications often suffer from inaccuracies since power distribution systems are inherently nonlinear, which may not reflect the realistic outcome [118]. Failure to consider mutual impedances can create an ineffective control signal, which may inadvertently increase the level of voltage unbalance.

These shortcomings can be overcome when meta-heuristics methods, such as Particle Swarm Optimisation (PSO) and Genetic Algorithm (GA), are applied to solve the optimisation problem with limited or fewer modifications required in the original problem. These methods also are not highly dependent on the dimensions and nonlinearity of the optimisation problem, and they can converge to a realistic solution where mathematical techniques fail [119]. Their main concern is to obtain the global best solution in the shortest possible time because of the large number of load flow calculations required in the solution process, limiting their use in online applications. However, the problem of computation time

is expected to be resolved by the next-generation of software and hardware, taking into consideration the rapid advancement of computer technology. For instance, the limitation of using meta-heuristics in online applications was addressed in [120] by operating the massively parallel architecture of graphics processing units, which significantly accelerated the computations process. Therefore, the development in computational intelligence with the advent of parallel processing capabilities and the use of supercomputer made using of meta-heuristics methods possible in real-time optimisation applications, such as [90], [121].

Various meta-heuristics methods and their variants have been proposed in the literature for solving the optimisation problem. PSO-based approach is one of the most popular techniques due to its ability to deal with highly nonlinear and mixed-integer problems [122]. Yet, the original PSO sometimes requires more time to move into the solution space's effective area, depending on the case. For this reason, various versions of PSO were proposed and hybridised with other meta-heuristics methods. For example, to alleviate the local minimum issue, a modification is applied to the PSO in [123], and the diversity of the optimisation variables is improved by applying GA mutation and crossover operators. A comparison investigation in [124] demonstrates that this hybridised PSO approach outperforms other heuristic approaches with regard to accuracy, robustness and speed. Furthermore, another version of PSO based on natural selection mechanism is reported in [125], where the number of the best particle is increased while the worst particle is reduced at each generation. This allows low assessed agents to move to the best adequate area straight using the selection method, and concentrated search primarily in the current effective area is realised. Taking advantage of the two modified PSO proposed in [123] and [125], and to improve the accuracy further and prevent premature convergence of the solution, a combination of both methods is proposed in chapter 6 to solve the optimisation problem involved in coordinated unbalanced voltage regulation.

2.7 Summary

This chapter has introduced a comprehensive literature review of different approaches used to address the challenges confronting the operation of modern power distribution systems. The chapter first covers the challenges encountered the modern power distribution systems topology and operation. Two main aspects associated with power distribution system operation are discussed; integration of RETs and voltage unbalance. The discussions indicate that RET's potential impacts will demand a paradigm change in the way power distribution systems are managed and designed. It also concludes that one of the major drawbacks of excessive integration of PVs and EVs is the increase in voltage unbalance in the power distribution system. Voltage unbalance can be significant, causing undesirable consequences to power distribution systems. In this regard, this chapter has also presented various related works on local and coordinated voltage regulation techniques to identify the challenges and the potential research gap.

There have been significant interests in the optimisation-based control schemes in distribution networks that are driven by the rapid growth of PVs and EVs in the recent few years. It involved coordination schemes of PVs and EVs with other existing voltage regulation devices. This has demanded developing a suitable optimisation framework that should accurately model all power distribution systems components under key operating conditions, which also involves using a load flow calculation. Therefore, this chapter has provided related work on load flow calculation methods and optimal power flow techniques to identify their limitation on a practical active power distribution system. It concludes that the need for faster, reliable, and accurate central-based control in unbalanced power distribution rich with RET connections consider as one of the potential research gaps.

Chapter 3: Unbalanced Power Distribution Systems Modelling

3.1 Introduction

Due to the modernisation of power distribution systems, many new network components, including smart meters, FACTS devices, and RETs, are being connected into the grid. The present power distribution system is rapidly developing and becoming more challenging to control. The introduction of the smart grid concept for the power distribution system offered many opportunities to solve unconventional and challenging problems, which involve collecting real-time data and the status of the network components to achieve various tasks, including reliable and optimal operation.

For smart power distribution systems to perform distribution automation, a repeated and accurate load flow solution is required [126]. A load flow solution provides the steady-state behaviour of the power system, which is one of the core elements for controlling and monitoring the operation of active power distribution systems. However, the most developed power flow calculation methods are exclusively employed for the power transmission system, and because of unbalanced operation and network complexity, they can no longer be directly applied to a power distribution system. This has led to propose different three-phase load flow calculation methods [97], which are also currently showing some limitations regarding their convergence and computation time. These limitations made them unsuitable for the application of real-time control and management of modern power distribution systems. Therefore, as power distribution systems become increasingly complex, there has been a significant interest in developing a new and reliable load flow calculation method. It should have the capability to accurately represent the operation of active power distribution

systems with their basic components and integrated active resources while considering a robust solution at high convergence speed, especially for real-time applications.

Thus, this chapter presents a new methodology for calculating unbalanced three-phase load flow for the power distribution systems. This method combines the three-phase current injection method [107] and the three-phase power injection method [127], reducing the number of equations that represent the voltage-controlled buses to further improve the convergence and computation time. The methodology also involves an accurate three-phase steady-state modelling of basic power distribution system components, including distribution lines, three-phase transformers, and loads. The chapter is structured as follows. Section 3.2 introduces the mathematical models of basic components of a power distribution system. Section 3.3 provides the mathematical formulation of the developed three-phase power and current injection mismatch (TPCIM) method. The accuracy of the developed model and the computational efficiency based on several case studies is demonstrated in section 3.4. Finally, section 3.5 brings a summary of the chapter. The study outcomes of this chapter have resulted in the publication of a conference paper [98] during the course of this Ph.D. work, which is being cited appropriately.

3.2 Modelling Power Distribution System Components

A power distribution system can be modelled as a network with a number of buses, which represent a system component such as DGs and load connected by branches through distribution lines or transformers. The transformer can be at distribution substations that are used to step down the incoming transmission-level voltage or at primary or secondary distribution circuits that are located near the load centres. The loads can be either residential loads supplied by single-phase or three-phase feeders or commercial loads supplied by a dedicated three-phase system. Figure 3.1 shows the basic component that can be seen in a typical power distribution system. In addition to these basic components, power distribution

systems tend to have many more complex elements and devices as compared to power transmission systems. These components must be carefully modelled to obtain accurate and reliable results regards to their contribution. The single-phase or balanced modelling of power system components is limited to the power transmission system, and consequently, new modelling needs to be carried out. This section presents the comprehensive models of basic components and devices that are usually used in power distribution systems.

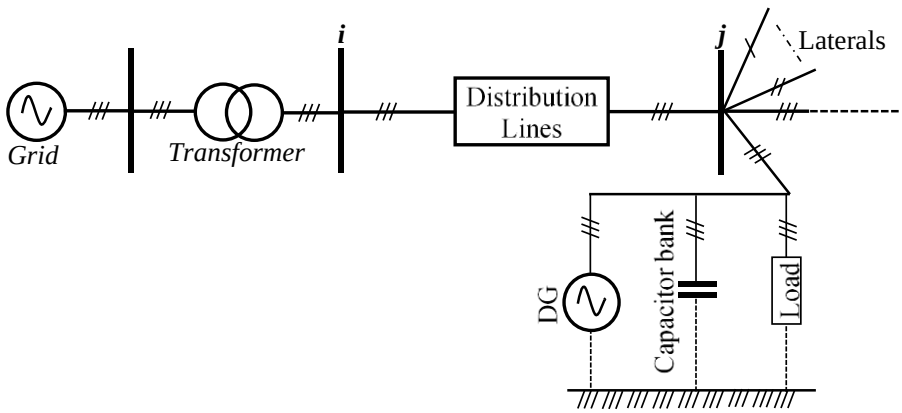

Figure 3.1. Basic power distribution system components

3.2.1 Distribution Lines Modelling

Balanced three-phase operation and the transposition of the conductors are the two main assumptions made in the analysis of a power transmission line. However, power distribution lines do not fall under either of these two assumptions. Therefore, it is important to establish a more precise mathematical model to represent the distribution lines. A general representation of power distribution system lines with a multi-number of conductors can be constructed by employing Carson's equations and Kron reduction [1], leading to a 3×3 primitive impedance matrix comprising of the self and mutual equivalent impedances for the three-phases multi-wires system. For a representation of distribution lines connected between bus *i* and bus *j*, commonly the π-model is used, which is composed by the series impedance (Z^{abc}) and the shunt admittance (y_{sh}^{abc}) of the line as shown in Figure 3.2.

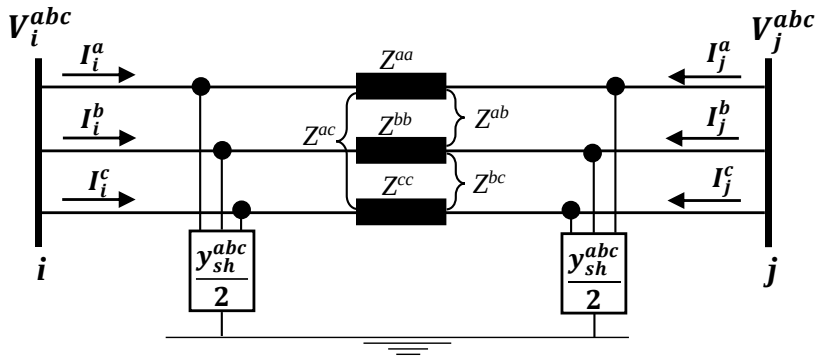

Figure 3.2. The π-model equivalent circuit of three-phase distribution line

Using Kirchoff's Current Law at each bus in the network, the mathematical interconnection between the injected current I^{abc} and the bus voltages V^{abc} for n number of buses is defined by the admittance matrix Y^{abc}:

$$\begin{bmatrix} I_1^{abc} \\ \vdots \\ I_n^{abc} \end{bmatrix} = \begin{bmatrix} Y_{11}^{abc} & \cdots & Y_{1n}^{abc} \\ \vdots & \ddots & \vdots \\ Y_{n1}^{abc} & \cdots & Y_{nn}^{abc} \end{bmatrix} \begin{bmatrix} V_1^{abc} \\ \vdots \\ V_n^{abc} \end{bmatrix} \tag{3.1}$$

where

$Y_{ii}^{abc} = \sum_{j=0}^{n}(y_{ij}^{abc} + \frac{y_{sh(ij)}^{abc}}{2}), i \neq j$ - are the diagonal components of the admittance matrix, which represent the sum of admittances and half shunt admittances connected to the bus i.

$Y_{ij}^{abc} = Y_{ji}^{abc} = -y_{ij}^{abc}$ -are the off-diagonal components of the admittance matrix, which are equal to the negative of the admittance between the buses. Therefore, the corresponding admittance matrix (Y_{bus}) for the whole power distribution network can be described as in (3.2).

$$Y_{bus} = \begin{bmatrix} Y_{11}^{aa} & Y_{11}^{ab} & Y_{11}^{ac} & \cdots & Y_{1n}^{aa} & Y_{1n}^{ab} & Y_{1n}^{ac} \\ Y_{11}^{ba} & Y_{11}^{bb} & Y_{11}^{bc} & \cdots & Y_{1n}^{ba} & Y_{1n}^{bb} & Y_{1n}^{bc} \\ Y_{11}^{ca} & Y_{11}^{cb} & Y_{11}^{cc} & \cdots & Y_{1n}^{ca} & Y_{1n}^{cb} & Y_{1n}^{cc} \\ \vdots & \vdots & \vdots & \ddots & \vdots & \vdots & \vdots \\ Y_{n1}^{aa} & Y_{n1}^{ab} & Y_{n1}^{ac} & \cdots & Y_{nn}^{aa} & Y_{nn}^{ab} & Y_{nn}^{ac} \\ Y_{n1}^{ba} & Y_{n1}^{bb} & Y_{n1}^{bc} & \cdots & Y_{nn}^{ba} & Y_{nn}^{bb} & Y_{nn}^{bc} \\ Y_{n1}^{ca} & Y_{n1}^{cb} & Y_{n1}^{cc} & \cdots & Y_{nn}^{ca} & Y_{nn}^{cb} & Y_{nn}^{cc} \end{bmatrix} \tag{3.2}$$

3.2.2 Three-phase Transformer Modelling

Transformers are one of the major components in the power distribution system that need careful modelling due to their effects on network losses, zero sequence current, grounding method, and protection strategies. Three-phase transformers are modelled in the three-phase load flow calculation by transformer admittance matrix Y_T^{abc} as described in (3.3), which reflecting also the connection type (e.g., YNyn0, Dyn1, etc.), transformer taps, and the leakage admittance [127].

$$Y_T^{abc} = \begin{bmatrix} Y_{pp}^{abc} & Y_{ps}^{abc} \\ Y_{sp}^{abc} & Y_{ss}^{abc} \end{bmatrix} \tag{3.3}$$

where Y_{pp}^{abc}, Y_{ss}^{abc} are self-admittance of the primary and secondary of the transformer, respectively and Y_{sp}^{abc}, Y_{ps}^{abc} are a mutual admittance of the transformer. The details of transformer admittance matrix elements for various transformer connections and tap ratio and location are given in Appendix A. The admittance matrix defined by (3.3) for the transformer can be included in the main admittance matrix described in (3.2).

A voltage regulator is also a device used to regulate or compensate for the voltage drop along a power distribution feeder. It can be installed either at a substation or along the feeder, which can be treated as an autotransformer with a load tap changing mechanism. The taps are specified through a dedicated control circuit that approximates the voltage drop or maintains the pre-defined bus voltage magnitude. Three-phase voltage regulators are typically installed in wye, closed-delta, or open-delta configurations in power distribution systems. A standard step regulation contains a reversing switch allowing a 10% regulation range of voltages, normally 32 steps. Therefore, a voltage regulator can be modelled as a three-phase transformer with controllable tap chargers, as proposed in [128].

3.2.3 Load and Generators Modelling

Loads are normally modelled as a fixed power demand interconnected at each bus in a single-phase or balanced load flow problem. Nevertheless, while the entire three-phase or asymmetrical scheme is taken into consideration, their characteristics and connection need to be addressed. For example, in power distribution systems, loads may be present in a different number of phases (e.g., single-phase load and three-phase load) with different connections (i.e., delta or wye connection). Moreover, according to the load characteristics, they can be classified into three different models: constant power, constant impedance, and constant current [129]. In a constant power model, the active and reactive power provided to the load are maintained constant, which is commonly used in transmission power system analysis. A constant impedance model is regarded as a more accurate load model for large industrial loads where the load's impedance is obtained using the defined active and reactive power at nominal voltage magnitude, and is maintained constant. Whereas in the constant current load model, the load current magnitude is determined by the fixed active and reactive power at nominal voltage magnitude, and is also maintained constant. There are various mathematical models for these loads, including the polynomial model or ZIP model, which combines all the different load models [130]. This model specifies the power consumption as the summation of elements of all three-load models, as follows:

$$P_i = P_{i_0} + P_{i_1}|V_i| + P_{i_2}|V_i|^2 \tag{3.4}$$

$$Q_i = Q_{i_0} + Q_{i_1}|V_i| + Q_{i_2}|V_i|^2 \tag{3.5}$$

where

P_{i_0}, Q_{i_0} - constant power elements for the load connected at bus *i*.

P_{i_1}, Q_{i_1} - constant current elements for the load connected at bus *i*.

P_{i_2}, Q_{i_2} - constant impedance elements for the load connected at bus *i*.

DGs are becoming much more common in power distribution systems as they can play a key factor in increasing operational efficiency and bringing financial benefits. Some of these generators are like any conventional generators that are used to control the real power (P) and the voltage magnitude ($|V|$), which are modelled as a voltage-controlled bus in the load flow formulation. Nevertheless, the majority of the small-scale DGs are incapable of controlling the voltage at the connected buses, and thus they cannot be modelled as a voltage-controlled bus. Therefore, based on the types of DG and its control mechanism, most buses connected with DG can be treated as load buses. Furthermore, besides the DGs, a shunt fixed capacitor bank is utilised to provide reactive power support, and its connected bus can be modelled as a load bus with zero active power and specified reactive power.

3.3 Proposed Unbalanced Power Flow Method

The formulation of power and current injection mismatch method developed in [107] is expanded to an unbalanced three-phase system. The developed technique is mainly a combination of two Newton-Raphson algorithms that are employed for the different types of buses. In load flow analysis, there are three types of network buses; slack bus, a generator bus (P-V bus), and a load bus (P-Q bus), which may correspond to a load, shunt capacitor bank or distributed generation connection. Load buses are specified by active power (P) and reactive power (Q), and generator buses are determined by active power (P) and voltage magnitude ($|V|$). Therefore, in the developed load flow calculation, the P-Q buses are modelled using current injection mismatches equations, whereas the P-V buses are represented by only active power injection mismatch equations [98]. This formulation increases convergence efficiency and computation time by reducing the complicity and number of equations of the proposed load flow algorithm.

3.3.1 Mismatch Equations

3.3.1.1 Current Injection Mismatch Equations

According to Kirchoff's Current Law, the injected current I_i^p at the bus *i* for phase *p* can be computed in rectangular coordinates using (3.6) [98].

$$I_i^p = \sum_{j=1}^{n} \sum_{q=a,b,c} Y_{ij}^{pq} V_j^q = \sum_{j=1}^{n} \sum_{q=a,b,c} \left(G_{ij}^{pq} + jB_{ij}^{pq}\right)\left((V_j^r)^q + j(V_j^m)^q\right) \tag{3.6}$$

Since the real power (p_i^{sp}) and reactive power (Q_i^{sp}) are specified at the P-Q buses, the specified current injection at bus *i* for phase *p* can be calculated using [98]:

$$(I_i^{sp})^p = \left(\frac{(S_i^{sp})^p}{(V_i)^p}\right)^* = \frac{(p_i^{sp})^p - j\,(Q_i^{sp})^p}{(V_i^r)^p - j(V_i^m)^p} \tag{3.7}$$

Separating the real and imaginary parts of these two expressions, and using the mismatch function $\Delta\left(I_i^p\right) = (I_i^{sp})^p - I_i^p$, the three-phase current injection mismatch equations for real ($\Delta(I_i^r)^p$) and imaginary ($\Delta(I_i^m)^p$) part expressing can be given as follows [98]:

$$\Delta(I_i^r)^p = \frac{(P_i^{sp})^p\,(V_i^r)^p + (Q_i^{sp})^p\,(V_i^m)^p}{((V_i^r)^p)^2 + ((V_i^m)^p)^2} - \sum_{j=1}^{n} \sum_{q=a,b,c} \left(G_{ij}^{pq}(V_j^r)^q - B_{ij}^{pq}(V_j^m)^q\right) \tag{3.8}$$

$$\Delta(I_i^m)^p = \frac{(P_i^{sp})^p\,(V_i^m)^p - (Q_i^{sp})^p\,(V_i^r)^p}{((V_i^r)^p)^2 + ((V_i^m)^p)^2} - \sum_{j=1}^{n} \sum_{q=a,b,c} \left(G_{ij}^{pq}(V_j^m)^q + B_{ij}^{pq}(V_j^r)^q\right) \tag{3.9}$$

where

$$(P_i^{sp})^p = P_{gi}^p - P_{li}^p \tag{3.10}$$

$$(Q_i^{sp})^p = Q_{gi}^p - Q_{li}^p + Q_{ci}^p \tag{3.11}$$

$j = \{1, 2, \ldots, n\}$ - set of buses, *n* is the total number of buses.

p, q $\in \{a, b, c\}$ - are the three phases notation. There are no current and power mismatch equations to represent the neutral point of buses in the system. Therefore, even if there is a neutral conductor, the neutral

point can be merged with other phases using Kron's reduction. In this case, the voltage at the neutral point and the neutral current cannot be computed directly from the bus admittance matrix.

P_{gi}^{p} , Q_{gi}^{p} , P_{li}^{p}, Q_{li}^{p} - the predefined active and reactive power of generators and loads, respectively at bus *i* for the given phase *p*.

$I_i^r, I_i^m, V_i^r, V_i^m$ - are the real and imaginary parts of the current and voltage at bus *i*

Q_{ci}^{p} - represent the shunt reactive power connected at bus *i* for the given phase *p*, which is defined as a positive reactive power load.

$Y_{ij}^{pq} = G_{ij}^{pq} + jB_{ij}^{pq}$ - is the bus admittance matrix element as described in (3.2).

3.3.1.2 Power Injection Mismatch Equation

Generator's nodes or P-V nodes are modelled using the power injection mismatch equations. Recall the power flow equation in polar form with admittance represented in the rectangular form [98].

$$S_i^p = V_i^p (I_i^p)^* = \sum_{j=1}^{n} \sum_{q=a,b,c} |V_i^p||V_j^q|(\cos\delta_{ij}^{pq} - j\,sin\,\delta_{ij}^{pq})(G_{ij}^{pq} - jB_{ij}^{pq}) \qquad (3.12)$$

Separating this expression into real and imaginary parts, then the mismatch equation for real power injection $\Delta(P_i^p) = (P_i^{sp})^p - P_i^p$ can be obtained using the following expression [98].

$$\Delta(P_i)^p = (P_i^{sp})^p - \sum_{j=1}^{n} \sum_{q=a,b,c} |V_i^p||V_j^q| \left(G_{ij}^{pq}\cos(\delta_i^p - \delta_j^q) + B_{ij}^{pq}\sin(\delta_i^p - \delta_j^q)\right) \qquad (3.13)$$

3.3.2 Newton-Raphson Method

In order to solve the set of nonlinear current and real power mismatch equations ($F(\vec{s})$) to obtain the voltage magnitude and angle variables ($\vec{s}$) , a Newton-Raphson method

is employed due to its quadratic convergence [99]. The linearised problem is constructed through the Jacobian matrix equation $(F(\vec{s}) = -J(\vec{s})\Delta(\vec{s}))$, as shown in (3.14).

$$\begin{bmatrix} \Delta(I_x^m)^{abc} \\ \Delta(I_x^r)^{abc} \\ \vdots \\ \Delta(P_y)^{abc} \\ \vdots \end{bmatrix} = -J \cdot \begin{bmatrix} \Delta(V_x^r)^{abc} \\ \Delta(V_x^m)^{abc} \\ \vdots \\ \Delta(\delta_y)^{abc} \\ \vdots \end{bmatrix} \tag{3.14}$$

where J is the square Jacobian matrix, which can be written in matrix form as follows:

$$J = \begin{bmatrix} \frac{\partial\Delta(I_{ix}^m)^{abc}}{\partial\left(V_{jx}^r\right)^{abc}} & \frac{\partial\Delta(I_{ix}^m)^{abc}}{\partial\left(V_{jx}^m\right)^{abc}} & \cdots & \frac{\partial\Delta(I_{ix}^m)^{abc}}{\Delta\delta_{jy}^{abc}} \\ \frac{\partial\Delta(I_{ix}^r)^{abc}}{\partial\left(V_{jx}^r\right)^{abc}} & \frac{\partial\Delta(I_{ix}^r)^{abc}}{\partial\left(V_{jx}^m\right)^{abc}} & \cdots & \frac{\partial\Delta(I_{ix}^r)^{abc}}{\Delta\delta_{jy}^{abc}} \\ \vdots & \vdots & \ddots & \vdots \\ \frac{\partial\Delta(P_{iy})^{abc}}{\partial\left(V_{jx}^r\right)^{abc}} & \frac{\partial\Delta(P_{iy})^{abc}}{\partial\left(V_{jx}^m\right)^{abc}} & \cdots & \frac{\partial\Delta(P_{iy})^{abc}}{\Delta\delta_{jy}^{abc}} \end{bmatrix} \tag{3.15}$$

x represents the element of P-Q buses only and y for P-V buses only, and submatrices of J, for example $\frac{\partial\Delta(I_{ix}^m)^{abc}}{\partial\left(V_{jx}^r\right)^{abc}}$ shown here are corresponding to nodes i and j, and the structure is:

$$\frac{\partial\Delta(I_{ix}^m)^{abc}}{\partial\left(V_{jx}^r\right)^{abc}} = \begin{bmatrix} \frac{\partial\Delta(I_{ix}^m)^{a}}{\partial\left(V_{jx}^r\right)^{a}} & \frac{\partial\Delta(I_{ix}^m)^{a}}{\partial\left(V_{jx}^r\right)^{b}} & \frac{\partial\Delta(I_{ix}^m)^{a}}{\partial\left(V_{jx}^r\right)^{c}} \\ \frac{\partial\Delta(I_{ix}^m)^{b}}{\partial\left(V_{jx}^r\right)^{a}} & \frac{\partial\Delta(I_{ix}^m)^{b}}{\partial\left(V_{jx}^r\right)^{b}} & \frac{\partial\Delta(I_{ix}^m)^{b}}{\partial\left(V_{jx}^r\right)^{c}} \\ \frac{\partial\Delta(I_{ix}^m)^{c}}{\partial\left(V_{jx}^r\right)^{a}} & \frac{\partial\Delta(I_{ix}^m)^{c}}{\partial\left(V_{jx}^r\right)^{b}} & \frac{\partial\Delta(I_{ix}^m)^{c}}{\partial\left(V_{jx}^r\right)^{c}} \end{bmatrix} \tag{3.16}$$

It can be noted that the number of equations used to represent the P-V buses is reduced to one equation only compared with the original current injection mismatch method. Consequently, the size of the Jacobian matrix is reduced from $3(2x + 3y) \times 3(2x + 3y)$ to $3(2x + y) \times 3(2x + y)$. For instance, considering the IEEE-37 buses test feeders having 10 P-V buses and 26 P-Q buses ($y = 10, x = 26$), the size of the Jacobian matrix will be 246×246 and 186×186 for the original current injection mismatch and developed

methods, respectively. This advantage of decreasing the size of the Jacobian matrix in the developed TPCIM can be considerably useful, especially at large-scale systems. The sub-matrices of Jacobian J components corresponding to only P-Q buses can be computed as follows [98]:

$$\frac{\partial \Delta(I_i^m)^{abc}}{\partial\ (V_i^r)^{abc}} = -B_{ii}^{abc} + \begin{bmatrix} A_i^a & 0 & 0 \\ 0 & A_i^b & 0 \\ 0 & 0 & A_i^c \end{bmatrix}$$
$$\frac{\partial \Delta(I_i^m)^{abc}}{\partial\ \left(V_j^r\right)^{abc}} = -B_{ij}^{abc} \quad for\ i \neq j \tag{3.17}$$

$$\frac{\partial \Delta(I_i^m)^{abc}}{\partial\ (V_i^m)^{abc}} = -G_{ii}^{abc} + \begin{bmatrix} B_i^a & 0 & 0 \\ 0 & B_i^b & 0 \\ 0 & 0 & B_i^c \end{bmatrix}$$
$$\frac{\partial \Delta(I_i^m)^{abc}}{\partial\ \left(V_j^m\right)^{abc}} = -G_{ij}^{abc} \quad for\ i \neq j \tag{3.18}$$

$$\frac{\partial \Delta(I_i^r)^{abc}}{\partial\ (V_i^r)^{abc}} = -G_{ii}^{abc} + \begin{bmatrix} C_i^a & 0 & 0 \\ 0 & C_i^b & 0 \\ 0 & 0 & C_i^c \end{bmatrix}$$
$$\frac{\partial \Delta(I_i^r)^{abc}}{\partial\ \left(V_j^r\right)^{abc}} = -G_{ij}^{abc} \quad for\ i \neq j \tag{3.19}$$

$$\frac{\partial \Delta(I_i^r)^{abc}}{\partial\ (V_i^m)^{abc}} = B_{ii}^{abc} + \begin{bmatrix} D_i^a & 0 & 0 \\ 0 & D_i^b & 0 \\ 0 & 0 & D_i^c \end{bmatrix}$$
$$\frac{\partial \Delta(I_i^r)^{abc}}{\partial\ \left(V_j^m\right)^{abc}} = B_{ij}^{abc} \quad for\ i \neq j \tag{3.20}$$

where the elements $A_i^p, B_i^p, C_i^P, and\ D_i^P$ are determined by the load models. For the constant load model, the elements are given as follows [98]:

$$A_i^p = \frac{(Q_i^{sp})^p(((V_i^r)^p)^2 - ((V_i^m)^p)^2) - 2\ (V_i^r)^p\ (V_i^m)^p(P_i^{sp})^p}{(((V_i^r)^p)^2 + ((V_i^m)^p)^2)^2} \tag{3.21}$$

$$B_i^p = \frac{(p_i^{sp})^p(((V_i^r)^p)^2 - ((V_i^m)^p)^2) + 2\ (V_i^r)^p\ (V_i^m)^p(Q_i^{sp})^p}{(((V_i^r)^p)^2 + ((V_i^m)^p)^2)^2} \tag{3.22}$$

$$C_i^p = -B_i^p \tag{3.23}$$

$$D_i^p = A_i^p \tag{3.24}$$

The elements of Jacobian matrix J , which are corresponding to P-Q and P-V buses, can be calculated as follows [98]:

$$\frac{\partial \Delta (I_i^m)^{abc}}{\Delta \delta_j^{abc}} = -\left|V_j^{abc}\right|\left(G_{ij}^{abc} \cos \delta_j^{abc} - B_{ij}^{abc} \sin \delta_j^{abc}\right) \ for\ i \neq j \tag{3.25}$$

$$\frac{\partial \Delta (I_i^r)^{abc}}{\Delta \delta_j^{abc}} = \left|V_j^{abc}\right|\left(G_{ij}^{abc} \sin \delta_j^{abc} + B_{ij}^{abc} \cos \delta_j^{abc}\right) \ for\ i \neq j \tag{3.26}$$

$$\frac{\partial \Delta (P_i)^{abc}}{\partial \left(V_j^r\right)^{abc}} = -\left((V_i^r)^{abc} G_{ij}^{abc} + B_{ij}^{abc} (V_i^m)^{abc}\right) for\ i \neq j \tag{3.27}$$

$$\frac{\partial \Delta (P_i)^{abc}}{\partial \left(V_j^m\right)^{abc}} = -\left((V_i^m)^{abc} G_{ij}^{abc} - B_{ij}^{abc} (V_i^r)^{abc}\right) for\ i \neq j \tag{3.28}$$

The last element of Jacobian matrix J, which corresponds to P-V buses only can be determined as follows [98]:

$$\frac{\partial \Delta (P_i)^p}{\Delta \delta_i^p} = -\sum_{i=j}^{n} \sum_{q \neq p}^{a,b,c} \left|V_i^p\right|\left|V_j^q\right| \left(-G_{ij}^{pq} \sin\left(\delta_i^p - \delta_j^q\right) + B_{ij}^{pq} \cos\left(\delta_i^p - \delta_j^q\right)\right) \tag{3.29}$$

$$\frac{\partial \Delta (P_i)^p}{\Delta \delta_j^q} = -\left|V_i^p\right|\left|V_j^q\right|\left(G_{ij}^{pq} \sin\left(\delta_i^p - \delta_j^q\right) - B_{ij}^{pq} \cos\left(\delta_i^p - \delta_j^q\right)\right) \tag{3.30}$$

It can be observed that Jacobian matrix elements associated with P-Q buses remain unchanged, and only the related P-V elements have been changed. After constructing the Jacobian matrix and current and power mismatch equations, the voltage magnitude and the angle must be then computed and updated for the next iteration (K+1). For P-Q buses, the bus voltage magnitude and angle are updated through the iteration process as follows [98]:

$$\begin{aligned} (V_{k+1}^r)^{abc} &= (V_k^r)^{abc} + \Delta (V_k^r)^{abc} \\ (V_{k+1}^m)^{abc} &= (V_k^m)^{abc} + \Delta (V_k^m)^{abc} \end{aligned} \tag{3.31}$$

$$\begin{aligned} \left|V_{k+1}^{abc}\right| &= \sqrt{((V_{k+1}^r)^{abc})^2 + ((V_{k+1}^m)^{abc})^2} \\ \delta_{k+1}^{abc} &= tan^{-1}\left(\frac{(V_{k+1}^m)^{abc}}{((V_{k+1}^r)^{abc}}\right) \end{aligned} \tag{3.32}$$

For P-V buses, the bus voltage angle δ is updated through the iteration process as follows:

$$\delta_{k+1}^{abc} = \delta_k^{abc} + \Delta\delta_k^{abc} \tag{3.33}$$

After the convergence is achieved, the power injection for each node can be found using (3.12). To calculate the power losses, the branch current must be determined as follows:

$$\begin{aligned} I_{ij}^{abc} &= Y_{ij-br}^{abc} * (V_i^{abc} - V_j^{abc}) \\ I_{ji}^{abc} &= Y_{ji-br}^{abc} * (V_j^{abc} - V_i^{abc}) \end{aligned} \tag{3.34}$$

where Y_{ij-br}^{abc} is the branch admittance matrix including the transformer model and series admittance element y_{ij}^{abc} and shunt admittance $(y_{sh}/2)_{ij}^{abc}$ of the line *i-j*. Then the complex power S_{ij}^{abc} flow from bus *i* to *j* and S_{ji}^{abc} from *j* to *i* are [98]:

$$\begin{aligned} S_{ij}^{abc} &= V_i^{abc}(I_{ij}^{abc})^* \\ S_{ji}^{abc} &= V_j^{abc}(I_{ji}^{abc})^* \end{aligned} \tag{3.35}$$

Thus, the active and reactive power losses of line $i - j$ is the algebraic sum of S_{ij}^{abc} & S_{ji}^{abc}.

$$S_{L-ij}^{abc} = S_{ij}^{abc} + S_{ji}^{abc} \tag{3.36}$$

Equations (3.34) - (3.36) reveal the contribution of mutual impedance effect on power losses and voltage drop. Due to unbalanced line coupling, the change in phase current in one phase can change the voltage magnitude of the other two phases. Moreover, load increase does not necessarily give a reduction in voltage magnitude. Therefore, ignoring mutual impedances offers an inaccurate representation of a power distribution system, creating incorrect and unrealistic outcomes of controlling and analysing active power distribution operations.

The flow chart of the developed TPCIM method is illustrated in Figure 3.3. After setting the buses and branches data, the bus admittance matrix (Y_{bus}) is constructed. Then the mismatch equations are calculated, and if they reach a pre-specified error tolerance (ϵ), the solution has been reached successfully. If not, then the Jacobian matrix equations are calculated, and the bus voltage magnitudes and angles are updated. The same procedure is

repeated for the next iteration until the solution is reached or stopped after reaching a maximum number of iterations [98].

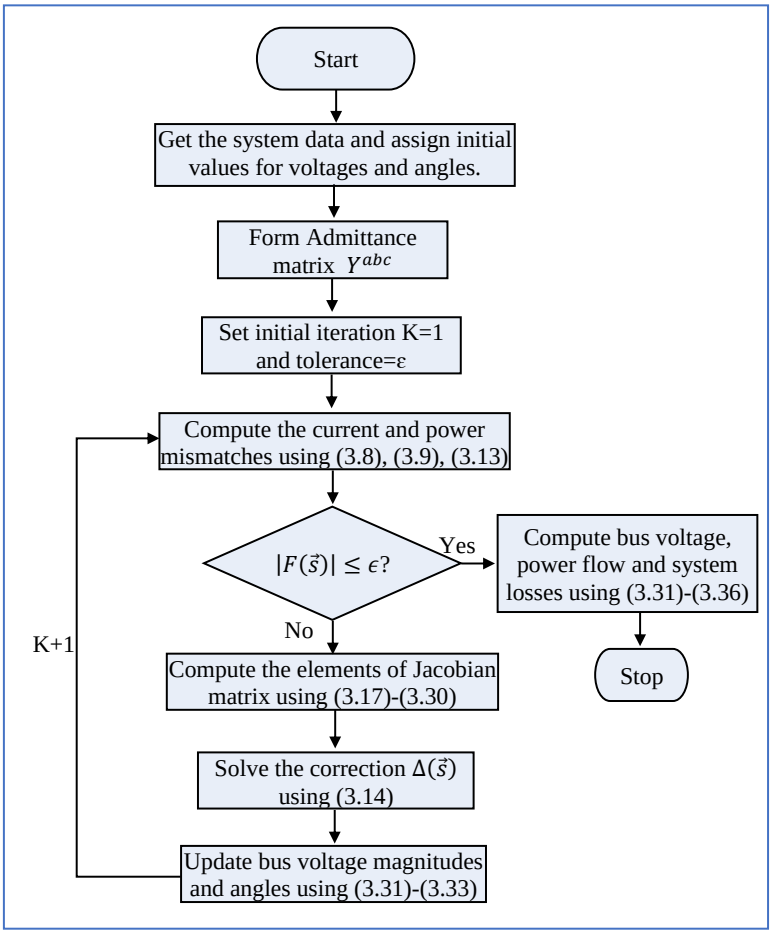

Figure 3.3. Flow chart of the proposed load flow (TPCIM) method [98]

3.4 Unbalanced Power Flow Studies

In order to validate and confirm the performance of the developed TPCIM method, three different studies are carried out on modified IEEE 13-node, IEEE 37-node, and IEEE 132-node test feeders [131]. In the first case study, the IEEE 13-node test feeder is used to validate the proposed unbalanced load flow calculation solution by comparing the result with other well-known Newton Raphson methods. For the second case study, all the test feeders are used to examine the performance of the proposed TPCIM formulation in terms of the number of iterations and execution times. In the final case study, the developed load flow calculation is tested under ill-conditioned unbalanced power distribution systems and

compared against other Newton Raphson methods. All load flow calculations methods are implemented in MATLAB®, and the related convergence tolerance ϵ is set to 1.E-06. The maximum number of iterations is set to 100. All simulations are executed on a computer with an Intel computer i7-6700 at 3.4 GHz CPU and 12GB RAM [98].

3.4.1 Power Flow Result and Validation

Figure 3.4 shows the modified IEEE 13-node test feeder that was used to validate the load flow results. All loads are supposed to be constant power load types in this test feeder and are connected in the Wye configuration. Bus number 1 is chosen as the slack bus, and bus 9 is a P-V bus with predefined reactive power limits. The data related to capacitor banks, loads, and distribution lines can be found in [131] [98].

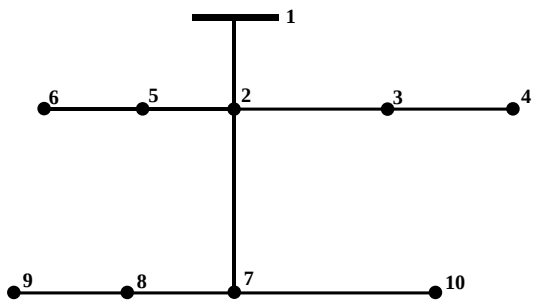

Figure 3.4. The modified IEEE 13-node test feeder

The well-known Three-phase Power Injection Mismatch (TPIM) load flow calculation method [127] is used to validate the proposed unbalanced load flow calculation result. After running the load flow calculation for both methods, the solution coverage at the 4th iteration and 5th iteration for TPCIM and TPIM methods, respectively. Figure 3.5-Figure 3.7 present the comparison of the voltage magnitude in per unit $|V_{pu}|$ for each phase obtained from solving the unbalanced load flow problem by the developed TPCIM and TPIM method. It can be noted that the results of the developed method are identical to the results of the TPIM method, which verified and validated the accuracy of the proposed load flow calculation. The voltage angles are also matching but are not given here for brevity [98].

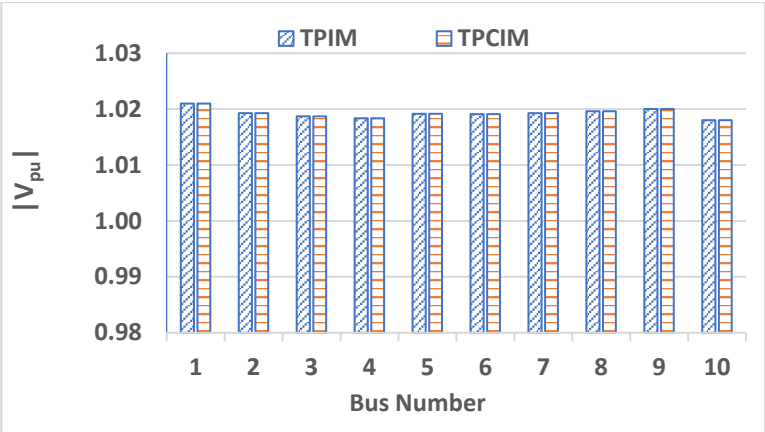

Figure 3.5. Voltage magnitude of phase a

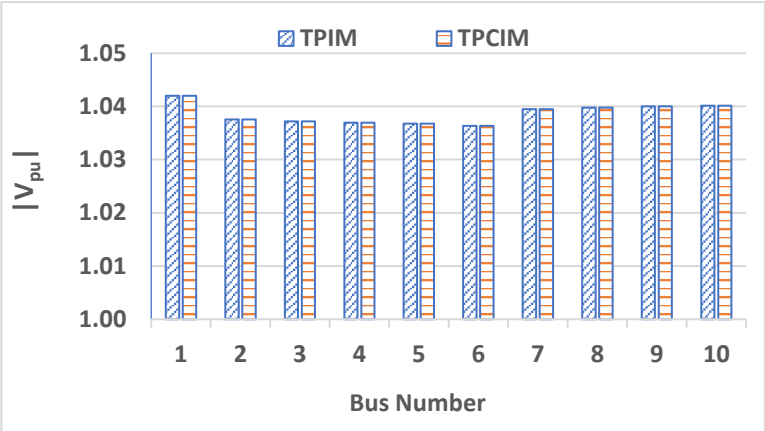

Figure 3.6. Voltage magnitude of phase b

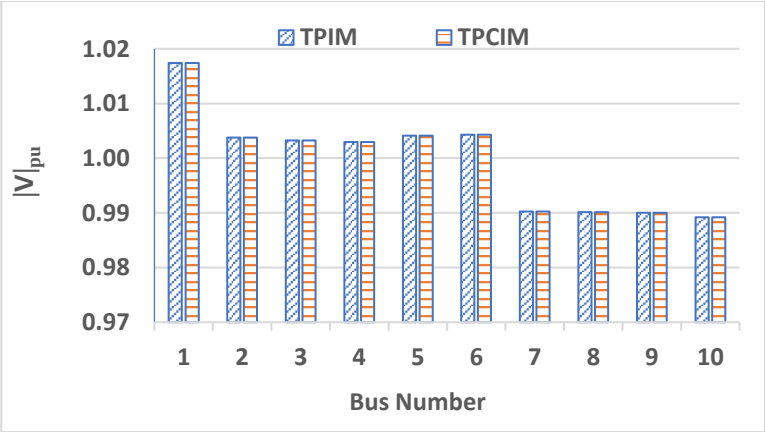

Figure 3.7. Voltage magnitude of phase c

Since voltage unbalance is inherent in the power distribution system and can cause significant implications, various definitions and standards were developed to evaluate the voltage unbalance level and its acceptable limits [20]. One of these definitions is based on

IEEE Std. 141-1993 [49], and it is referred to as phase Voltage Unbalance (VU%) , which should be limited to 2 %. It is determined as the ratio between the maximum deviation of phase voltage magnitude ($V^p, p \in \{a, b, c\}$) from average phase voltage magnitude and average phase voltage magnitude, as given in (3.37). This indicates that the modified IEEE 13-node test feeder experience a maximum of 1.66% VU%, which can be higher if the connection of RETs connection is considered.

$$\mathrm{VU\%} = \frac{\left|\mathrm{Max.}\left\{V^{a,b,c} - \frac{1}{3}\sum_{p=a,b,c} V^p\right\}\right|}{\frac{1}{3}\sum_{p=a,b,c} V^p} \times 100 \tag{3.37}$$

3.4.2 Power Flow Calculation Performance

In this study, three unbalanced distribution networks, IEEE 13-bus, IEEE 37-bus, and IEEE 132-bus test feeders [131], are used in this case study to assess the performance of the developed load flow method compared to the other Newton-Raphson methods. The aim of the comparison is to examine the convergence and execution time rate taking into account different numbers of P-V buses that exist in the test feeders. First, the convergence characteristics and execution time of the developed TPCIM method are compared with the TPIM method [109] and TCIM method [106]. Then, a comparison is made to check the effect of the increased number of P-V buses on convergence and execution time [98].

Since a new representation of P-V bus is developed in this chapter, several P-V buses were randomly added to all test feeders. Table 3.1 shows the convergence characteristics and average computation time per iteration (average of 20 load flow runs) of TPIM, TCIM, and the proposed TPCIM methods. It can be observed that in all test feeders, the developed TPCIM method execute the solution in less or same number of iterations compared with other methods. At the same time, the average execution time per iteration for the proposed TPCIM is by far less than the TPIM method, especially when the number of buses on the test feeder is high. Although both TCIM and TPCIM have relatively the same computing

time per iteration on the IEEE 13-bus test feeder, the computing time difference is increased as the number of buses increases. For example, at the IEEE 37-bus test feeder, the average total computing time is 0.0764s and 0.0552s for TCIM and TPCIM, respectively, given the superior performance of the proposed load flow calculation in terms of computing time. In practice, this helps to achieve an average 31% speedup in the computation time when the test benched against state of the art Newton Raphson power flow. Moreover, as the number of P-V buses and feeders increase, the computation time difference will be high because the required equations for representing the P-V buses are reduced to only one equation compared with the TCIM method. As a result of reducing problem size complexity, the proposed TPCIM offers better convergence characteristics and computing time than any Newton-Raphson methods, making the proposed TPCIM more perforable for an online application that requires high-speed computation [98].

Table 3.1. Convergence characteristics and execution time comparison

Methods	Test Feeder					
	IEEE 13-Node		IEEE 37-Node		IEEE 132-Node	
	No. of iterations	Time per iteration(s)	No. of iterations	Time per iteration(s)	No. of iterations	Time per iteration(s)
TPIM	5	0.0029	4	0.0329	4	0.4055
TCIM	4	0.0019	4	0.0191	3	0.2231
TPCIM	4	0.0018	3	0.0184	3	0.2065

The IEEE 37-node test feeder is used to examine the influence of increasing P-V buses on computing time and convergence. The simulation started with only one P-V bus, and the number of P-V buses is constantly increased to count 40% of the total number of network buses. The load flow results show that all three methods have preserved the same number of iterations while increasing the number of generators buses. On the other hand, the result demonstrated in Figure 3.8 shows that the execution time per iteration for the

proposed TPCIM is always the lowest compared with other methods regardless of the number of P-V connections. Since the TPIM method and the proposed TPCIM method have the exact size of the Jacobian matrix, they have shown an identical pattern of computing time where it keeps decreasing as the number of P-V connections increases. This is because the mismatch equation used to represent the P-V buses of both methods are identical. However, the computing time of the TPIM method is much higher due to transcendental functions (sine and cosine) that are involved in the Jacobian matrix. In contrast, the computing time for the TCIM method is increased as the number of P-V node connections increases due to the increased size of the Jacobian matrix resulting from the additional number of equations used to represent P-V buses. It concludes that the proposed TPCIM method maintains its superior convergence and computing time efficiency while the connection of voltage control devices in the power distribution systems is increasing [98].

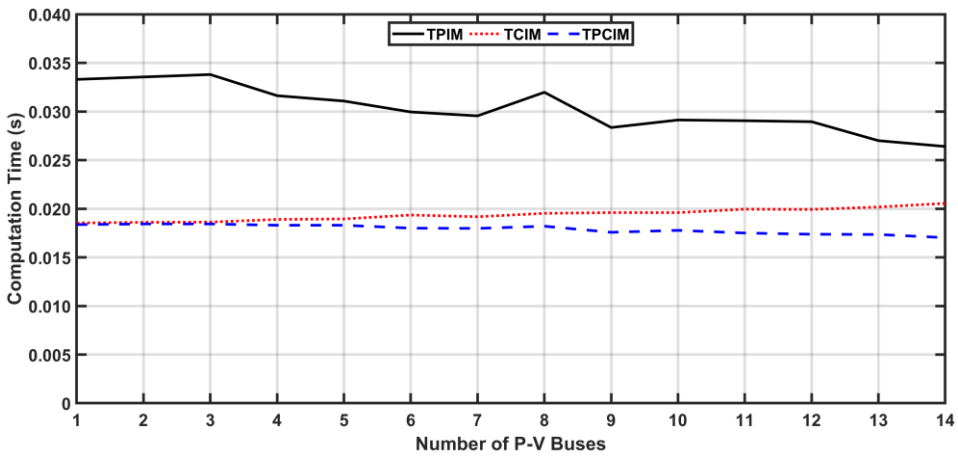

Figure 3.8. Computing time for different numbers of P-V buses

3.4.3 Power Flow Calculation in Ill-Conditioned System

To confirm the robustness of the proposed TPCIM method, the ill-conditioned system (i.e., system experience a divergence in load flow calculation) of IEEE 37-node test feeder is used by steadily increasing the R/X ratio of the feeder and loading conditions. Different R/X ratios are obtained by multiplying each branch resistance by a constant k as $Z = k \times R + jX$. Similarly, various loading conditions are introduced by multiplying each

P-Q bus's power S by h as $S = h \times (P + jQ)$ for each phase. Two scenarios are carried out in this case study. The first scenario considers all buses are P-Q buses, and the second scenario considers 40% of total buses are P-V buses to examine the influence of developed mathematical modelling of P-V buses in an ill-conditioned system. Due to the same convergence characteristics of both TPIM method and TCIM method in an ill-conditioned system, the proposed TPCIM is compared with only TPIM method in this case study [98].

For the purpose of evaluating the load flow methods performance under large R/X ratios, the line resistance increases by 50% until the solution fails to converge. It can be observed from Table 3.2 that the number of iterations remains the same while increasing the R/X ratio in the absence of P-V buses, and the solution has diverged at 650% and 700% for TPIM method and TPCIM method, respectively. Nevertheless, in the presence of P-V buses, the number of iterations is slightly increased as the R/X ratio increases, and the solution is not converged for both methods when the ratio reaches 400% [98].

Table 3.2. Convergence characteristics under different R/X ratios

R/X ratio	only P-Q buses		40% P-V buses	
	TPIM	TPCIM	TPIM	TPCIM
100%	4	3	4	4
150%	4	3	4	4
200%	3	3	4	4
250%	4	3	4	5
300%	4	3	4	5
350%	4	3	5	6
400%	4	3	NC	NC

NC= No Convergence.

Similarly, the IEEE 37-node test feeder was examined by increasing the loading percentage level by 100% at each step until reaching the upper limit where the convergence is not achieved. It can be noted from Table 3.3 that there is a slight increase in the number

of iterations while keep increasing the loading of the network. Although there are slightly fewer iterations to converge with respect to the TPIM method, both methods diverged at 600% of the loading level for both scenarios (i.e., test feeder having only P-Q buses and test feeder having 40% P-V buses). These case studies illustrate that the new representation of P-V buses for the load flow calculation has reduced the computation burden while keeping its superiority convergence properties in well-conditioned and ill-conditioned unbalanced power distribution systems [98].

Table 3.3. Convergence characteristics under different loading conditions

Loading Factor	only P-Q buses		40% P-V buses	
	TPIM	TPCIM	TPIM	TPCIM
100%	4	3	4	4
200%	4	3	4	5
300%	4	3	4	5
400%	5	4	5	7
500%	7	6	6	9
600%	NC	NC	NC	NC

NC= No Convergence.

3.5 Summary

This chapter has introduced a mathematical model to represent the operation of an unbalanced power distribution system. A new representation of generator buses and modelling of some basic power distribution system components are developed for the unbalanced load flow calculation. The new model of P-V buses of the three-phase current injection mismatch (TCIM) method is improved using the power injection mismatch equation. The proposed method is validated, and its convergence characteristics and execution time are compared with other load flow methods. The case studies outcomes show that the mathematical formulation of the proposed unbalanced load flow calculation is robust, and the solution converges in a fewer number of iterations than the TPIM method

and TCIM method, depicting added values for smart grid application. The results also demonstrate a good performance of the proposed TPCIM method, particularly with ill-conditioned systems such as heavily loaded power distribution systems and systems that carry high R/X ratios.

The new developed three-phase load flow is the key essential tool for analysing and real-time operation of the modern power distribution system. Speed and accuracy are the main features of the proposed load flow calculation, which can be used for the application of effective management and control of the power distribution system. It can analyse different network topologies such as radial, weakly meshed, and meshed networks, including high degrees of unbalance. It can also accommodate the various types and phases of load connection and power transformer, including the phase shift introduced by various transformer connections. The unbalanced modelling of the power distribution system proposed in this chapter is the primary tool used to assess the different proposed techniques to address the problem of voltage unbalance throughout this thesis. However, some modern power distribution components need to be included, such as FACTS devices and RETs, which will be discussed in the following chapter.

Chapter 4: Modern Power Distribution Components Modelling

4.1 Introduction

Rooftop PVs and EVs have recently received significant attention because of their major role in decarbonising the electricity and transportation sectors. However, introducing EV charging stations infrastructure and expanding the connection of PVs makes the power distribution system more vulnerable to voltage regulation problems and unbalanced operating conditions. This has increased the demand for FACTS devices such as SVC and STATCOM at some operating conditions due to their fast response. Moreover, to reduce the adverse consequences of high PV penetration, on-grid connection standards of a PV system have been introduced to allow the PV inverters to inject/absorb reactive power to regulate the voltage locally [64]. The modelling of these devices and their role in fast and slow voltage regulation is well established for the power transmission application. However, for unbalanced power distribution system applications, there is a gap in the exploration. Therefore, to assess SVC, STATCOM, and PV inverters contribution to the power quality improvement and make them adequate for online application, it is essential to advance the power flow algorithm taking into consideration the unbalanced operation and achieving high solution convergence speed.

This chapter presents a novel simplified steady-state model of a three-phase SVC and STATCOM for an unbalanced three-phase load flow formulation. The contribution of the developed SVC and STATCOM mathematical model lies in decreasing the complexity of the unbalanced three-phase load flow algorithm and computing time. Moreover, this chapter investigates the influence of unbalanced EVs interconnection on an unbalanced power distribution system taking into account semi-fast charging station, accurate modelling

of EV load, and the autonomous control of PV inverter for reactive power support. The investigation involves studying the impact of different EV connections among the three phases and PV penetration levels on voltage unbalance and network power losses. Another primary goal of this investigation is to evaluate the local voltage regulation on addressing the problem of voltage unbalance and highlight its limitation.

The chapter is structured as follows. Section 4.2 describes the key facts of FACTS devices and their roles in the modern power distribution system. Section 2.5 provides the mathematical formulation of the developed three-phase SVC and STATCOM models into the TPCIM load flow method. The accuracy of the improved SVC and STATCOM models and the computational efficiency based on several case studies are demonstrated in section 4.3. Section 4.4 introduces unbalanced modelling of EVs and PV inverters, and section 4.5 investigates their impact on an unbalanced power distribution system. Finally, section 4.6 brings a summary of the chapter. The study outcomes of this chapter have resulted in the publication of two conference papers [132], [133] during the course of this Ph.D. work, which are being cited appropriately.

4.2 FACTS Devices

In power distribution systems, bus voltages are primarily affected by load deviations and by network structure variation. EV charging stations can be one of the main sources of sharp voltage variation, especially at a fast-charging station. Voltages can drop significantly and even could collapse at some critical operating conditions if fast corrective actions are not in place [19]. On the other hand, overvoltage can occur when the load demand in the system is relatively low, and can be extreme with the presence of excessive PV systems penetration [134]. With the increased exploitation of these technologies, the present voltage regulation devices such as OLTC and switched capacitors cannot necessarily deliver practical timing responses to the instant load and PV generation variation [7].

The development of power electronics-based devices such as FACTS devices recently offered a great opportunity to rapidly control the power flow and regulate the voltage under diverse operation conditions, consequently improving power system stability. The potential of FACTS devices is based on the opportunities to increase or diminish the power flow in specific lines or inject or absorb reactive power at a particular location with responding almost instantaneously. Despite the fact that FACTS devices have been developed principally for power transmission system applications, these devices have also been suggested to power distribution systems as well [103], [135]. Presently, these devices have been successfully utilised in some power distribution systems because of their instant operation, compact structures, multi-function, and minimal maintenance. They are also considered as one of the most effective devices for load compensation in active three-phase power distribution systems integrated with RETs [136].

FACTS devices can be grouped based on their connection at the power system, such as series-connected devices, shunt-connected devices, or combining series and shunt connected devices. Thyristor Controlled Series Compensator (TCSC) is among one of the series-connected FACTS devices used to influence the effective impedance on the line to affect the stability and power flow in a power network. SVC and STATCOM are among the shunt connected FACTS devices that are mainly used for voltage regulation and improve the network power factor by providing a rapid and adequate amount of reactive power support. It is also regarded as the most effective approach to resolve the unbalanced voltage problem and enhance other power quality in modern power distribution systems [137].

The connection of SVC and STATCOM is one of the alternative approaches that meet the purpose of voltage unbalance mitigation, which also needs to be involved in the unbalanced load flow formulation. STATCOM or SVC has been recently used in the power distribution systems to participate in mitigating the challenges associated with the increased

connection of PV systems. However, their present three-phase load flow models involve an increased number of iterations, and their convergence characteristic is subjected to the assigned initial values of control parameters, which can add uncertainties in the convergence. This chapter addresses this problem by proposing a new simplified model that is more robust and demonstrates a significant reduction in the number of iterations, which consequently reduce the computation burden of load flow calculation. Thus, the developed SVC and STATCOM models provide extended opportunities for examining modern power distribution system performances with the presence of increased RETs.

4.2.1 Proposed SVC Modelling

The SVC comprises a set of shunt-connected capacitors and reactor banks with rapid control action through thyristor switching. In the most typically used SVC device, the SVC consist of a thyristor-controlled reactor connected in parallel with a fixed-capacitor (FC-TCR). The firing-angle controls the thyristor to supply or absorb reactive power. From the operational perspective, the SVC can be viewed as a variable shunt reactance that automatically varies according to system operation conditions. It operates as a capacitive or inductive mode to exchange reactive power for the desired voltage regulation [137] [132].

SVC can be modelled as a P-V type bus in the load flow calculation, and either the SVC's firing angle, α_{svc}, or the SVC's equivalent susceptance, B_{svc}, are considered as controlled parameters. Their limits are then examined during the iteration procedures. The three-phase SVC comprises of a delta-connected Thyristor Controlled Reactor (TCR) in parallel with a star connected capacitor bank. For the purpose of power flow formulation, the capacitor bank is transformed to a delta configuration where the firing angle or total susceptance model is applied. The total susceptance model of the three-phase delta connected SVC is shown in Figure 4.1[132].

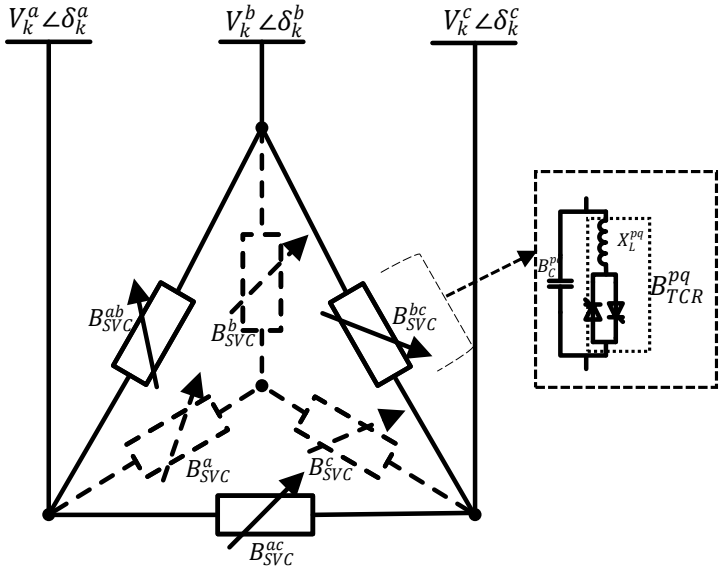

Figure 4.1. Three-phase SVC equivalent circuit [132]

The control variables of the SVC model displayed in Figure 4.1 considering star configuration can be determined at each iteration using (4.1) [132].

$$B_{SVC}^{p} = \left(\frac{Q_{sh}^{p}}{(V_k^p)^2}\right) \tag{4.1}$$

where Q_{sh}^{p} is the amount of reactive power absorbed or injected by the SVC at phase *p*, which can be determined through the iteration process using (4.2). Equation (4.2) is basically the mismatch between the calculated reactive power at the connected bus and the connected loads (Q_{k-load}^{p}) [132].

$$Q_{sh}^{p} = \sum_{j=1}^{n} \sum_{q=a,b,c} |V_k^p||V_j^q| \left(G_{kj}^{pq} \sin(\delta_k^p - \delta_j^q) - B_{kj}^{pq} \cos(\delta_k^p - \delta_j^q)\right) + Q_{k-load}^{p} \tag{4.2}$$

Then, the parameters of the SVC model considering delta connection can be computed using star-delta transformation, as shown in (4.3) [132].

$$B_{SVC}^{pq} = \frac{B_{SVC}^{p} B_{SVC}^{q}}{\sum_{j=a,b,c} B_{SVC}^{j}}, \quad p \neq q \in \{a, b, c\} \tag{4.3}$$

If the parameters of SVC violate its limits during the load flow calculation, then the bus type is changed to the P-Q bus type, and the injected or absorbed reactive power is set

to the corresponding violated limit values. It is also possible to determine the thyristor firing angle α_{svc} using (4.4) [132].

$$B_{SVC}^{pq} = B_C^{pq} - B_{TCR}^{pq}$$

$$B_{SVC}^{pq} = \frac{B_c^p B_c^q}{\sum_{j=a,b,c} B_c^j} - \frac{(2(\pi - \alpha^{pq}) + \sin(2\alpha^{pq}))}{\pi X_L^{pq}}, p \neq q \tag{4.4}$$

4.2.2 Proposed STATCOM Modelling

The STATCOM was developed as advanced technology of SVC where voltage source converter was used instead of thyristor control to give a similar function as the SVC, but with more robustly and superior performances [137]. Based on the operating principle of the STATCOM, Figure 4.2 shows the three-phase equivalent model of STATCOM. The impedance (Z_{sh}) represents the mutual and self-impedance of STATCOM's transformer and converter. The controllable voltage source ($V_{sh}\angle\delta_{sh}$) is used to regulate the voltage at the bus where the STATCOM is connected. However, the voltage magnitude of STATCOM is limited by the upper and lower values, while its phase angle can change from 0 to 2π [132].

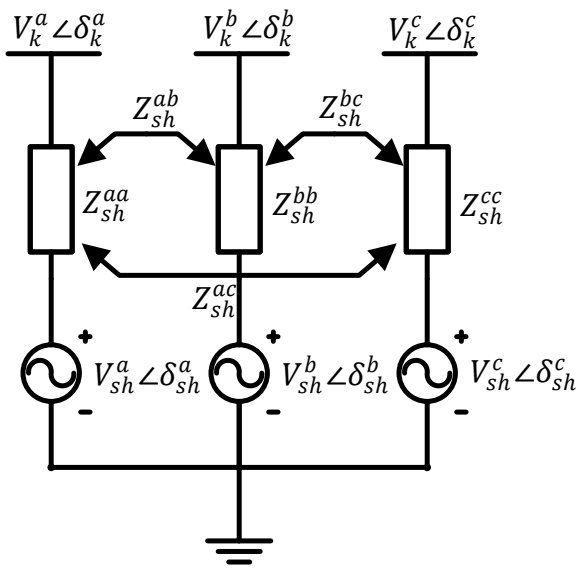

Figure 4.2. Three-phase STATCOM equivalent circuit [132]

Under ideal conditions and steady-state studies, it can be considered that there is no active power interchange between the network and the STATCOM device, and only reactive

power can be injected or absorbed by the STATCOM. Consequently, similar to SVC modelling, the STATCOM connected bus is represented as a P-V type bus with a predefined voltage magnitude and zero active power production when it operates within limits. The parameters of the STATCOM model for each phase given in Figure 4.2 can be obtained using (4.5), which can be applied to check the operation limits of STATCOM at the end of each iteration process of load flow calculation [132].

$$V_{sh}^{p}\angle\delta_{sh}^{p} = (V_{k}^{p}\angle\delta_{k}^{p}) + \sum_{q=a,b,c} Z_{sh}^{pq}\left(\frac{P_{sh}^{q} + jQ_{sh}^{q}}{V_{k}^{q}\angle\delta_{k}^{q}}\right)^{*} \tag{4.5}$$

where p & $q = \{a, b, c\}$ and, since there is no active power production or consumption from STATCOM, $P_{sh}^{p} = 0$ and Q_{sh}^{p} can be computed during the iteration process using (4.2). If the control voltage V_{sh}^{p} of STATCOM violates its bounds ($V_{sh-min}^{p} < V_{sh}^{p} < V_{sh-max}^{p}$), the bus type is switched to P-Q bus, and the supplied or absorbed reactive power is corresponded to the controllable voltage source limit [132]. Thus,

$$\begin{aligned} V_{sh}^{p} &= V_{sh-max}^{p}, \text{ if } \quad V_{sh}^{p} \geq V_{sh-max}^{p} \\ V_{sh}^{p} &= V_{sh-min}^{p}, \text{ if } \quad V_{sh}^{p} \leq V_{sh-min}^{p} \end{aligned} \tag{4.6}$$

4.3 SVC and STATCOM Model Studies

Two case studies are performed in this section to check the developed SVC and STATCOM model performance on unbalanced power distribution systems. The first case study validates the proposed SVC and STATCOM model, and the second case study investigates their convergence characteristics on the developed load flow calculation. A flowchart of the load flow incorporates the SVC and STATCOM modelling shown in Figure 4.3 is used for the studied case. All load flow algorithms were implemented on MATLAB®, and the relative convergence tolerance ϵ was set to 1.E-12. The maximum number of iterations was set to 50. All tests were conducted on an Intel computer i7-6700 at 3.4 GHz CPU and 12GB RAM [132].

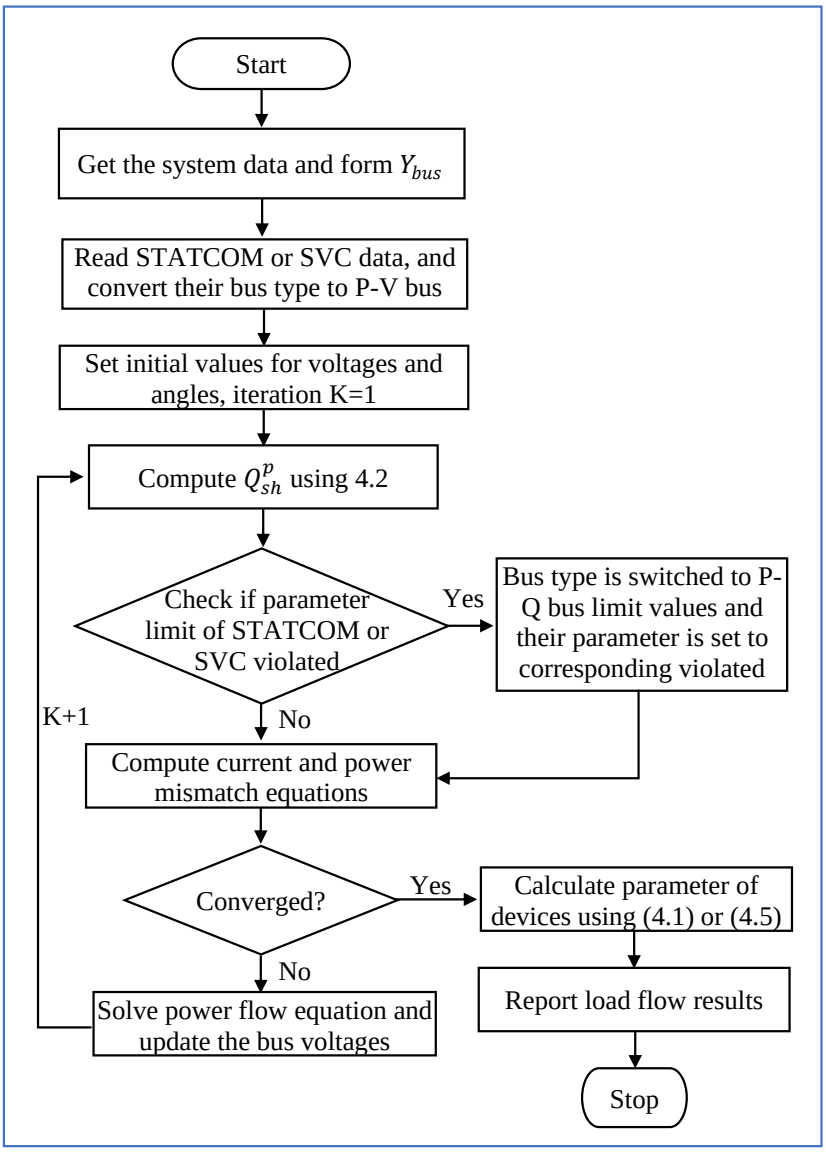

Figure 4.3. Flowchart of the load flow incorporates the SVC and STATCOM modelling

4.3.1 Validation of the Proposed Models

This study aims to validate the result obtained from the proposed three-phase SVC and STATCOM models with other well-established models. A 5-bus network shown in Figure 4.4 was used to validate the three-phase SVC and STATCOM models and compare them with the models used in [109], [138]. For the purpose of this study, an imbalance in operating conditions was introduced into the test network by changing the load at each phase as illustrated in [109]. All the loads, generators and transmission line data of the 5-bus test network can be found in [109], and they are presented in appendix B [132].

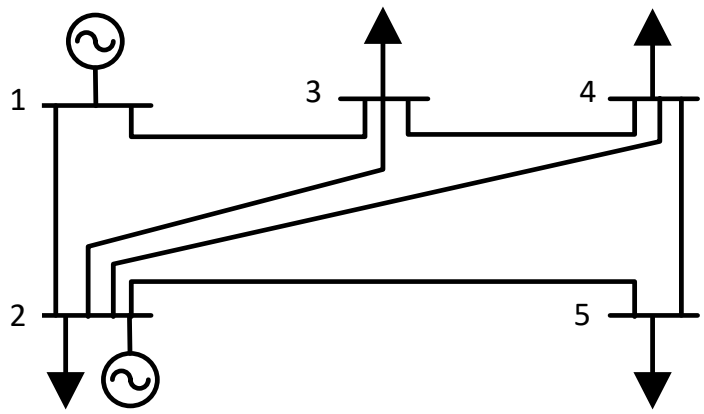

Figure 4.4. The five-bus test network [109]

First, the unbalanced three-phase load flow was carried out with no SVC or STATCOM connection in the network. In the developed load flow calculation (TPCIM), the convergence was achieved in four iterations, whereas in the TPIM method was achieved in five iterations. The voltage at each bus and the total power losses are presented in Table 4.1. Then, the three-phase load flow calculation is carried out by incorporating the proposed SVC and STATCOM models separately to regulate the voltage at bus 5 to be 0.98 pu for each phase. In this case, the total susceptance model is used for SVC, and the upper and lower susceptance values are considered as -0.25 pu and 0.25 pu, respectively, for each phase. The source impedances of STATCOM are $X_{sh} = 0.1$ pu for each phase, and the upper and lower voltage source values are 0.95 pu and 1.05 pu, respectively.

The power flow result and the voltage control devices variables are provided in Table 4.2, which are matching to the results found in [109]. This validates and illustrates the accuracy result of the proposed SVC and STATCOM models. It should be mentioned that the connection of SVC and STATCOM can deteriorate the voltage unbalance (i.e., at bus 4, Table 4.2) if balanced voltage is assigned at the connected bus due to the inter-phase coupling between the lines. However, their connection is not limited to regulate the voltage only but also to reduce the network power losses, as demonstrated in Table 4.1 and Table 4.2 [132].

Table 4.1. Unbalanced load flow results for base case [132]

Bus No.	Phase Voltage Magnitude (pu) and Angle (deg.)		
	a	**b**	**c**
1	$1.060\angle 0.00^{\circ}$	$1.060\angle -120.00^{\circ}$	$1.060\angle 120.00^{\circ}$
2	$1.000\angle -2.02^{\circ}$	$1.000\angle -121.84^{\circ}$	$1.000\angle 117.58^{\circ}$
3	$0.982\angle -4.67^{\circ}$	$0.988\angle -124.74^{\circ}$	$0.991\angle 115.38^{\circ}$
4	$0.981\angle -4.84^{\circ}$	$0.983\angle -125.05^{\circ}$	$0.987\angle 114.88^{\circ}$
5	$0.979\angle -5.96^{\circ}$	$0.975\angle -124.74^{\circ}$	$0.960\angle 113.23^{\circ}$
Total Real Power Losses =18.72 MW			

Table 4.2. Unbalanced load flow results after incorporating SVC and STATCOM [132]

Bus No.	Phase Voltage Magnitude (pu) and Angle (deg.)		
	a	**b**	**c**
1	$1.060\angle 0.00^{\circ}$	$1.060\angle -120.00^{\circ}$	$1.060\angle 120.00^{\circ}$
2	$1.000\angle -2.04^{\circ}$	$1.000\angle -121.84^{\circ}$	$1.000\angle 117.61^{\circ}$
3	$0.982\angle -4.64^{\circ}$	$0.989\angle -124.83^{\circ}$	$0.995\angle 115.37^{\circ}$
4	$0.981\angle -4.79^{\circ}$	$0.984\angle -125.16^{\circ}$	$0.992\angle 114.86^{\circ}$
5	$0.980\angle -5.76^{\circ}$	$0.980\angle -125.19^{\circ}$	$0.980\angle 113.09^{\circ}$
$\mathbf{B_{SVC}}$	0.0500 pu	0.0882 pu	0.1588 pu
$\mathbf{E_{sh}}$	$0.985\angle -5.76^{\circ}$	$0.989\angle -125.19^{\circ}$	$0.995\angle 113.09^{\circ}$
Total Real Power Losses =18.54 MW			

4.3.2 Performance of the Proposed Models

IEEE 13-node, IEEE 37-node, and IEEE 132-node test feeders are used to compare the convergence characteristics of the proposed SVC and STATCOM models with other developed models. The comparative SVC and STATCOM models used in the case study are described in [138] and [109], respectively, and are also simulated in MATLAB. The voltage control devices are connected randomly into the test network to regulate the connected buses voltage to 1.0 pu for each phase. Table 4.3 shows the comparison of convergence characteristics under different test feeders. It can be noted that the proposed model has better

convergence characteristics than comparative SVC and STATCOM models. Using the conventional SVC and STATCOM models has increased the number of calculation iteration. For example, the number of iterations required to converge the load flow calculation for IEEE 132-node test feeders with a comparative STATCOM model is three times higher than with the developed model. It can also be observed that the number of iterations in the developed model stays the same when including the SVC and STATCOM [132].

As the convergence of the comparative method is affected by the initial values of the control variables, the number of iterations is increased as the initial values are changed. For instance, the number of iterations for the comparative SVC model on the IEEE 37-node test feeder is increased from 6 to 9 when the initial value of B_{svc} is changed from 0.2 pu to 0.05 pu. This gives the developed model superiority with respect to the convergence characteristics, computing time, and accuracy, allowing the proposed models of SVC and STATCOM to be more applicable for online applications. This case study also suggests that these devices can be utilised to reduce the diversity of voltage unbalances. The unbalanced control of these devices can further improve the overall voltage unbalance in the network and reduce the power losses while applying an optimisation model for centralised-based voltage management. For instance, the voltage unbalance is reduced from 2.7% to 1.5% when regulating the voltage at the connecting bus to balanced 1.0 pu, whereas assigning appropriate unbalanced voltage magnitude (i.e., V_a=1.02 pu, V_b=1.005 pu, V_c=1.01 pu), the voltage unbalance is limited to 1% [132].

Table 4.3. Comparison of convergence characteristics [132]

IEEE System	**Comparative Models**		**Proposed Models**	
	STATCOM Model	**SVC Model**	**STATCOM Model**	**SVC Model**
IEEE 13	9	8	5	5
IEEE 37	6	8	5	5
IEEE 132	12	6	4	4

4.4 Modelling of Renewable Energy Technologies (RETs)

PV systems, especially rooftop-mounted, have gained popularity among different renewable energy sources and have been progressively connected to power distribution systems. Various PV inverter control schemes have been proposed to allow more PV energy system hosting capacity and improve network power quality. The growing number of EVs and their technologies have led to an increase in charging facilities. Nowadays, different charging stations are distributed across the countries, and they are mostly connected to the power distribution system. Both EVs and PVs are becoming the most significant components that contribute to improve or worsen the power quality at the power distribution system, depending on the control scheme adopted in these devices [13], [32]–[35]. Therefore, it is essential to model these devices and study their impact accurately.

4.4.1 PV Inverters

Depending on the available open-scale areas, customer type, and the number of phases, the size of the PV system can vary from several kW for residential purposes to hundreds of kW for a sizeable commercial purpose [36]. Substantial shares of the connected PV systems are rooftop mounted that are electrically coupled to the low voltage power distribution systems [139]. They can be a single-phase unit connected randomly across the three-phase system or a three-phase unit subjected to the required demand and accessibility of a three-phase feeder. Because of the uncertain nature of PV systems, the injected power cannot be precisely predicted, and therefore their contributions to the grid are independent of load demand. On the contrary, traditional distributed generation can adjust their generated power according to the load demand [8].

Reactive power and active power control can be integrated into PV inverters. Due to the high R/X ratio in power distribution systems, controlling active power has shown better

voltage regulation. Nevertheless, active power control is probably an undesirable control due to active power curtailment. Consequently, the reactive power control option of the PV inverter became more popular and is considered in this study because of its capability of mitigating both voltage magnitude variation and unbalanced voltage problems [9]. However, the exchange rate of reactive power (power factor range) is restricted by the rating of the PV inverter. For the inverter to exchange sufficient reactive power support despite the active power production capacity, oversizing of PV inverter is essential. Thus, in this study, the inverter is oversized by 25% of the rated active power production of the PV system, allowing the PV inverter to operate in the range of 0.8 leading and 0.8 lagging power factor regardless of active power generation [140] [133]. More details of PV inverter size and reactive power capability are presented in the next chapter (section 5.3.1) [133].

In load flow formulation, the PV inverter could be treated as a voltage-controlled bus or load bus. For large-scale controllable distribution generators, the voltage-controlled model is commonly adopted. On the other hand, at the domestic size, the PV inverter is treated as a P-Q bus with specified active power (P) and reactive power (Q). The generated active power of the inverter is subjected to sunlight exposure, and hence fluctuates. In contrast, reactive power depends on the measured voltage magnitude at the connecting bus and the availability of active power. Therefore, the connected PV inverter bus is modelled as a P-Q bus in this study. The active power output (P_{pv}^{abc}) of the PV system is predefined, and the reactive power (Q_{pv}^{abc}) can be obtained using (4.7). The power factor (PF^{abc}) values are determined based on the voltage at the connected PV. This means that the reactive power support of a PV inverter is governed by the assigned power factor, which represent a linear droop control, as proposed in [43]. Three parameters can define the linear droop characteristic; minimum voltage (V_{min}), deadband width (D), and maximum voltage (V_{max}), and are set to 1.07 pu, 0.02 pu, and 0.93 pu, respectively, as shown in Figure 4.5 [133].

$$Q_{pv}^{abc} = \frac{P_{pv}^{abc}}{PF^{abc}} \times \sqrt{1 - (PF^{abc})^2} \tag{4.7}$$

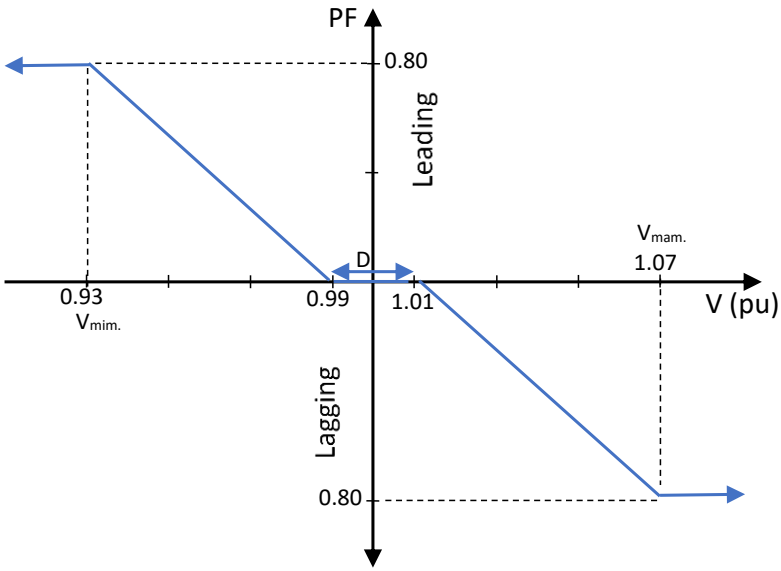

Figure 4.5. The linear droop control characteristic of the PV inverter

4.4.2 EV and Charging Station

As a result of rapid EV growth, there will be a demand for more charging facilities, which are generally interconnected to the power distribution system. According to [8] , the charging speed can be categorised into three groups, namely “slow” charging units (up to 3 kW), “semi-fast” chargers (7-20 kW), and “fast” charging units (+ 20 kW) [8]. A large share of EVs are currently charged residentially with a slow charging speed [141]. Nevertheless, it is anticipated that the number of dedicated charging stations will grow considerably, and all the public car parking and workplace will be equipped with charging facilities as a way of attracting customers [142]. Among these charging stations, the car parking-based charging stations are expected to contribute to the large scale of the overall charging station, which is usually equipped semi-fast charging facilities [141]. Nevertheless, EV integration is an added heavy load demand for the low-voltage power distribution system. The different types of charging events can take place any time during the day. However, for residential types, EVs are charged mostly throughout the night where the demand is relatively low, and

their impact on the power distribution system might be neglectable. On the other hand, semi-fast (up to 20 kW) and fast (up to 250 kW) charging speed is usually demanded at peak time [2]. Therefore, their connection could bring some benefits for the electricity grid, for example, phase balancing and peak power shaving [143]. Still, they can post significant challenges such as introducing power losses and voltage violations due to the inherent intermittency of EVs charging demand [133].

The battery charging demand and detailed characteristics of an EV determine the influence on the power distribution system. Their load characteristics vary from other traditional system loads, and therefore need to be carefully modelled to study and analyse EV integration's real impact. Constant power load models and ZIP load models are commonly used in the literature to represent EV characteristics. However, a more precise EV load representation is to model EV load characteristics as a merger of two components, a constant power component and a voltage-dependent component which depends on the charger, as expressed in (4.8)[8]. The EVs load is assumed operated at unity power factor such as [143], [144], and therefore no reactive power is exchanged by the EV [133]. However, the reactive power can be calculated using the relation (4.9), and the value of the power factor can be taken as 0.97. A single-phase charger that fed by a three-phase feeder is considered for this study which has two stages. Front end AC–DC rectifier with power factor correction that provides constant DC-link voltage at unity power factor and DC–DC buck converter at the battery end [145].

$$P_{EV} = P(\alpha + \beta V^{a}) \tag{4.8}$$

$$Q_{EV} = P_{EV} \tan(\theta) \tag{4.9}$$

where α, β and a are the parameters of the load model, and are 0.9279, 0.0721, and −3.101, respectively, and P and V are the specified voltage and real power input of charger, respectively [143]. As pointed out previously, semi-fast charging is expected to represent

the high portion of the overall charging stations [40]. Consequently, the input power (P) of the chargers at these stations are selected to be 7.4 kW. The EVs connection at the charging station is represented as a P-Q bus in the load flow calculation, and their values are updated at each iteration using (4.8). Moreover, the elements A_i^p, B_i^p, C_i^P , and D_i^P of the Jacobian matrix presented in equations (3.16)-(3.19), which are used for the constant loads model, are replaced with the following equations [133].

$$A_i^p = -\frac{(V_i^m)^p (V_i^r)^p (\beta P_i^p a (V_i^a)^p - 2\alpha P_i^p - 2\beta P_i^p (V_i^a)^p)}{(((V_i^r)^p)^2 + ((V_i^m)^p)^2)^2} \tag{4.10}$$

$$B_i^p = \frac{((V_i^m)^p)^2 (\alpha P_i^p + \beta P_i^p (V_i^a)^p - \beta P_i^p a (V_i^a)^p) - ((V_i^r)^p)^2 (\alpha P_i^p + \beta P_i^p (V_i^a)^p)}{(((V_i^r)^p)^2 + ((V_i^m)^p)^2)^2} \tag{4.11}$$

$$C_i^p = \frac{((V_i^r)^p)^2 (\alpha P_i^p + \beta P_i^p (V_i^a)^p - \beta P_i^p a (V_i^a)^p) - ((V_i^m)^p)^2 (\alpha P_i^p + \beta P_i^p (V_i^a)^p)}{(((V_i^r)^p)^2 + ((V_i^m)^p)^2)^2} \tag{4.12}$$

$$D_i^p = A_i^p \tag{4.13}$$

4.5 Impact of PVs and EVs Studies

The proposed unbalanced load flow (TPCIM) calculation is applied to evaluate the impact of EV connections and the autonomous control of PV inverters on a power distribution system. The simulated test network employed in this case study is presented in Figure 4.6, which is the modified IEEE 37-node test feeder [131]. In the provided test feeder, the loads are unsymmetrically connected among the phases and are assumed to be constant load types. Star configurations are considered in this study for all three-phase loads. For the purpose of case studies, each load bus forms a group of residential loads, fed either by only a single-phase or multi-phase feeder. The information associated with the peak loads demand and the distribution lines is available in [131]. Bus number 1 was chosen as the slack bus, which connects the substation transformer's outgoing feeder [133].

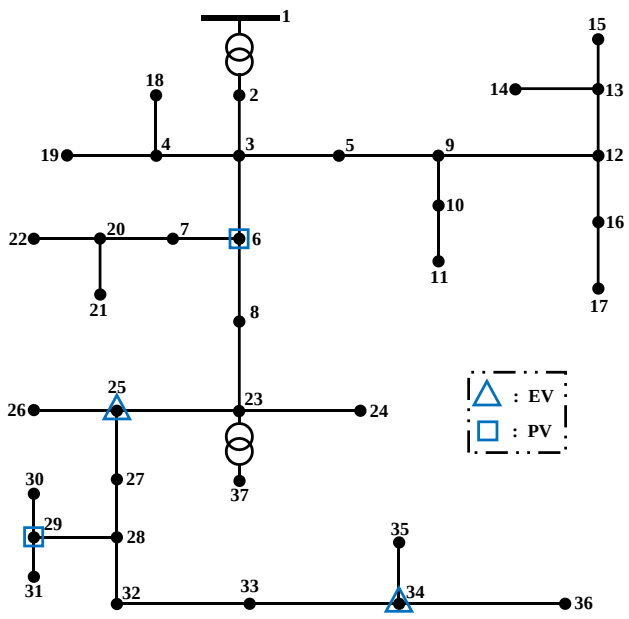

Figure 4.6. The modified IEEE 37-bus test feeder [133]

Two units of three-phase PV systems were connected to bus 6 and 29 of the test feeder, which are marked by square. Two EV charging stations that emulate real parking were also considered in this study, and were connected to bus 25 (charging station 1) and bus 34 (charging station 2). Both were assumed to be commercial parking lots that provided a semi-fast charging facility to EVs with a rating of 7.4 kW. Each parking lot was supplied by a three-phase feeder where the EV represents a single-phase load connected in one of the three phases. The maximum number of connected EVs into parking station lots 1 and parking station lots 2 were 15 and 20, respectively. Figure 4.7 displays the total EVs connected at two different parking lots during a day, which are identical to the typical EVs parking lot profiles used in [146]. The real data of PV power production on a sunny day and an actual load demand profile of a typical three-phase feeder for 24-hours during a day with a time step of 10 minutes are presented in Figure 4.8. These data were documented by HCT GreenNest Eco House [147]. The provided demand profile curve was merged into all load nodes in the test network, considering various rated loads and phase numbers. Although the measured power reflects the active power demand, it can be employed to represent the reactive power demand [133].

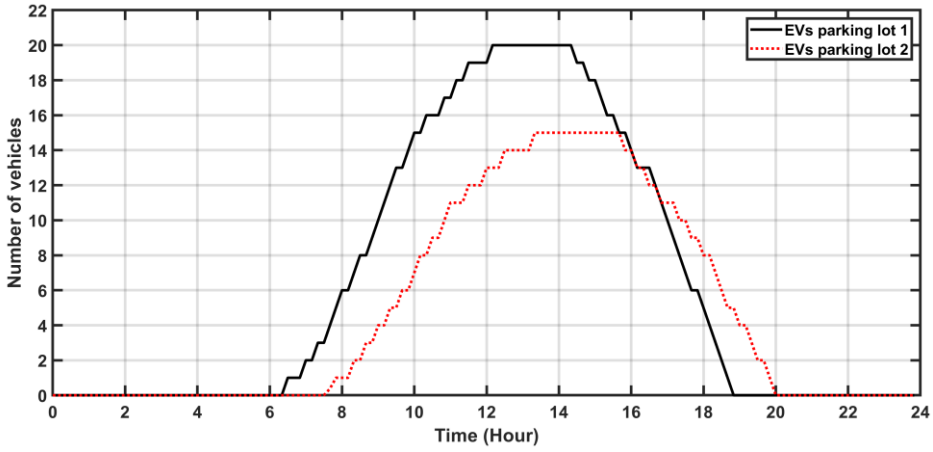

Figure 4.7. The number of EVs in parking lots [133]

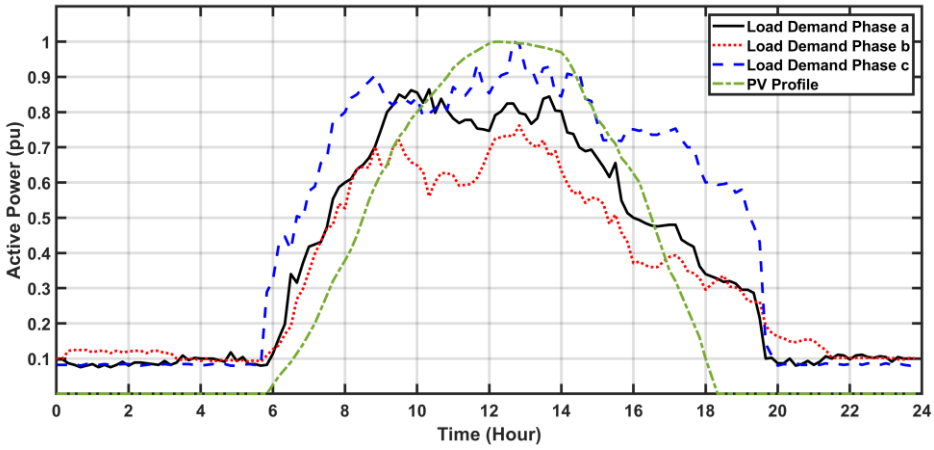

Figure 4.8. Three-phase load and PV output power profile [133]

One of the assumptions considered in case studies is that the feeder's size and transformers rating of the simulated network is intended to handle excessive PV and EV connections. Several criteria were adopted in different studies to describe the level of PV penetration [148]. The criterion used in this study is the percentage of the total peak injected active power ($P_{PV-Peak}$) of PV connected systems to the total peak demand of the apparent power (S_{L-Peak}) in the whole feeder [149]. Since the 24-hours load and PV profile are applied here, the PL % termed to the highest penetration level reported throughout the day, which is determined by (4.14) [133].

$$PL\ \% = \frac{P_{PV-Peak}}{S_{L-Peak}} \times 100 \tag{4.14}$$

A repeated unbalanced three-phase power flow calculation with a time step of 10-minutes for 24-hour is performed in MATLAB®. Two prominent cases were studied on the

IEEE 37-bus test feeder, where the first case study is to examine the influence of EVs connection on voltage unbalances. The second case study investigates the effects of the local voltage control of PV inverters on mitigating the voltage unbalance and the associated power losses under different load profiles and penetration levels of PV systems. Due to the intermittency of EV charging behaviours, a different pattern of EV connections among the three phases is generated every hour during the day, which is shown in Figure 4.9. These connection patterns resemble the ideal scenario (all are connected equally among the phases) and worst-case scenario (unbalanced connected) of EVs connection [133].

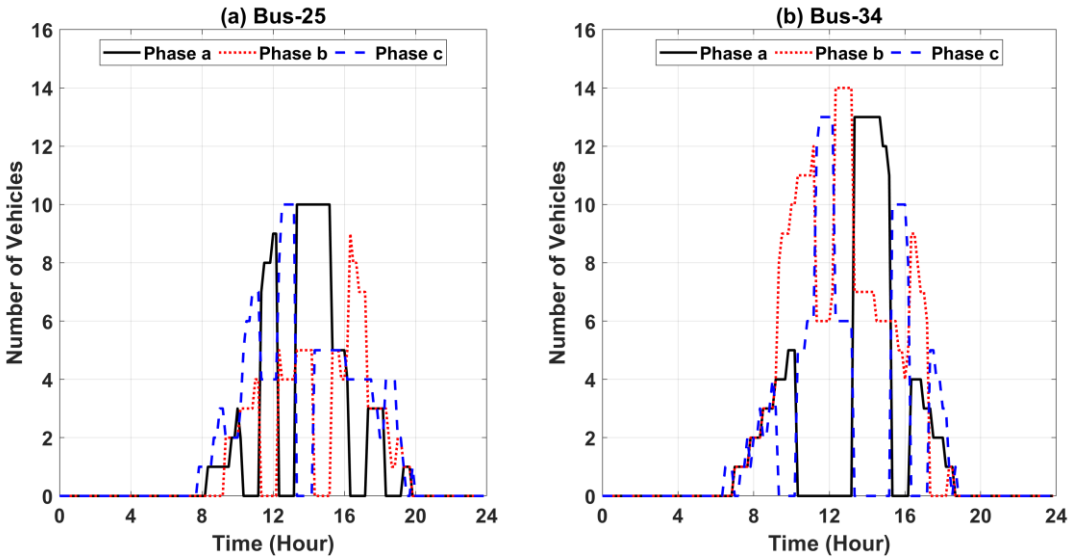

Figure 4.9. The generated random connection of EVs [133]

To study the influence of EVs connection on voltage unbalance, the unbalanced load flow calculation is carried out before and after EVs connection. In this case study, the network was tested under 20% of the PV penetration level while assuming the PV inverter is operating at a unity power factor. Due to the unbalanced load distributed in the test network, it can be noted from Figure 4.10 that the maximum recorded voltage unbalances at some buses was very significant and crossed the boundary of 2%, approaching 2.8% for a few hours during the day. It exhibits that the level of unbalance begins rising at the receiving end of the feeder, specifically the feeder starting from bus 23. After EVs connection,

considering the connection profile presented in Figure 4.9, the highest voltage unbalance level recorded at each bus increases significantly and reaches up to 3.4% at bus 36 [133].

Figure 4.11 also shows the highest voltage unbalance level recorded during the day prior to and after EVs connection, which illustrates the effect of random connection of EV on voltage unbalance. The voltage unbalance during the day can increase or decrease depending on the EV connections. For example, between 9:30 and 10:30, the voltage unbalance is reduced because the majority of EVs are connected at phase 'b' at the parking lots located at bus 34, as shown in Figure 4.9. The loading at phase 'b' was relatively low and high at phase 'a' and 'c', and by increasing the loading at phase 'b' the voltage unbalance can be minimised. On the other hand, connecting more vehicles at phase 'c' increased the unbalanced voltage level, especially at 12:00. Power losses are another major issue arising from EVs connection. The connection of EVs has increased the total energy losses during the day from 300 kWh to 376 kWh. It is important to mention that the voltage-dependent loads model of EVs shows slightly higher voltage unbalance levels and power losses than the constant load model of EV. However, this difference, especially on power losses, can be significant if a fast-charging speed is employed due to the high-power consumption and high voltage magnitude. Therefore, accurate representation of the EVs load model can be crucial in analysing and controlling the operation of the power distribution system [133].

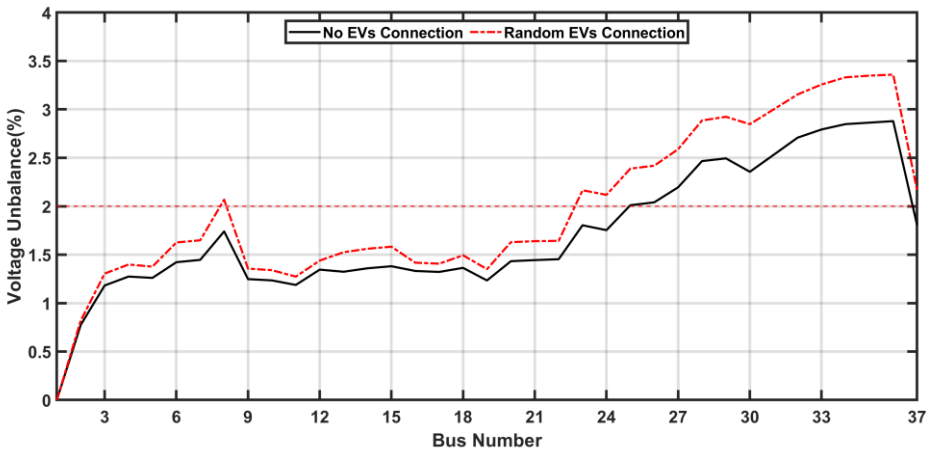

Figure 4.10. Comparison of maximum voltage unbalance recorded at each bus [133]

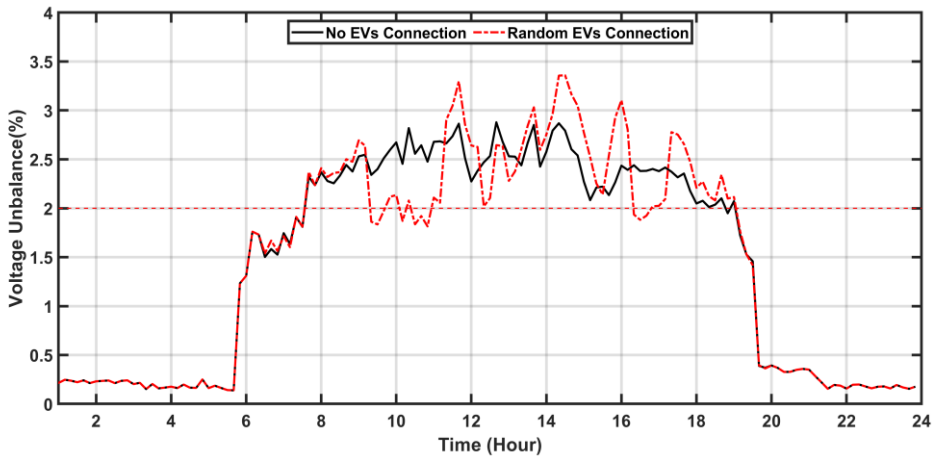

Figure 4.11. Comparison of maximum voltage unbalance recorded during the day [133]

To examine the consequence impact of local PV inverter control on voltage unbalance and power losses, the network is simulated under two scenarios; *(i)* the PV inverters are operating at unity power factor where there is no reactive power provision to regulate the voltage, *(ii)* the PV inverters are operating to manage the voltage magnitude by changing its power factor based on the linear relation with the voltage magnitude. In the beginning, the simulation is initiated at a low level of PVs penetration (20%), and the penetration of the integrated PV systems is increased to reach 120% [133].

Figure 4.12 (a) displays the highest voltage unbalance reported over the day at various penetration levels. Although the injection of PVs active power among the phase is equal, the voltage unbalance decreases as the penetration level of PVs increases. This is because of the mutual impedance of the distribution line, resulting in a different voltage drop at each phase, which can reduce the voltage unbalance. Injection of reactive power from PV inverters has reduced the voltage unbalance slightly at low penetration levels and significantly at high penetration levels. Nevertheless, the voltage unbalance still exceeds the allowable limits (2%) due to the fact that the reactive power control of the PV inverters was mainly designed to regulate the voltage magnitude and has less impact on voltage unbalance. For this reason, the voltage magnitude at each node and under various PVs penetration levels was maintained with the standard limit [133].

On the other hand, the total energy losses decreased slightly for both scenarios as the PV penetration level increased, and then at a high penetration level, the power losses increased significantly. It can be seen from Figure 4.12 (b) that the power losses keep increasing after adopting the voltage regulation capability of the PV inverter at a high penetration level (60% >). For example, at 80% penetration level, the total energy losses rise by 98% due to excessive reactive power absorption to regulate the voltage at PV connected buses. It concludes that the lack of coordination between various voltage regulation devices and EV connections can sometimes improve the voltage unbalance, but the energy losses increase [133].

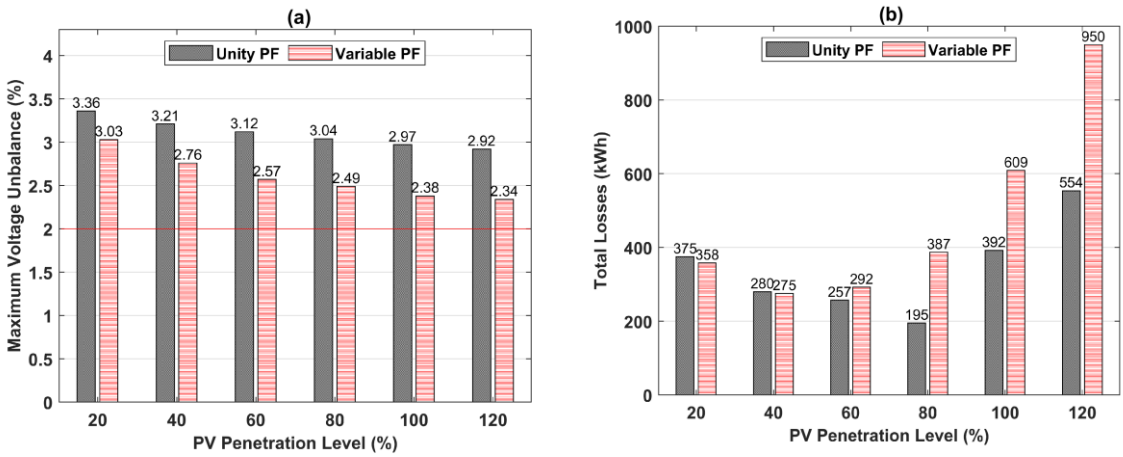

Figure 4.12. Comparison of (a) peak voltage unbalance and (b) total energy losses [133]

The results presented throughout the case studies underline the fact that voltage unbalance is significantly high in power distribution systems. EVs connection can further increase the voltage unbalance even if they are equally connected among the three phases. The impact of voltage unbalance on power losses can be identified by load flow calculation. Nevertheless, its implications on equipment derating and ageing cannot be easily quantified and are excluded in this study. Besides that, a slight imbalance in the phase voltages can produce a considerable imbalance in the phase currents, which could pose significant implications on various power system equipment. The neutral current also cannot be

accurately estimated in the study because the neutral transformation matrices were not given (used to calculate the neutral current) from the simulated test system [133].

Nevertheless, as the unbalanced voltage percentage goes beyond 2%, there will be a possibility of derating and reducing the lifespan of all connected three-phase power equipment. For instance, if the unbalanced voltage goes beyond 2%, the three-phase induction motor can become overheated when operating near full rating [49]. Furthermore, the higher flow of current in neutral wires may also heighten the overall power losses on three-phase power equipment, which was excluded in the case studies because of the lacking information on the connected network components. Consequently, maintaining the voltage unbalance at the minimum can reduce the overall energy losses [133].

The detection of voltage unbalance is the first and crucial step in developing a practical solution to alleviate the unbalanced problem that cannot be achieved by autonomous-based control. Furthermore, minimising the voltage unbalance using a local control scheme can sometimes increase the power losses, which can be significant under a high PV penetration level. Besides that, an unbalanced connection of EVs among the three phases can sometimes reduce the severity of voltage unbalance, which can be achieved by adopting the optimisation model. Thus, implementing centralised-based control solutions could become the way forward in the infrastructure design of active power distribution systems, providing an adequate monitoring platform and efficient operation [133].

4.6 Summary

This chapter has presented robust SVC and STATCOM models for unbalanced power flow calculation. The proposed model of SVC and STATCOM enables a reduction of the computational time and an improvement in the calculation convergence, offering additional values for monitoring and control of power distribution systems that require rapid decision making. The connection of SVC and STATCOM is one of the alternative

approaches that fit the purpose of voltage unbalance improvement and provides extended opportunities for assessing modern power distribution system performances with the presence of expanded RETs. Illustrative studies with the developed models indicate that SVC and STATCOM can be exploited to improve the voltage profiles and reduce the voltage unbalance, depending on the targeted phase voltage magnitude, which can be determined by solving an optimisation problem.

With a growing number of RET connections, new challenges are confronting the operation of power distribution systems. This chapter has also presented a methodology to assess the effects of EVs connection and the local voltage control of PV inverters under unbalanced power distribution system conditions. It involves modelling of PV inverters and EVs load on unbalanced load flow calculation. Several case studies using typical data illustrate the significant impact of EV connections on voltage unbalance and power losses. The study outcome further justified the limitation of the autonomous control scheme of PV inverters on voltage unbalance and energy losses reduction and highlighted the importance of a central-based control.

Finally, this chapter has shown the potential of reactive power management of the PV inverters in reducing the severity of voltage unbalance. However, they still failed to maintain the unbalanced voltage level below the standard limits, requesting a new control strategy. The next chapter proposes advanced reactive power control for the PV inverters to address this limitation.

Chapter 5: Unbalanced Voltage Regulation Using PV Inverters

5.1 Introduction

The increased connection of rooftop PV system in a low-voltage power distribution system causes additional difficulties in regulating the voltage at buses because of the severity of voltage rise and voltage unbalance issues. As a result, these factors have become a major obstacle to the further integration of PVs. Traditional voltage regulation approaches are ineffective in tackling these challenges due to their limitation to deal with the unbalanced voltage conditions and the intermittent PV power generation. For these reasons, the distribution system operators in some countries have recently amended grid codes and regulations to include PV systems as active elements to provide ancillary services by controlling their power exchanged with the grid. PV inverters can provide reactive power support when operated at a capacity less than the rated value, and therefore can contribute to the voltage regulation. However, voltage regulation using reactive power control in the unbalanced power distribution system is a challenging problem and was only adopted to mitigate the voltage rise effects. As mentioned in chapter 4, the present reactive power control of the PV inverter approach has failed to alleviate the problem of voltage unbalance. Consequently, with the enormous integration of PV systems in unbalanced power distribution systems, it is vital to deploy a new control strategy for voltage unbalance compensation and leverage the reactive power capability of PV inverters.

This chapter proposes an innovative reactive power control approach for rooftop PV inverters as an effective method to address the voltage unbalance problem in a power distribution system. The significance of the developed approach is that it avoids the violating of voltage magnitude and voltage unbalance limit simultaneously at affected network buses

by exchanging a specified amount of reactive power provided by the PV inverters. The proposed control scheme can also significantly relieve the operational strain of the PV inverters, promoting a power distribution system with increased reliability and integration of renewable energy.

The chapter is structured as follows. Section 5.2 describes the potential of PV systems in voltage regulation in modern power distribution systems. Section 5.3 presents the proposed voltage regulation approach for the PV inverter. Section 5.4 describes the PV inverter model used for load flow calculation. The effectiveness and the performance of the proposed reactive power control based on several case studies are demonstrated in section 5.5. Section 5.5 also discusses the potential of the proposed voltage control and its limitation. Finally, section 5.6 brings a summary of the chapter. The study outcomes of this chapter have resulted in the publication of a journal paper [140] during the course of this Ph.D. work, which is being cited appropriately.

5.2 PV Inverters for Voltage Regulation

Integrating a PV system into a power distribution system can change the direction of power flow, leading to fluctuating voltage at nodes and rising beyond the standard limits. To assess the causes of voltage rise and voltage unbalance, and to develop an adequate approach to restrain such problems, a simplified two-bus low voltage power distribution system with a PV system connection is given in Figure 5.1. V_o^{abc} is the three-phase voltage at the low voltage side of the transformer, and V_s^{abc} is the three-phase voltage at in PCC. The self and mutual impedance of lines ($Z^{abc}= R^{abc}+jX^{abc}$) are included to accurately represent the distribution lines in an unbalanced power distribution system. The generated active power P_{pv} and reactive power Q_{pv} of a PV system are fed to the nearby load P_L+jQ_L, and the excess power or net power P_n and Q_n are injected into the grid [140].

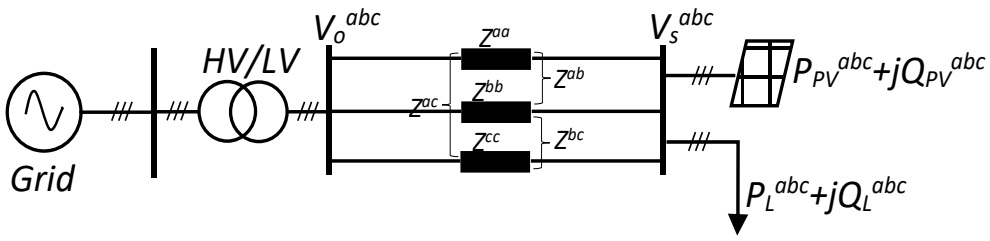

Figure 5.1. The basic structure of a low-voltage power distribution system integrated with a PV system [140]

The phase voltage (V_s^p) for each phase (p =a, b, c) at PCC in an unbalanced three-phase system can be determined using (5.1). Equation (5.1) points out that the increase of PCC voltage depends on the voltage at the transformer low-voltage side (V_o^{abc}), the network line impedance, and the net injected power while assuming the grid voltage is constant. It can be observed that the excessive injection of active power (PV penetration is high) can cause a reverse power flow, leading to an increase in the voltage magnitude in some network buses. Depending on the grid configuration, some nodes may experience an overvoltage problem, especially those close to the connected PV system. As a result, applying negative reactive power injection can potentially reduce the voltage rise. It is also noted that the injection of balanced active power from the three-phase PV system will have a relatively minor impact on voltage unbalance. On the other hand, the unbalanced connection of loads between the phases is considered the primary cause for extreme level voltage unbalance, which can be significantly reduced by adopting appropriate controlling of reactive power compensation [140].

$$V_s^p = V_o^p + \sum_{q=a,b,c} Z^{pq} \left(\frac{P_n^q + jQ_n^q}{V_s^q} \right)^* \tag{5.1}$$

Traditional approaches to control V_o^{abc}, and therefore address voltage regulation problems include utilising OLTC, autotransformers, and switched capacitors, but still, they are incapable of providing reliable timing responses to the rapid PV generation variation. Moreover, the high penetration of PV systems and their stochastic nature can also lead to

excessive wear and tear of voltage regulator devices. It may also lead to improper decisions of these control devices if both overvoltage and undervoltage take place simultaneously in the feeders [150]. Reconfiguring power distribution networks can change the effective network impedance (Z^{abc}), and thus reduce the associated voltage drop. The main drawbacks of this procedure are the high investment cost, increase in transient switching, and complexities of the power distribution operation [151]. To cope with these challenges, on-grid PV systems have been allowed to actively contribute to voltage regulation besides other devices as they might offer better outcomes than conventional approaches from an investment and time response perspective [152]. Control-side development in inverters can lead to efficient interfacing of the PVs and enable them to participate in compensating the unbalanced load distributed among the three phases. Therefore, the PV inverter circuit topology and its corresponding control strategy are key factors in tackling the voltage rise and unbalance problems [140].

5.3 Proposed Voltage Regulation Approach

The voltage regulation approach developed in this chapter depends on controlling the exchanged amount of reactive power of the PV inverters to simultaneously maintain the voltage magnitude and voltage unbalance within the standard limit. There are various techniques employed for voltage regulation in the local reactive power control, and these are divided into static and dynamic control strategies [55]. In static approaches, the Power Factor (PF) is predefined to a fixed value, and the supplied reactive power is proportional to the active power generation. In the case of low active power generation and peak load, the likelihood of voltage rise is very low, and reactive power support would be unnecessary. On the contrary, a dynamic PF based on the injected real power *PF(P)* may not guarantee the proper voltage regulation. This is because the voltage will not permanently rise with the

increase of active power production if the load variation is neglected. Thus, for effective voltage regulation, the reactive power is adjusted according to the local voltage [140].

5.3.1 Reactive Power Capability

There are various reactive power capability options available for PV inverters, which are commonly identified by the country's standards and grid code, such as IEEE Standard 1547 [153]. Among them is to apply PF adjustment according to the measured voltage regardless of generated active power. These standards determine the upper and lower constraints on reactive power exchange with regard to generated active power and inverter size. This means that reactive power injection is a function of active power and the assigned PF that depends on the PCC voltage. On the other hand, although it is technically feasible to design a PV inverter to supply reactive power at low injected power or no solar input, this practicality is not standard and yet not adopted by system operators [76]. Therefore, the PV inverters are usually not functioning at night and the support of reactive power is not possible. This practicality can be amended if operating conditions require the backing of reactive power support during the periods of zero power generation of PV systems. However, operating PV inverters at night or at $P=0$ will increase their operational stress and reduce their lifespan. Moreover, additional configuration to the PV inverter is required because the limitation of reactive power ($Q = \sqrt{S^2 - P^2}$) needs to be recomputed at every period. Therefore, in this investigation, no reactive power support is considered while there is no solar power, and the adjustment of PF is taken into account disregarded of PV generated power [140].

In regard to the PF limit, the rate of reactive power is restricted by the size of the PV inverter. For a PV inverter to provide sufficient reactive power support, extra capacity needs to be introduced in the design so that the inverter can deliver or absorb reactive power regardless of rated active power production. Thus, for a given inverter, the maximum

reactive power capacity ($Q_{PV-max.}$) at the rated active power ($P_{PV-rated}$) is governed by inverter size (γ) as follows [140]:

$$Q_{PV-max.} = P_{PV-rated}\sqrt{\gamma^2 - 1} \tag{5.2}$$

However, identifying the appropriate size of the inverter depends on application requirement, inverter sizes availability in the market, the country's regulations, and PV penetration level. For example, some power regulators mandate the operation of PV inverter between ±0.9 PF [154] (inverter oversized by 10%) to avoid excessive reactive power injection. Nevertheless, the current increase in PV penetration level has led to a rise in the occurrence of overvoltage and voltage unbalance problems, which have caused manufacturers to increase the size of PV inverters to allow sufficient reactive power capability [155]. As a result, some PV inverters are currently available in the market with a size up to 125% of P_{pv} rating, such as SMA Sunny Tripower Inverter [156], which allow the inverter's PF to operate between ±0.8. Moreover, several studies have suggested oversizing the PV inverters by more than 25%, such as in [157], [158], to address the voltage variation problem that arises from the excessive PV systems penetration. Besides that, the importance of oversizing the PV inverter in various control schemes for a multifunctional purpose, such as harmonic mitigation and reactive power compensation, was also addressed in [159] [140].

For the reasons mentioned above, the PV inverter is oversized by 25% of rated active power in this investigation, considering the high PV penetration level associated with a power distribution system, the availability of PV inverter with this size in the market, and PV application inverter to mitigate voltage unbalance. Thus, γ=1.25 ($S_{inv} = 1.25 \times P_{PV-rated}$), allowing reactive power of $\pm 0.75 \times P_{PV-rated}$ to be produced or absorbed by the inverter. With this size, the inverter can be operated between 0.8 leading (provides reactive power) and 0.8 lagging (absorbs reactive power) PF regardless of active power

output. Figure 5.2 below illustrates the inverter capability for this case, where the shaded area represents the inverter's range operation [140].

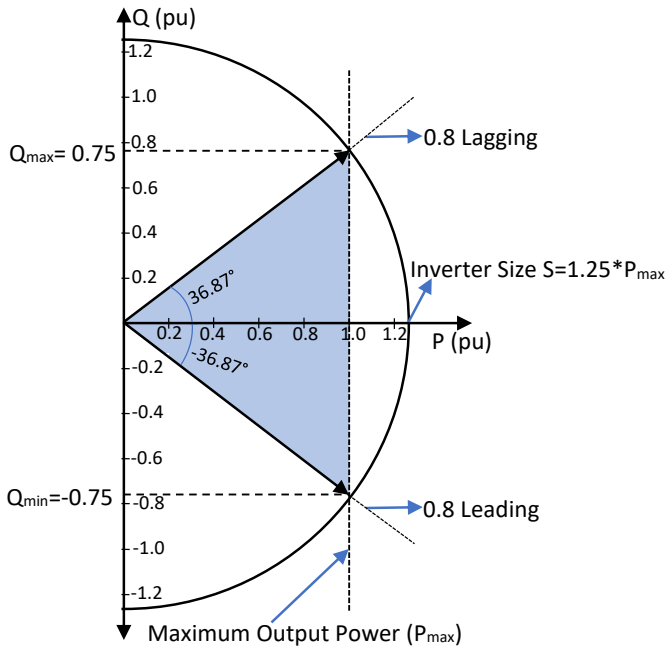

Figure 5.2. Capability curve of a PV inverter [140]

5.3.2 Proposed Step Droop Control Method

To address the limitation of the currently available reactive power control of PV inverter, A step control approach is developed in this chapter, as given in Figure 5.3. To establish a universal PV inverter control, the VU% is limited to 2%, and the voltage variation is set to ±7%. In the proposed step control, the PF of the PV inverter varies according to the measured voltage. Therefore, the PV inverter can adaptively alter its reactive power generation while maintaining its PF within the operational range. Due to the high R/X ratio in the power distribution system, the range operation of the inverter's PF is divided into four steps to guarantee a high impact on voltage magnitude in each phase, and hence reduce the voltage difference between the phases. As noted in equation (3.37) in chapter 2, violating the voltage unbalance limit (VU%) stars when the difference between any phase voltage magnitude and average voltage magnitude is more than 0.02 pu. For example, if the phase voltage magnitude ($V^{a,b,c}$) as follows, $V^a = 0.98$ pu, $V^b = 1.0$ pu, $V^c = 1.02$ pu, then the

VU% will be 2%. Consequently, applying steps control with the 0.02 pu voltage difference will allow different PF values to be allocated at each phase, which eventually decreases the voltage variation between the phases and keeps it within the permissible limitations [140].

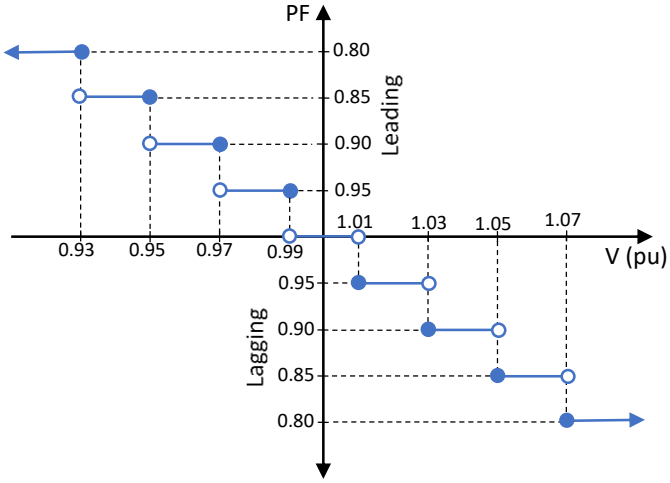

Figure 5.3. Proposed PF(V) control [140]

The adopted stepped function is also used to reduce the PV inverter degradation because of the deadband. At the same time, its impact could be significant on voltage regulation and maintaining the voltage unbalance under 2%, allowing more PV system integration without causing overvoltage, or severe voltage unbalance level. On the other hand, the conventional linear droop control assigns relatively the same PF for all phases unless the difference of voltage magnitude between any two phases is considerably high, which then the voltage unbalance level can be reduced. The linear droop characteristic parameters mainly depend on the demanded voltage limit, deadband width and PV inverter size. If these parameters change, their influence on voltage magnitude will differ, but their impact on voltage unbalance remains the same. For example, if the deadband width is increased by more than 0.02 (1.01-0.99), there will be no reactive power injected or absorbed at this deadband. This means that the probability of having voltage unbalance is high even if the phase voltage magnitude is within the specified limit. Wider deadband will allow voltage unbalance to occur mainly if all phase voltages are in the deadband interval. It is

important to mention that the transient intermittent characteristic of PVs and loads are not focus on this study. This is because the voltage unbalance and overvoltage are steady-state parameters of the network and are measured at 10 minutes intervals [140].

The block diagram of the PV system is shown in Figure 5.4. The variation of solar irradiation due to weather conditions and PV panel's locations cause fluctuations in the output voltage. The DC-DC converter is applied to keep the output voltage to a constant level and delivers the maximum power point tracking. Along with the phase-locked loop and anti-islanding function, the control system is employed to adjust the inverter's PF operation in response to the measured voltage V_{inv}. Several control structures can be applied for both control schemes (traditional droop control and the developed control) [160], which may require almost the same computational resources. The developed control scheme can use a digital sinusoidal pulse width modulation, which is more fixable and accurate in controlling the PF than used in conventional control because of the broad specificity and range of PF involvement. The main features of this control structure are fewer computational requirements and simple hardware implementation [161]. Therefore, controlling the PF is relatively simple to implement, either using reference frame theory or a digital control design, as suggested in [162]. In most linear droop control methods, the maximum reactive power must be recomputed at every operation period, adding complexity to the inverter's control circuit. Whereas in the developed control, the reactive power is computed according to the PF's assigned value [140].

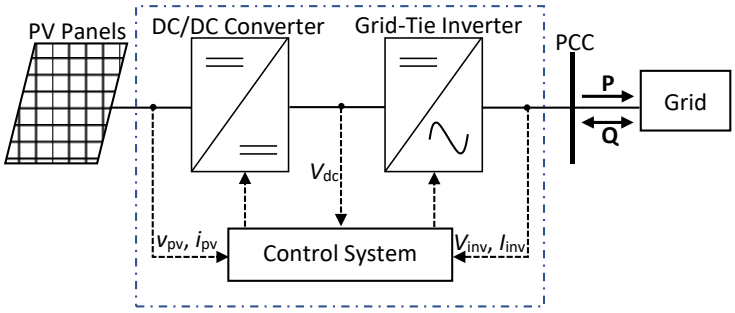

Figure 5.4. Block diagram of the PV system [140]

5.4 PV Inverter Model for Load Flow Calculation

To confirm the performance of the developed voltage unbalance improvement approach, modelling of a PV inverter for load flow calculation considering an unbalanced power distribution system needs to be addressed first. Most studies on voltage regulation use balanced load flow calculations [68], [76], [77], which can produce inaccurate results and predictions in actual unbalanced power distribution systems. To evaluate the performance of the developed control strategy of a PV inverter for voltage regulation, an Unbalanced Three-phase Load Flow Calculation (UTLFC) was developed in chapter 3. The developed TPCIM load flow method treats the node where the PV inverter is connected as a load bus. The active output power (P_{pv}^{abc}) of PV is known, and the reactive power (Q_{pv}^{abc}) can be determined using (4.7). The power factor (PF^{abc}) is determined according to the proposed *PF(V)* piecewise step function shown in Figure 5.3. Figure 5.5 shows the flow chart of UTLFC with the implementation of the PV inverter's proposed voltage control. The load flow is repeated at 10-minute intervals to generate a 24-hour time series of load flow values. Since the developed control scheme targets local control, the voltage magnitude measurement is assumed to be traced through the inverters or installed sensors at smart meters. Thus, to perform the simulation studies, instead of the actual data tracing through smart meters, a load flow calculation is performed to determine the voltage magnitudes, representing Step 1. In Step 2, the load flow calculation is conducted to examine the impact of the developed control on voltage magnitude and voltage unbalance [140].

The Y bus matrix is formulated after determining the buses and branches data. Next, the UTLFC is started by giving the initial values of voltages magnitude and angles and PF of the connected PV inverter. Then, at time $t = 0$, the load and PV generation profiles are used for the load flow calculation. After the UTLFC converges, the PV inverter's PF is updated according to the voltage obtained in Step 1, and accordingly, the reactive power is

calculated. Then, to verify the performance of the developed control, the UTLFC is carried out again in Step 2 after assigning the new value of PF. The same procedure is repeated every 10 minutes for each case study to form a 24-hour time series of UTLFC [140].

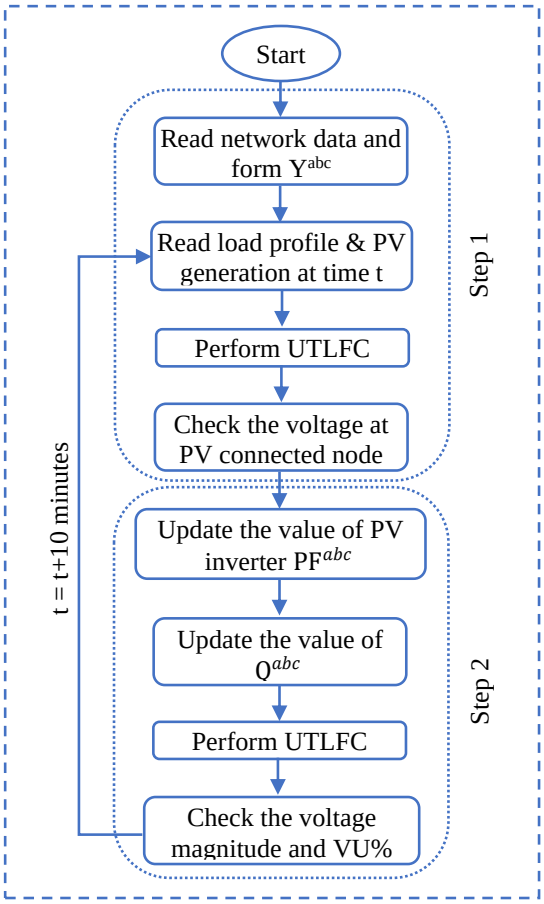

Figure 5.5. The flow chart of the proposed PV inverter model in UTLFC [140]

5.5 Case Studies and Analysis

A 24-hour time series of UTLFC is simulated in MATLAB®. Two main case studies are performed on the simulated network to assess the viability of the proposed control strategy. Different PV power output profiles and various PV penetration levels are first applied to assess the effects of the proposed control method on voltage regulation and voltage unbalance reduction. Then, the performance of the proposed control method in terms of voltage unbalance mitigation and inverter operation stress is compared with the conventional linear droop control method [140].

The voltage magnitude and unbalance of each case study are first determined without considering the control scheme (base case) to the connected PV inverter. Then, when the control strategy is adopted, two UTLFC are carried out. The first load flow calculation results are utilised to define the voltage at the connected PV buses, which represent the measured voltage taken either by the inverters or smart meters. Then, the second UTLFC is applied to confirm the effectiveness of the proposed control method by examining the voltage magnitude and unbalanced voltage, as shown in Figure 5.5 [140].

5.5.1 Test Network

Figure 5.6 shows the modified IEEE 37-bus unbalanced radial distribution feeder [131]. All the assumptions applied in chapter 4 for this test feeder and the typical load profile for a three-phase feeder (Figure 4.8) are considered here. Figure 5.7 shows the actual PV active power generation under various weather conditions throughout a day with a time step of 10 minutes [147]. It is assumed that all the connected PV systems would have the same irradiance profile as they are geographically close in proximity, and hence the PV production profile shown in Figure 5.7 can be used for all connected PV systems. With this typical data, an accurate and practical evaluation of the proposed control can be achieved [140].

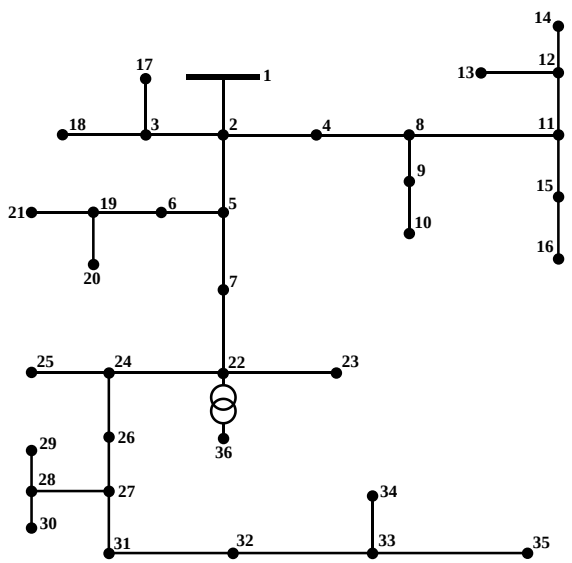

Figure 5.6. The modified IEEE 37-bus test feeder [140]

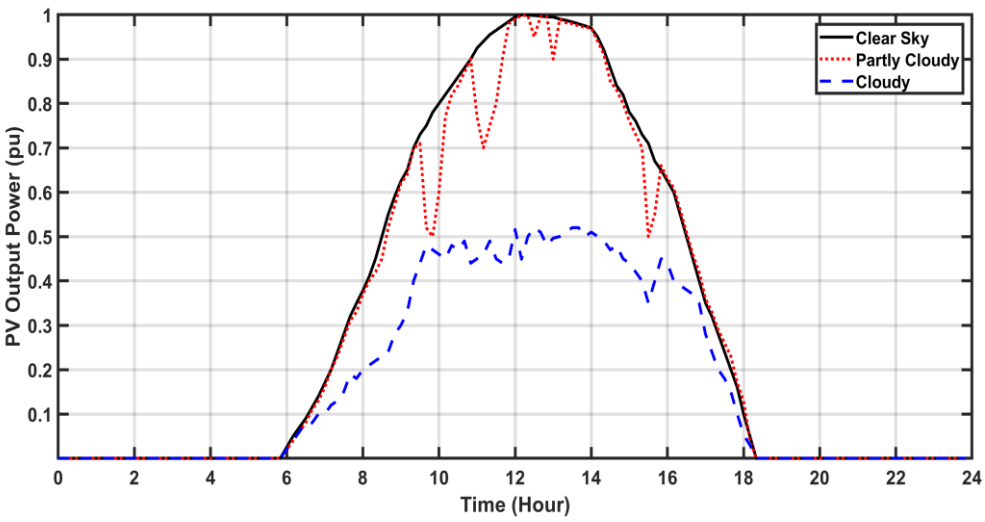

Figure 5.7. PV output power profile for 24 hours under different weather conditions [140]

5.5.2 Proposed Voltage Control Method Performance

Four three-phase PV power generation units are connected to the unbalanced distribution feeder with different ratings. Although the PVs can be connected anywhere in the simulated test feeder, for this study, they are connected at buses with high load densities, i.e., buses 32, 33, 34, and 35, to check their performance on voltage unbalance reduction. This is because voltage unbalances usually occur at the end of the feeder. First, the network has been stimulated with no reactive power control at the base case, and PV inverters only provide active power. This means that the inverters are operating at unity PF. The simulation was initiated with a lower PV power penetration level (25%) considering clear sky, partly cloudy and fully cloudy scenarios. Then, the buses voltage magnitude profile and unbalanced voltage level were investigated [140].

Statistical analysis of the voltage unbalance range over 24 hours for each node through a standard box plot is presented in Figure 5.8. The line inside each box is the median, and the left and right edges of each box are the upper and lower quartiles, respectively. For the base case (Figure 5.8. (a)), the unbalanced voltage range is the same for all PV power generation scenarios. It is noted that the VU% exceeded the limit of 2%, reaching 2.7% during some hours of the day. It proves that the unbalances in voltage start increasing at the

far end of the feeder, specifically feeder segments originating from node 27. On the other hand, the voltage magnitudes at every node in the simulated network were within the assigned limit, as indicated by the result of the load flow calculation. This is because the PV penetration level is relatively low, and the probability of having overvoltage is low. Hence, at this stage, the developed control scheme would be mainly applied to decrease VU% [140].

To minimise the voltage unbalance, the local voltage is measured, and then, according to Figure 5.3, the PF of the inverter is adjusted. Each phase would have different PF values, and thus, various amounts of reactive power are absorbed or injected depending on the measured voltage. The previous simulation has been repeated with the same data except that the PV inverters can now control their PCC voltage. The simulation steps presented in the flow chart given in Figure 5.5 is used in this case study. As shown in Figure 5.8 (b), the unbalanced voltage is reduced after incorporating the developed control strategy and appears within the limit during the clear sky day. On a partly cloudy day, the VU% exceeds 2% for a few minutes, as shown in Figure 5.8 (c), but it was within the limit for most of the time. The generated PV power is reduced to more than 50% during the cloudy day, causing less impact of reactive control on voltage magnitude. This can be noted in Figure 5.8 (d), where the VU% is reduced comparatively. As a result of low PV penetration, the voltage magnitudes were within limits in all PV generation scenarios, and with the support of the proposed control scheme, the VU% was reduced significantly [140].

Figure 5.9 shows the related PF angle (δ_{PF}^{abc}) values of the connected PV inverters for each phase during the clear sky day. It reflects the amount of reactive power exchanged and how often the inverter changes its PF values during a day. It can be observed that most of the day, the PV inverters absorb the reactive power at phase ‘b’ and supply the power at other phases. This is because the load is relatively low at phase ‘b’ and high at phase ‘a’ and ‘c’. Although the PV inverter can provide reactive power up to 75% of active power, at this

stage, around 32 % is utilised to achieve limited VU%. Therefore, the inverters were operated between 0.95 leading and 0.95 lagging PF, ensuring that the total power absorption stayed at the lowest levels while maintaining the VU% at the limited bounds [140].

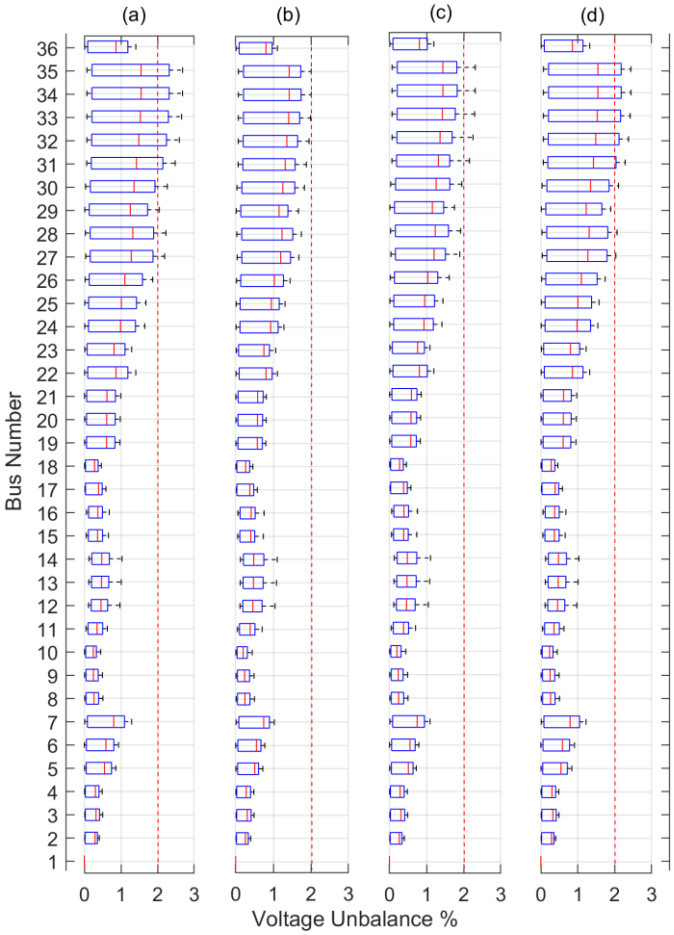

Figure 5.8. Voltage unbalance for (a) the base case, and with the proposed control strategy at (b) clear sky day, (c) partly cloudy day (d) cloudy day [140]

To confirm the superiority of the developed control scheme under a high PV penetration level, the rating of the connected PVs is increased. Since a high PV penetration level is considered here, the PV output power profile at the clear sky is employed for this case study. While increasing the PV penetration level, the phase voltage rises, particularly in phase 'b', and at a level of 70%, the voltage starts to go out of the permitted limits. Therefore, in the absence of the control strategies of PV inverters, the penetration level should be limited to 70%. For instance, Figure 5.10 shows the highest voltage recorded throughout the day at each phase when the level of 85% PV penetration level is applied. It

can be noted that without adopting the developed control of reactive power, the voltage at phase ‘b’ from bus 31 to 35 exceed 1.07 pu [140].

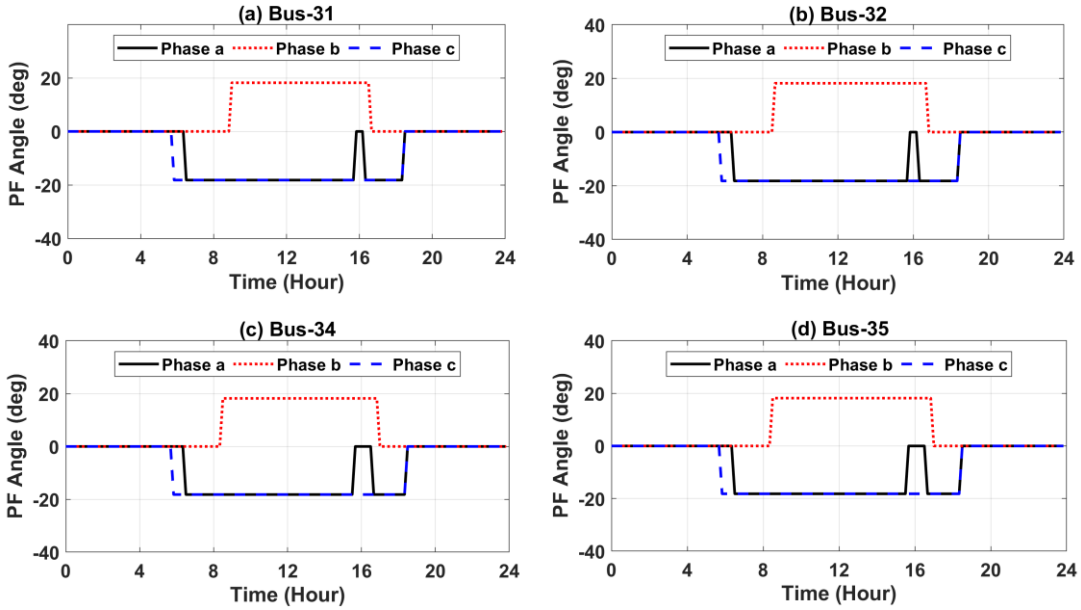

Figure 5.9. Corresponding PF angle of the connected PV inverter at low penetration level during the clear sky day [140]

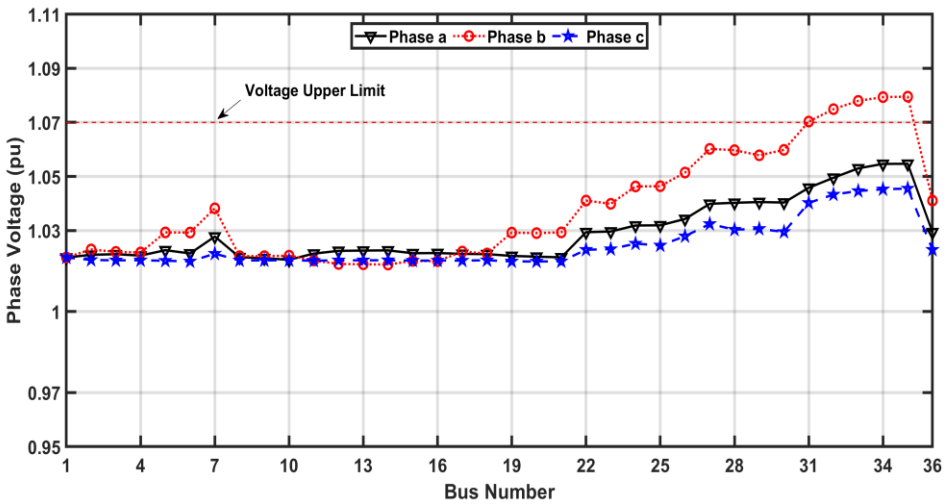

Figure 5.10. The maximum voltage recorded during the day at each bus for the base case at 85% PV penetration level [140]

After adopting the developed control scheme with the same penetration level (85%), the load flow calculation results demonstrate the effectiveness of the proposed approach. For example, Figure 5.11 indicates that the recorded maximum voltage is decreased to 1.04 pu. Although, at high PV penetration, the VU% is relatively low, applying the proposed

control scheme further reduces the VU% and is kept within the specified limit, as indicated in Figure 5.12. The newly developed control scheme allows the penetration level of PV generation to increase up to 150% without violating the voltage magnitude and voltage unbalance limit. For this reason, the PV inverters constantly absorb reactive power at each phase, as shown in Figure 5.13, where only phase 'b' of PV inverters were operated at rated PF, especially at peak generation time between 12 PM to 2 PM [140]. Moreover, it can also be noted that, although the developed control has a local impact, it could also benefit the nearby nodes (e.g., node 31), and reduce the severity of voltage unbalance [140].

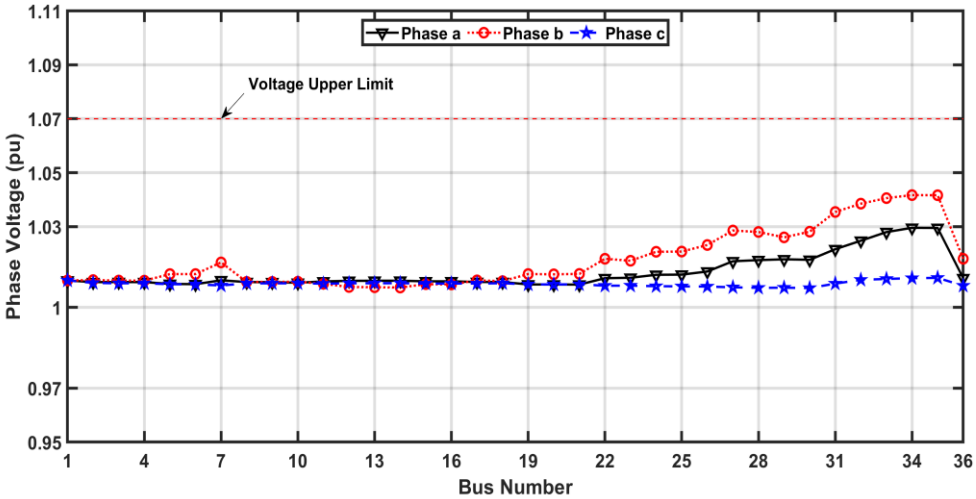

Figure 5.11. The maximum voltage recorded during the day at each bus after adopting the proposed control strategy at 85% of PV penetration level [140]

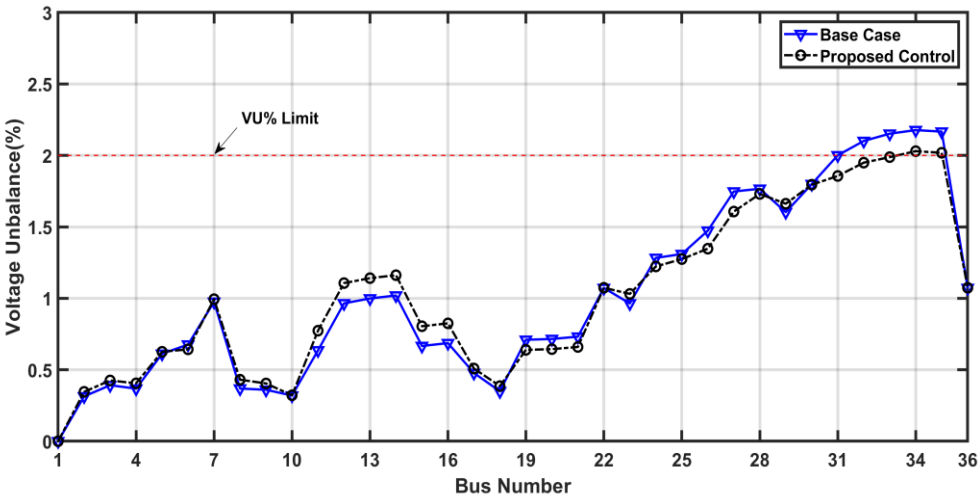

Figure 5.12. The maximum voltage unbalance during the day at each bus before and after using the proposed control strategy at 85% of PV penetration level [140]

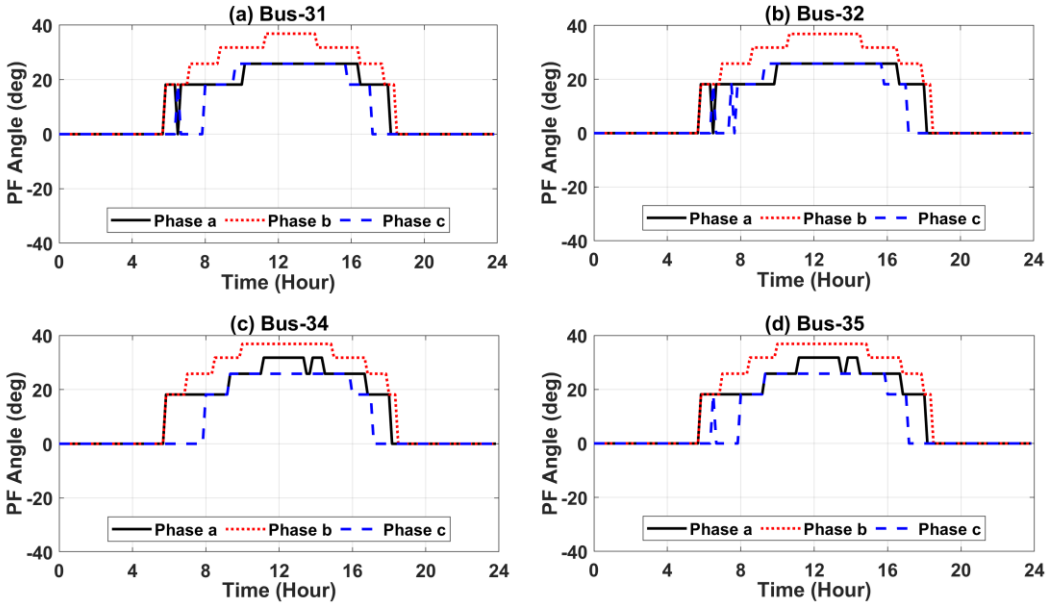

Figure 5.13. Corresponding PF angle of the connected PV inverter at 85% of PV penetration level [140]

5.5.3 Voltage Control Methods Comparison

In the final case study, the developed voltage control approach is compared with the conventional linear droop control approach, as suggested in [55]. The exact size and PF limit of the inverter are applied for both approaches. This means that both approaches should have the same voltage limit (±7%) and PF operation range (±0.8), as presented in Figure 4.5 and Figure 5.3. Both methods inject their full capacity of reactive power at a high PV penetration level when the voltage magnitude exceeds the limit, which cause a reduced influence on voltage unbalance. Nevertheless, as shown in Figure 5.14, they demonstrate different impacts on the voltage unbalance at a low PV penetration level (25%) on a clear day. The VU% is reduced only to 2.45% in the linear droop control scheme, leaving its value above the violated limit. The results further depict that the developed control scheme succeeds to keep the percentage of voltage unbalance within the limit, showing its superior benefit in reducing the voltage unbalance in a power distribution system [140].

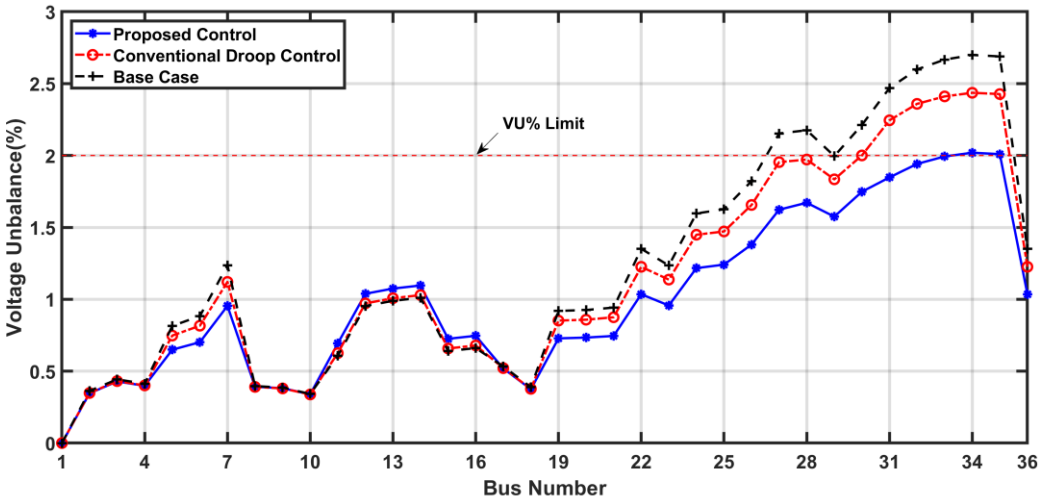

Figure 5.14. The maximum unbalanced voltage recorded during the day at each bus before and after applying the proposed control and conventional droop control methods [140]

With the application of the proposed step control of reactive power, the frequency of changes in inverters' PF in a day can be observed in Figure 5.9 and Figure 5.13. Although the PV power generation and load demand vary throughout the day, the PV inverter is operated for several hours with the same PF, particularly at phases 'b' and 'c'. On the other hand, as shown in Figure 5.15, the PF in the linear droop control approach frequently changes, especially at the phase 'a' and 'c'. This depicts that the developed control reduces the inverter's operating strain while keeping the voltage variation and voltage unbalance at certain bounds, giving superior benefits compared to the linear droop control method [140].

Figure 5.9 and Figure 5.15 show that both the developed control and linear droop control schemes establish almost the same amount of injected or absorbed reactive power from PV inverters, leading to the same overall network power losses. However, they demonstrate different voltage unbalance levels reduction, and thus different consequences and neutral current flows across the inverter or any nearby connected three-phase appliances. A small unbalance level in the phase voltages can cause a large neutral current, which can provoke adverse outcomes on the inverter and other three-phase power equipment. Moreover, the high level of voltage unbalance can lead to a possible derating and reduce the lifetime of any connected three-phase appliance, as mentioned in [49] and chapter 4. In

addition, the increased neutral current can also increase the overall network power losses. Therefore, adopting the proposed control of PV inverter can significantly reduce the voltage unbalance at network buses, and hence the power losses and derating factors associated with connected three-phase appliances can be minimised [140].

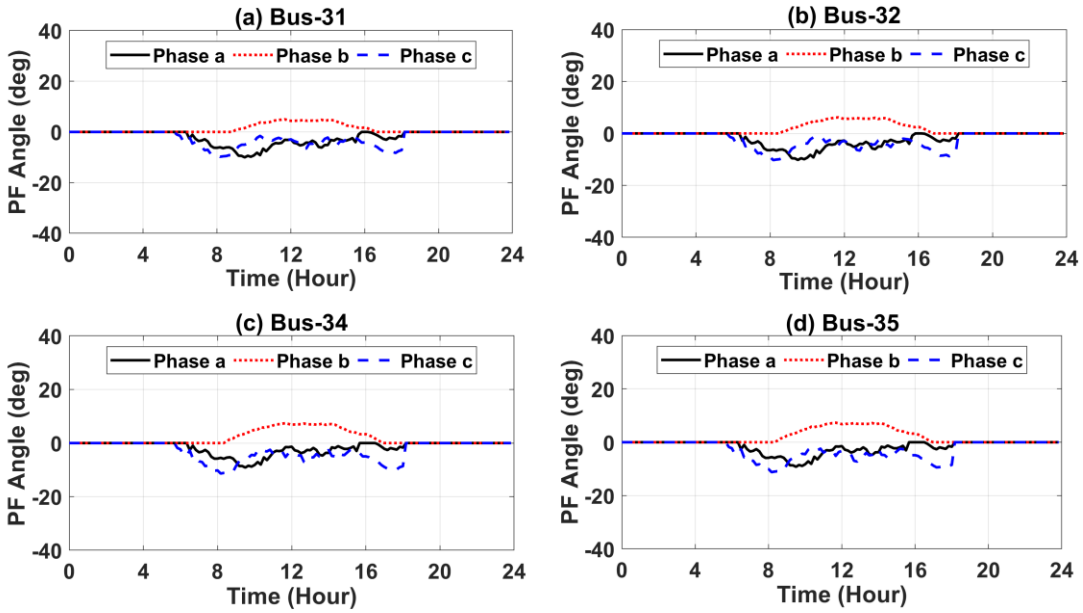

Figure 5.15. Corresponding PF angle of the connected PV inverter when conventional droop control method is applied [140]

5.5.4 Discussion

All three case studies demonstrated the developed reactive power strategy's ability to maintain the voltage magnitude and voltage unbalance within the specified limit in an unbalanced power distribution system. The proposed control strategy was studied under low PV penetration levels and different weather conditions in the first case study. The evaluation found that the severity of voltage unbalance can be reduced significantly without excessive reactive power injection. As shown in the second case study, the voltage rise and unbalance were also minimised at a high PV penetration level. The proposed control scheme allows the penetration level to increase from 75% to 150% without violating the operational voltage limits in the feeder. To validate the superiority of the developed control, a comparison between the proposed control and linear droop control has also been made in the last case

study to compare their performance on voltage unbalance reduction and frequency change of PV inverter PF. As expected, the proposed control managed to keep the voltage unbalance under 2% and the operating strain of the PV inverter at a minimum level [140].

The developed control scheme can be implemented for any integrated PV inverter and can be simply modified by the distribution network operator before being connected to meet their statutory standards. It can also be used to regulate the voltage at the connected PV and nearby nodes, which can increase the extended usage of renewable energy. The developed control approach can also be implemented to a single-phase PV inverter because it is designed to control each phase individually. While a single-phase inverter connection can regulate the voltage magnitude at PCC, the other nearby connected single-phase PV inverters may also contribute to voltage unbalance reduction in the feeders. In the absence of solar irradiation, the developed reactive power control with minor modifications can be used as a practical solution to overcome overvoltage and undervoltage problems. Besides that, the developed control approach can limit OLTC and voltage regulators' ageing because of frequent switching actions that they would normally face in the absence of alternative fast response voltage regulation action. Furthermore, employing the proposed PV inverter on an unbalanced power distribution system can also decrease the overall network power losses that are resulted from the increased neutral current and can increase the availability of power distribution system components [140].

5.6 Summary

With the continuous expansion of PV systems connections in power distribution systems, an innovative approach to effectively regulate the unbalanced voltage is required. This chapter has proposed an advanced approach for unbalanced voltage regulation for power distribution systems using the reactive power capability of PV inverters. Investigations on typical feeders with actual PV generation profile and load data found that

using a developed step droop control of reactive power at each phase using locally measured voltage can effectively maintain the voltage magnitude and voltage unbalance within the standard limit. Furthermore, the developed deadband reactive power control can potentially decrease the operating stress of the inverter control system, providing a higher inverter life expectancy and permitting an increase in PV penetration level. The analysis result further validates the significance of the proposed control scheme in comparison to the traditional linear droop control of PV inverter from voltage unbalance level reduction and PV inverter operational strain perspective. Finally, the study outcome illustrates the potential of extending the PF operation range of PV inverters to provide adequate unbalanced voltage regulation, which might be helpful to power distribution system operators and policymakers.

Despite the fact that local control approaches of PV inverters respond instantly at almost no extra investments required, it can sometimes increase the network power losses. As demonstrated in chapter 4 and this chapter, autonomous voltage regulation, including controlling of PV inverters, can provide acceptable voltage magnitude and unbalance levels at certain PV generation levels. However, it can be harmful to the power system at some extreme PV integration levels, such as high-power losses due to a lack of coordination between various voltage regulation devices. Therefore, the findings promote the demand for coordinated voltage regulation approaches for unbalanced power distribution systems experiencing extreme PV systems penetration, which will be developed in the next chapter.

Chapter 6: Optimal Coordination of Unbalanced Power Distribution Systems

6.1 Introduction

Introducing semi-fast stations (i.e., single-phase charging stations) for EVs has also contributed to exacerbating the level of voltage unbalance in power distribution systems besides the integration of PV systems. Due to unbalanced line coupling, ordinary voltage regulation devices that are based on autonomous control, such as OLTCs and reactive power compensators, are sometimes incapable of adequately addressing this issue without proper coordination with PVs and EVs. As illustrated in chapter 4, the uncoordinated voltage regulation devices can potentially lead to unnecessary reactive power compensation or insufficient voltage support, which may significantly increase power losses, especially at high PV penetration levels. Moreover, the local control of these devices cannot effectively avoid frequent operation and overloading of a transformer, which may outweigh the benefits of RETs connection. For these reasons, centralised or coordinated control has become essential to maximise the benefits and penetration levels of RETs and allow optimal control and operation of the network assets to achieve various operation goals, including mitigation of voltage unbalance problems and minimising network power losses.

This chapter presents a novel optimal real-time coordination scheme for various modern voltage regulating devices and RETs. The proposed scheme aims to keep the voltage magnitude and unbalanced level within the statutory limits while minimising the power losses in an active power distribution network. The main contribution and novelty of the study presented in this chapter are twofold: First, this chapter develops a novel mathematical framework for optimisation-based coordination control scheme incorporating the natural intermittency and practical operation of unbalanced power distribution systems to achieve

various objectives. The mathematical framework integrates robust, computationally efficient, and more accurate models (including realistic constraints and inter-phase coupling) of the controllable devices, making them flexible, effective, and scalable for a practical operation of a power distribution system. Second, this chapter proposes an advanced optimisation method combining two modified particle swarm optimisation (PSO) techniques. The advanced hybrid particle swarm optimisation (AHPSO) facilitates the proposed optimisation algorithm escaping from premature convergence and improving the local minimum problem, thereby improving the accuracy, convergence, and effectiveness of the proposed optimisation framework.

The chapter is structured as follows. Section 6.2 describes the coordinated control schemes in an unbalanced power distribution system and the proposed methodology. Section 6.3 presents the mathematical formulation of the optimisation problem. Section 6.4 describes the developed AHPSO that was applied to solve the optimisation problem. The performance and the effectiveness of the proposed optimal coordination scheme based on several case studies are illustrated in section 6.5. Section 6.5 also demonstrate the accuracy and robustness of the employed AHPSO. Finally, section 6.6 presents a summary of the chapter. The study outcomes of this chapter have resulted in the publication of a journal paper [163] during the course of this Ph.D.

6.2 Proposed Methodology

The increased integration of PVs and EVs introduce operational challenges on conventional control devices, such as the increased frequent operation of OLTC due to the absence of coordination between them. Moreover, they can negatively impact network performance by deteriorating the network voltage profile, making voltage regulation difficult, especially under unbalanced operation. As shown from Figure 6.1(a) and equation (5.1), the injected power or connected EV in one phase can also affect the voltage magnitude

of the other two phases because of the mutual impedance effect. This makes autonomous voltage regulation in an unbalanced network complicated and sometimes ineffective to address unbalanced voltage problems [80]. Moreover, the trend toward fast-charging facilities at the charging station brings more challenges in controlling the voltage unbalance in the power distribution system. Therefore, to a certain extent, the un-coordinated operation of voltage control devices can provide a limited solution to the problem of overvoltage, but it can increase the unbalanced voltage level and the total power losses. To limit such issues, it becomes fundamental for the modern power distribution system integrated with extreme RETs to utilise a centralised control approach of different voltage control devices and make use of smart technology (e.g., communication infrastructure, smart meters, etc.).

This chapter proposes a methodology for coordinating different voltage regulation devices in the power distribution systems with PV and EV connections. This coordination involved centralised control, where the control action is processed by a common entity accountable for collecting the required data about the network. This information is then processed in accordance with some desired optimisation objectives and constraints. Finally, the centralised control is dispatching the set-points back to the controllable devices through a communication medium. In such a scheme, the computation involved in processing the control action usually depends on solving an optimisation problem, which desires an expanded communication infrastructure and a network model. The conceptual diagram of the proposed coordination method is presented in Figure 6.1.

The proposed supervisory control systems coordinate four types of voltage regulation devices: OLTC, STATCOM, PVs, and EVs. The suggested coordination scheme identifies the optimal values of the reactive power absorbed/supplied from the PV inverters and STATCOM, the tap settings of the OLTC, and the phase connection of EVs. The optimal control signals of these controllable devices aim to improve the voltage profile, limit voltage

unbalance, minimise the total energy losses, and limit the frequent operation of OLTC. To limit affecting customers' comfort, like controlling their EVs charging rate and state of charge, especially at charging stations, only switching the phase where the EV is connected is considered as a control variable. In addition, the connection of EVs with slow charging speed (e.g., charged residentially) can be excluded from central-based control due to their insignificant impact. This will also reduce the required supervision and control facilities that go beyond the central controller capability to reach hundreds of EVs connected to the network. The low-scale PV system or residential-scale can be excluded from central-based control and can be locally controlled (as proposed in chapter 5). At the same time, the large-scale such as in industrial or commercial buildings (50 kW and above) are included in the optimisation model.

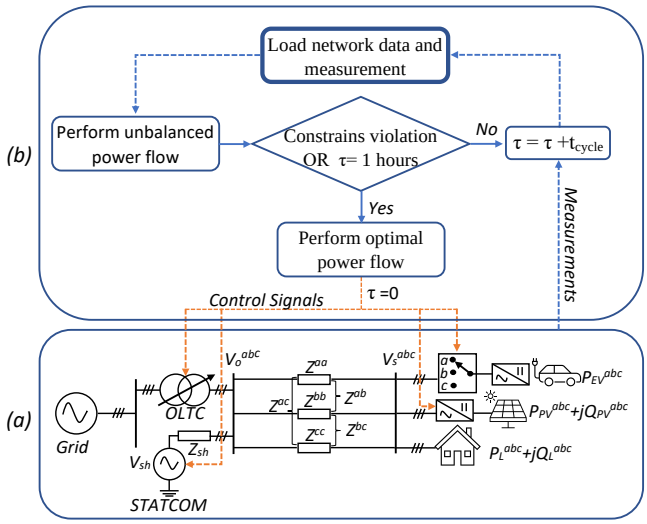

Figure 6.1. Conceptual diagram of the proposed centralised control

In the proposed centralised control, the central unit receives the required network measurement such as PVs generated power, loads profile, and current set-points of controllable devices (e.g., OLTC tap position) at each control cycle (t_{cycle}). An unbalanced three-phase load flow is then routinely calculated (i.e., every 10 minutes) to check for limit violation issues, such as voltages magnitude, and voltage unbalances violation. After that, the optimisation model is exclusively applied when there is constrains violation (e.g., a

voltage violation) or after a specified time (e.g., 30 minutes, 1 hour, etc.) of the last control signal action. If the optimisation model's criteria are still not activated, the unbalanced load flow is performed again for the next control cycle on a sampled time-wise basis.

The main components for deploying the proposed schemes are smart meters, sensors, controllers, and communication medium. Smart meters and sensors provide the necessary energy consumption, voltage measurements, and the set-points of controllable devices. The controller can be a central controller where all information and measurement are processed to generate a control signal to be sent to the controller installed at a controllable device (e.g., PV inverters, STATCOM and OLTC). A static transfer switch is also one of the controllable devices used at the charging stations to allow easy and flexible EV switching among the three phases. 3G/4G/5G, optical fibre ethernet and Zigbee are all different communication methods that can be used in centralised control, which have already been utilised in power transmission and distribution systems [29].

6.3 Problem Modelling and Formulation

The coordination between reactive power control capability of PV, voltage control option of OLTC and STATCOM, and phase switching of EV is an optimisation problem. It has various operational goals as it must meet the various network operational constraints and component characteristics (e.g., integer variables of OLTC). The optimisation formulation minimises the energy losses, the operational switching of OLTC, the voltage magnitude violation limit, and the voltage unbalance level. Thus, the objective function is constructed as a mixed-integer nonlinear problem, which can be expressed as follows:

$$\text{Minimise:} \quad f(x,u), \qquad \text{Subject to :} \quad \begin{aligned} g(x,u) &\leq 0 \\ h(x,u) &= 0 \end{aligned} \tag{6.1}$$

where $f(x,u)$ is the objective function that requires to be minimised. $x=\{x_1,x_2,x_3,..,x_m\}$ is the vector of dependent variables or the state variables. $u=\{u_1,u_2,u_3,..,u_n\}$ is the vector of

independent variables or the control variable (i.e., decision variable) used to achieve the optimisation problem. g*(x,u)* is the set of inequality constraints, and *h(x,u)* is the equality system operating and control variable constraints.

6.3.1 Objective Function

The main objectives of the optimisation model are to minimise the power losses and switching operation of OLTC and limit the unbalanced voltage while satisfying the other operation constraints and control variable constraints. The multi-objective optimisation problem can be solved either by converting multi-objective functions to a single objective function with different weighting factors or applying pareto-based methods [164]–[166]. Treating all objective functions as one objective function is commonly used because it has less computation burden than pareto-based methods, and the optimisation of one objective function could be achieved without the aggravation of another objective function. However, choosing an appropriate value for weighting factors could be challenging. To address this problem, some objective functions can be treated as a constraint in the optimisation problem by limiting their values, which is not the case for power losses as they cannot be limited. Therefore, the primary objective function is to minimise the total three-phase power losses in a power distribution system where the number of OLTC switches, voltage magnitude, and voltage unbalance factor is limited.

Different formulations are used to describe the power losses in literature. Most of them are based on an approximation to reduce the complexity of the optimisation problem, mainly when analytical approaches are used. When metaheuristic optimisation techniques are used, any formulation can be used without compromising the accuracy. Therefore, the difference between power generation ($P_{G\_i}^{p}$) and loads ($P_{L\_i}^{p}$) at each at phase *p* and node *i* is the most precise presentation of the total three-phase power losses (f^{PL}), and thus, the objective function can be formulated as given in (6.2).

$$f^{PL} = \sum_{i=1}^{N} \sum_{p=a,b,c} (P_{G\_i}^{p} - P_{L\_i}^{p}) \tag{6.2}$$

6.3.2 Equality Constraints

Equality constraints represent the typical load flow equations. These constraints are strictly enforced during the load flow procedure when metaheuristic optimisation techniques are used, which are satisfied by performing load flow calculations to obtain the fitness function. Therefore, solving the developed unbalanced load flow method (TPCIM) presented in (3.9) would fulfil the equality constraint for the optimisation problem.

6.3.3 Inequality Constraints

6.3.3.1 State Variables

The state variables represent the power system operating limit as follows:

- Voltage Limit: voltage magnitude (V_i^p) at all buses i and phases p in the power distribution system must be kept with the defined limits.

$$V_{i_{min}}^{p} \leq V_i^p \leq V_{i_{max}}^{p} \tag{6.3}$$

- Thermal limit: the rated amount of current ($|I_{ij}^p|$) flow between any two nodes ij is restricted by the feeder thermal limit.

$$|I_{ij}^p| \leq I_{ij\_rated.} \tag{6.4}$$

- Voltage Unbalance: because it can produce undesirable operation conditions in the power distribution systems, the steady-state voltage unbalance (VU%) at any bus i should be limited.

$$VU\%_i \leq VU\%_{Limit.} \tag{6.5}$$

All these state variables are incorporated into the formation of the comprehensive objective function with penalty factors to maintain the state variables inside their allowable

boundary and reject any infeasible solution. The penalty function can be specified by a quadratic term as follows:

$$F = f^{PL} + k_1 \sum_{i=1}^{N} \sum_{p=a,b,c} \nabla V_i^p + k_2 \sum_{i=1}^{Nl} \sum_{p=a,b,c} \nabla I_i^p + k_3 \sum_{i=1}^{N} \nabla VU\%_i \tag{6.6}$$

where

$$\nabla V_i^p = \begin{cases} (V_i^p - V_{min.})^2 & V_i^p < V_{min.} \\ 0 & V_{min.} \leq V_i^p \leq V_{max.} \\ (V_i^p - V_{max.})^2 & V_i^p > V_{max.} \end{cases} \tag{6.7}$$

$$\nabla I_i^p = \begin{cases} 0 & I_{ij}^p \leq I_{ij\_limit}^p \\ (I_{ij}^p - I_{ij\_limit}^p)^2 & I_{ij}^p > I_{ij\_limit}^p \end{cases} \tag{6.8}$$

$$\nabla VU\%_i = \begin{cases} 0 & VU\%_i \leq VU\%_{limit} \\ (VU\%_i - VU\%_{limit})^2 & VU\%_i > VU\%_{limit} \end{cases} \tag{6.9}$$

VU% can be calculated using (3.37). In this research study, $VU\%_{limit}$ is restricted to 2%, and the voltage variation ($V_{min.}, V_{max.}$) is limited to ±7%. $k_1, k_2, and\ k_3$ represent penalty factors for voltage limit constraint (∇V_i^p), thermal limit constraint (∇I_i^p), and voltage unbalance limit constraint ($\nabla VU\%_i$), respectively. Violating of these constraints could compromise network stability and often lead to network components failure. Therefore, the penalty factors are chosen to be a large number to avoid violation of relevant constraints.

6.3.3.2 Control Variables

The inequality constraints of the control variables are self-limiting. The optimisation solver chooses a feasible value for each control variable in the specified range. These control variables represent the control parameter of STATCOM, OLTC, EV, and PV inverter.

- **STATCOM**

According to the operating concept of the STATCOM, the controllable voltage source ($V_{sh}\angle\delta_{sh}$) is used to control the rate of reactive power (Q_{sh}^p) to be injected or consumed. Nevertheless, the voltage magnitude of STATCOM is constrained by the upper and lower

limit, but its phase angle can differ from 0 to 2π. Therefore, the control variable of STATCOM is constrained as follows:

$$V_{sh-min}^{p} < V_{sh}^{p} < V_{sh-max}^{p}$$
$$Q_{sh-min}^{p} < Q_{sh}^{p} < Q_{sh-max}^{p} \tag{6.10}$$

The unbalanced model of STATCOM that was developed in chapter 4 for the unbalanced load flow calculation is used in this study, where its connected bus is modelled as a voltage-controlled bus with a predefined voltage magnitude and no real power exchange while it operates within limits. In the optimisation problem, the voltage magnitude is treated as a control variable, and then STATCOM model parameters for each phase can be calculated at the end of each iteration of the load flow calculation to check its limits. Such a model would improve the convergence characteristic of load flow calculation, and thus, significantly enhance the scalability and speed of the optimisation solution.

- **OLTC**

Three-phase transformers are modelled in the three-phase load flow calculation by an admittance matrix Y_T^{abc} that is represented by equation (3.3). The transformer taps ($Tap(t)$) are supposed to be at the primary side (i.e., high voltage side), and the transformer connection is Delta Wye-G. A typical tap changing transformer has 21 discrete positions (nominal, 10 above and 10 below), and each tap has ±1% regulating range of voltage, therefore, the equivalent voltage ratio a_T is practically determined by the tap positions [26].

$$a_T(t) = 1 + 0.01 \times Tap(t) \tag{6.11}$$

where $Tap(t)$ must be an integer value, and the limit on tap position of OLTC can be expressed by:

$$-10 \leq Tap(t) \leq 10 \tag{6.12}$$

Regular OLTC tap position changing shortens their operation life and increases the coupled maintenance costs because of the intermittent generation of PVs. Power system

operators are usually interested in reducing the number of switches due to financial and technical considerations. These number depends on the switching type of OLTC (e.g., oil or vacuum) [167], which can vary between 600,000 and 1,000,000 switches [81]. According to [85], the maximum number of tap switching of the OLTC has been supposed equivalent to the average number of tap changes of 700,000 by the manufacturers without the need for maintenance [85]. Taking into account this value and projected lifetime of 40 years, the maximum average number of taps switching each day must be restricted to 48 (700,000/(40×365)), which can avoid excessive tap operations of OLTCs, and therefore preserve their service life. To satisfy this requirement and avoid unrealistic tap operation, the optimisation problem restricts the number of tap position changes between two consecutive times to be less than 3. Consequently, the constrain of tap position at each control cycle can be expressed by (6.13) considering the maximum and minimum tap position given by (6.12).

$$Tap_{t-1} - 3 \leq Tap_t \leq Tap_{t-1} + 3 \tag{6.13}$$

where Tap_t is the tap position at time step t and Tap_{t-1} represent the previous tap position.

- **EV**

EVs have been recently involved in voltage management of smart power distribution systems by optimally controlling their charging rate, state of charge, and either charging or discharging. However, these control options may affect EV owners' comfort level in charging stations or parking lots while waiting for their vehicle to be quickly charged. Moreover, EV manufacturers are competing to provide fast charging facilities to their vehicles, making fast charging demand increase. This can be seen in public and workplace car parking, which are usually equipped with semi-fast charging speed supplied by three-phase feeders, which are projected to represent the high portion of the overall charging stations [40]. The various control options of EV at home can be feasible; however,

controlling many connected EVs makes the optimisation problem very complicated, and the time burden increases in multifold. Therefore, a charging station or parking lots equipped with semi-fast charging facilities and a static transfer switch is considered in the optimisation problem. According to the desired objective function, a static transfer switch is used to re-connect the single-phase EVs charging port between the three-phase system. One of the main features of a static transfer switch is to ensure instantaneous and quick load transfers without tolerating voltage disturbance limits. Many researchers identified static transfer switch as a potential cost-effective remedy to power quality problems in various applications such as dynamic switching residential customers between three phases and re-phase of single-phase PV system connection among the three phases [168].

Therefore, selecting the phase at which the EVs should be connected will be used as a control variable. Three variables represent each parking lot despite the number of EVs connected at the parking site. Each variable identifies which phase that one-third of the total number of EVs should be connected to. Consequently, the control variables of parking lots are discrete, and their value represents by (6.14). In the load flow calculation, the bus with a charging station would be represented by a load bus, and its load depend on the number of vehicles connected at each phase and parking lots.

$$EV_{i\frac{1}{3}}^{phase} = \begin{cases} 0; & phase\ a \\ 1; & phase\ b \\ 2; & phase\ c \end{cases} \tag{6.14}$$

where i is express the first, second and third groups of the connected EV at each parking lot.

- **PV Inverter**

The reactive power capability of the PV inverters developed in chapter 5 is applied here. However, the assigned power factor (PF_i^{abc}) value, which is constrained by (6.15) is now depending on solving the optimisation problem. To design a reliable and realistic optimisation model, only large scale (>50 kW) residential or commercial PV systems can

be included in the optimisation model. This reduces the monitoring and control infrastructure required to reach the vast number of connected small-scale PV inverters. Moreover, the small-scale PV system has a local effect and can be controlled locally using droop control, as proposed in chapter 5 or linear droop control.

$$0.8_{i-leading}^{abc} < PF_i^{abc} < 0.8_{i-lagging}^{abc} \tag{6.15}$$

6.4 Advanced Hybrid Particle Swarm Optimisation (AHPSO)

Various optimisation methods can be employed to solve the optimisation problem; however, since the non-convexity and non-linearity of the proposed problem, a heuristic-based method is employed. As discussed in chapter 2, the modified variant of PSO provides enhanced performance with respect to accuracy, robustness, and speed [124]. In this research study, a new version of PSO (AHPSO) is proposed to further enhance the optimisation solution by combining and advancing two well-developed PSO, [123] and [125]. The developed AHPSO combines these two methods' merits and demerits by applying GA mutation, crossover operators and natural selection mechanism to the specified number of particles. After updating the speed and position of the particle, mutation and crossover operators are employed to half of the particles at every optimisation iteration. After that, all particles are sorted based on the objective function, and then the speed and position of the worst half of the particles are swapped by the other best particles. The complete flowchart of implementing the proposed AHPSO to solve an optimisation problem is shown in Figure 6.2. The specific procedure of the proposed AHPSO algorithm is given below.

1. Initialise the parameter of PSO and GA, and then the velocity V_i and position X_i of each particle are initialised randomly.
2. Evaluate the objective function (6.6) of each particle after performing an unbalanced load flow calculation.

3. Update personal best positions (p_{best-i}) for each particle that has a new better objective value than the old personal best value, and then updates the global best position (g_{best}), which represents the best ever solution achieved so far.
4. Update the speed and position of the particle for the next iteration *k+1* as follows:

$$V_i^{k+1} = \chi\left(V_i^k + c_1 r_1\left(p_{best-i} - X_i^k\right) + c_2 r_2\left(g_{best} - X_i^k\right)\right) \tag{6.16}$$

$$X_i^{k+1} = X_i^k + V_i^{k+1} \tag{6.17}$$

where χ is the constriction factor coefficient that is used to ensure the convergence of the search processes and produce better-quality solutions than the standard PSO. c_1, c_2 are the acceleration coefficients, and r_1, r_2 are two random numbers between 0 and 1 with uniform distribution. In this research study, the acceleration coefficients are set $c_1 = c_1 = 2.05$. The constriction factor coefficient (χ) is calculated as follows:

$$\chi = \frac{2}{\left|2-\varphi-\sqrt{\varphi^2-4\varphi}\right|} \quad , \varphi = c_1 + c_2, \varphi > 4 \tag{6.18}$$

5. Apply crossover and mutation operators to half of the particle. Then check if the inequality constraints enforce the limits of positions. If not, then they are replaced by their respective boundaries. In this research study, the crossover and mutation rate are set as 1 and 0.1, respectively.
6. Apply the natural selection approach by sorting the practice according to their objective function values, and then only the speed and position of the worst half of the particles are substituted by the speed and position of the other best half of the particles.
7. Repeat steps 2–6 until a stopping condition is achieved, which can be achieving the maximum number of iterations or an adequately good fitness value is attained.

For the purpose of case studies, the proposed centralised control is initialised by loading the network data and the control variable's initial setting. In this research study, the optimisation process has been executed over a period of 24-h with a 10-minutes time step. The initial value of OLTC tap, STATCOM V_{sh}, and PV inverter PF was set at unity value,

and the number of connected EVs at each phase was set to be equal. Then, an unbalanced three-phase load flow is performed to check the operational constraints of a power distribution system, such as voltage unbalance and magnitude. The optimisation model is employed either when the voltage magnitude, voltage unbalance, and thermal limit exceed the corresponding limit or after one hour of the last activated optimisation model. When the optimisation model is activated, the objective function presented in (6.6) is calculated using another load flow calculation and, then AHPSO is employed. The optimisation solution provides a new setting of coordinated devices that enforce the efficient operation of the power distribution system. These processes are repeated every 10 minutes until the optimisation model has produced 24 hours of network operation.

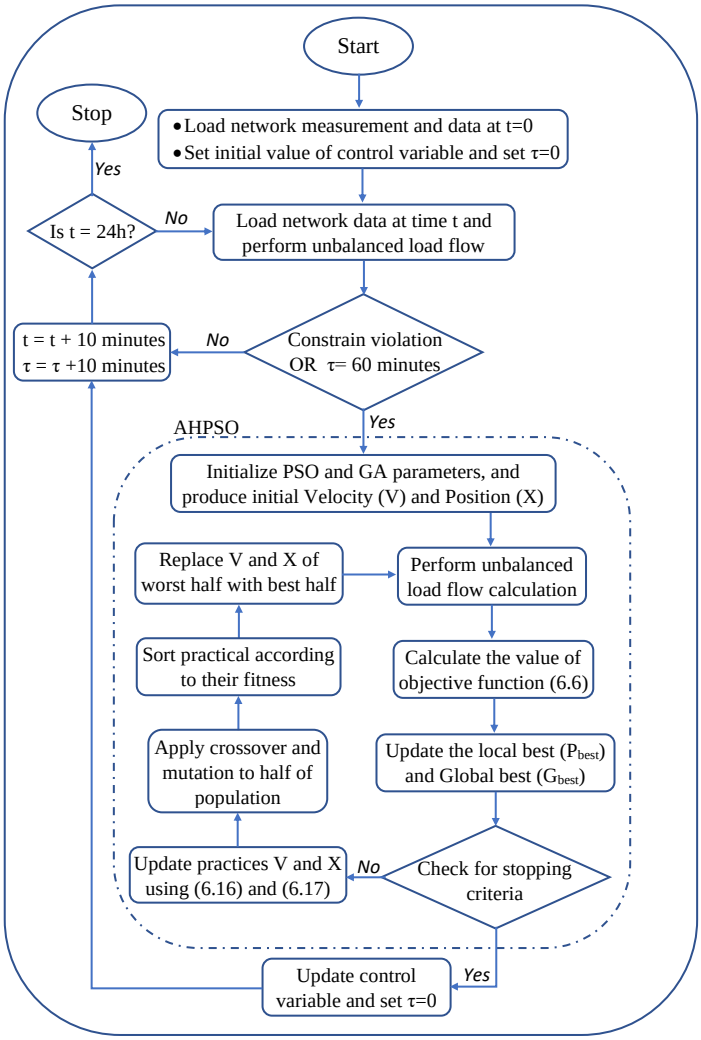

Figure 6.2. The flowchart of the proposed AHPSO and centralised control

6.5 Case Studies and Analysis

In order to verify the performance of the developed optimal coordination scheme, various scenarios are performed on the modified IEEE 37-node and IEEE 123-node test feeders [131], and the strength of the developed method is examined in detail under various operating conditions (i.e., different PVs penetration level and load profiles). First, the contribution of the suggested control scheme on the unbalanced condition improvement and power losses reduction under different PV penetration levels is evaluated on the modified IEEE 37-node test system. After that, several case studies are conducted on the IEEE 123-node test system to confirm the proposed method's scalability on the severe unbalanced conditions. Three scenarios are adopted on each test network to analyse and compare the effectiveness of the developed optimal coordination scheme with the autonomous voltage regulation scheme. The considered scenarios are:

Scenario 1: network is operating without any voltage regulation devices (base case). There is no OLTC and STATCOM, and the PV inverters are operated at unity power factor. The EVs are connected equally among the three phases.

Scenario 2: network is operating under the local control of connected voltage regulation devices. STATCOM and PV inverters are locally controlled, whereas the EVs are still connected equally among the three phases. The conventional rule-based control method of OLTC is used, where the tap position changes to maintain the secondary bus voltage variation from the pre-set reference with a voltage regulation bandwidth is 0.012 pu.

Scenario 3: network is operating with the proposed voltage regulation approach. All the voltage regulation devices and EVs' connections are now controlled by the proposed optimisation model described in the flowchart shown in Figure 6.2.

Finally, both test systems are used to confirm the accuracy and robustness of the employed AHPSO. The proposed strategy and simulation were implemented in

MATLAB®. The numerical experiments were conducted on an Intel computer i7-6700 at 3.4 GHz CPU and 12GB RAM. For all case studies, the population size and maximum number generation are set to 20 and 100, respectively.

6.5.1 IEEE-37-Bus Test System

Figure 6.3 shows the modified IEEE 37-bus unbalanced radial distribution feeder [131]. The assumptions applied in chapter 4 for this test feeder and the typical PV generation, load profile, and EVs parking lots profile shown in Figure 4.7 and Figure 4.8 are employed here. In addition, to study the performance of the developed optimal coordination scheme method, it assumed that the substation transformer (at bus 1) is equipped with OLTC. Moreover, this research study supposes that the size of the feeder's conductors and transformer of the simulated IEEE 37-bus test feeder is designed to handle the excessive connection of PVs and EVs. Thus, the power loading of lines and transformers are assumed to be within limits. In this regard, two units of three-phase PV generation systems are randomly interconnected to the tested feeder, specifically at buses 25 and 33. Two EV charging stations that emulate typical car parking equipped with charging facilities are considered in this study, and both are assumed to provide a semi-fast charging facility to EVs with a rating of 7.4 kW. The maximum number of connected EVs into the parking lots 1 and 2 are 20 and 15, respectively, and are connected into bus 20 and bus 9, respectively. A three-phase STATCOM is installed at bus 8, having a capacity of 3 × 200 kVAr.

Initially, the simulated system is tested under a low PV penetration level (20%) to identify the system's detailed behaviour under various scenarios and point out the significance of the proposed optimisation model. It is important to highlight that both local and proposed control (Scenario 2 and 3) have managed to keep the voltage magnitude within the limit, and therefore the evaluation of voltage unbalance and power losses would be the main interest in this research study.

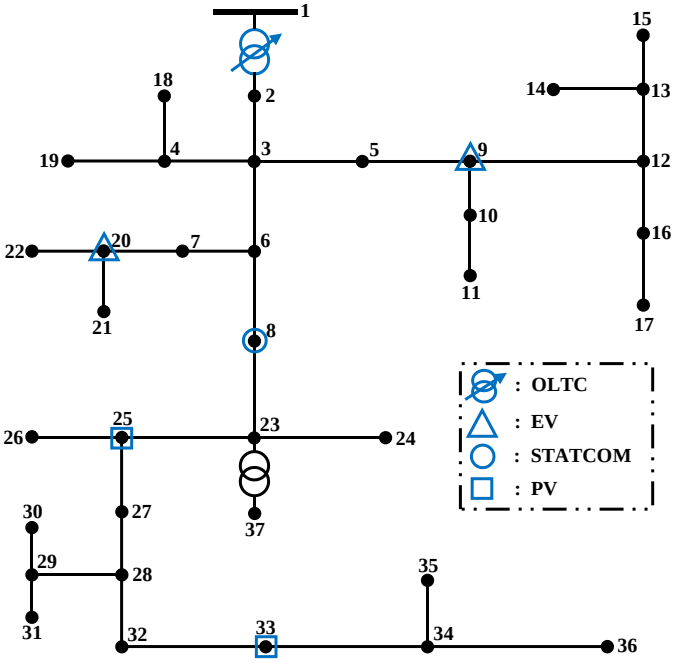

Figure 6.3. The modified IEEE 37-bus test feeder

The statistical analysis of voltage unbalance under the three scenarios for 24 hours at each bus is demonstrated through a standard box plot displayed in Figure 6.4. Similarly, in this box plot, the line inside each box is the median, and the left and right edges of each box are the upper and lower quartiles, respectively. It shows that the voltage unbalances at the base case (Figure 6.4 (a)) crossed the limit of 2% and reached up to 3.7% throughout several hours of the day. It proves that the voltage unbalance limits are violated most of the day at some buses, particularly bus 27 to bus 36. The operation of local control of voltage regulator devices representing scenario 2 manages to reduce the voltage unbalance to 2.6%, as shown in Figure 6.4 (b), but still, the network is suffering from voltage imbalance problems for a significant amount of time. Moreover, if the number of EVs connected at each phase are not assumed equal in the local control, the voltage unbalance level could be considerably high. On the other hand, after adopting the developed optimisation model, the voltage unbalances are further minimised and kept within standard limits, as demonstrated in Figure 6.4 (c).

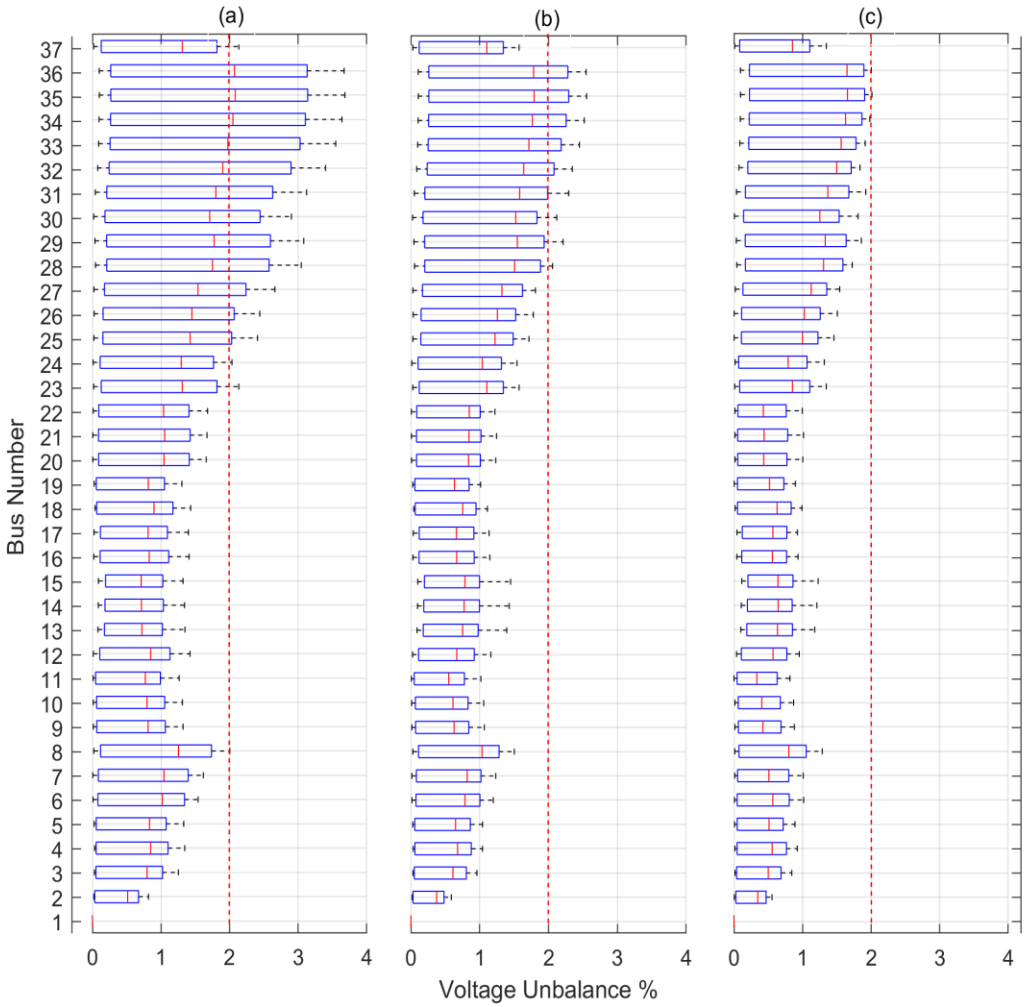

Figure 6.4. Voltage unbalance for (a) Scenario 1, (b) Scenario 2, and (c) Scenario 3

As far as scenario 3 is concerned, Figure 6.5 presents the related PF angle (δ_{PF}^{abc}) of the two integrated PV inverters for each phase throughout the day, which reflect the rate of reactive power exchanged with the network. It can be noted that the PV inverters connected at bus-33 most of its operating time absorb the reactive power at phase 'b' and supply the reactive power at the other two phases to reduce the voltage variation among the phases. This is because the connected load at phase 'b' is comparatively light compared with phase 'a' and 'c', which are heavily loaded, making the voltage unbalance level significant.

It can also be observed from Figure 6.6 that most of the EVs are connected at phase 'b' to balance the power between the phases. On the other hand, the exclusion of EVs' connections in the optimisation problem has shown an increase in the total energy losses per

day by 6%. This is because the network is forced to consume more reactive power (from STATCOM and PV inverters) to compensate for the voltage unbalance, especially at a high PV penetration level. Involving EVs' connections in the optimisation model may demand oversizing the charging stations infrastructure (sizing of each phase). However, shifting the EV's load from one phase to another can reduce the overall loading to other phases in three-phase systems. This is because the optimisation algorithm tries to minimise the loading difference in the three-phase system, which leads to maintaining a reasonable feeder loading and hence, avoids upgrading feeder size. For example, the loading of phase 'c' of the substation transformer is reduced from 120% to 105% (with respect to the transformer' rating at each phase) after applying the proposed coordination scheme.

To accommodate the voltage drop and reduce the power losses at peak load, the OLTC operates at tap position 3, and the STATCOM operates at its limit to provide reactive power, as shown in Figure 6.7. It is important to note that the total number of taps changed during the day was 25, which is less than the maximum average number of tap changes per day (48 tap changes). Moreover, the loading of the substation transformer at peak load is reduced by 5% compared with local control approaches due to power losses and voltage unbalance reduction.

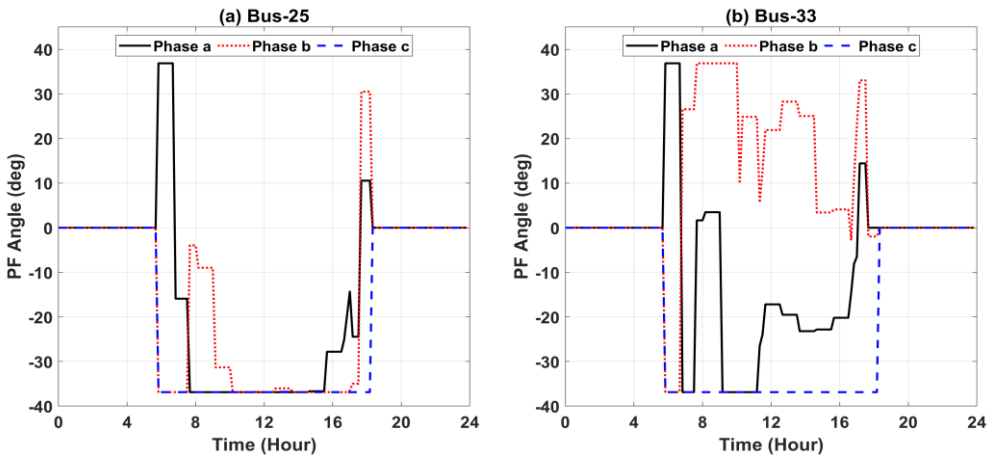

Figure 6.5. The PF angle of the connected two PV inverters

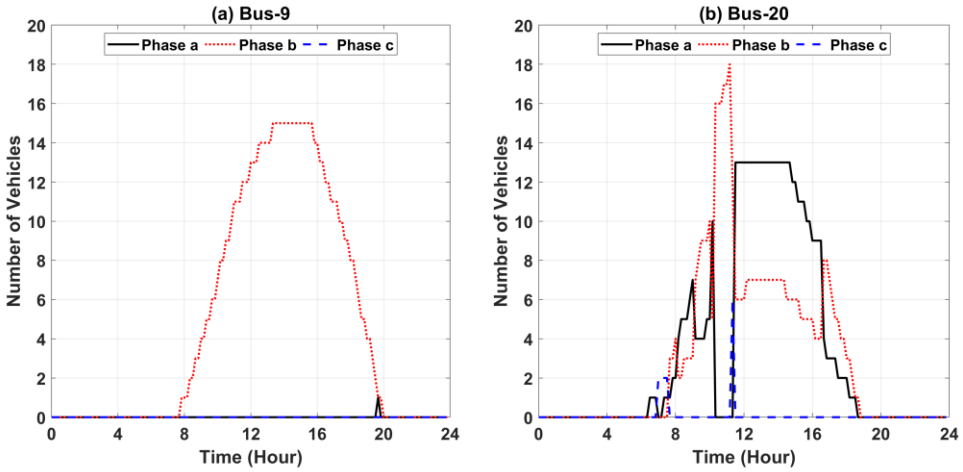

Figure 6.6. Number of connected EVs at each phase at the parking lots

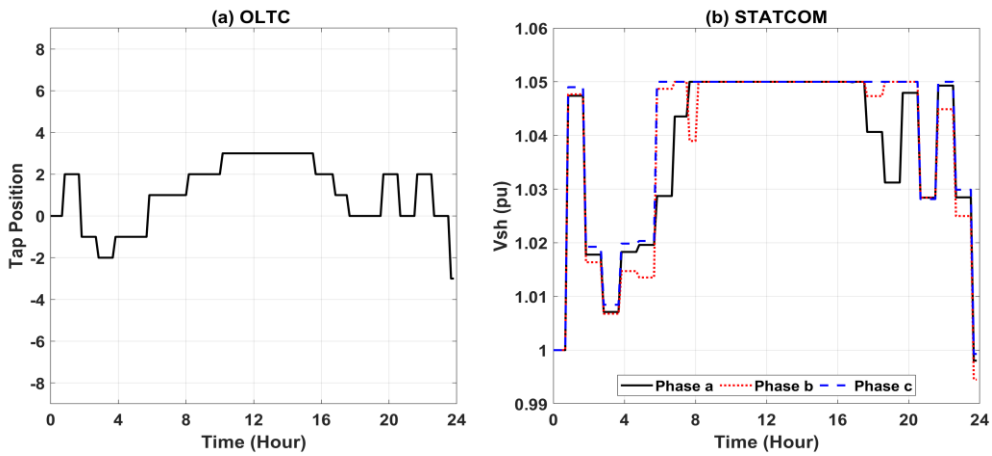

Figure 6.7. Tap position of OLTC and controllable voltage source of STATCOM

To examine the superiority of the developed coordination control approach at different PV penetration levels, the size of the integrated PV systems is increased to reach 100%. Figure 6.8 displays the total energy losses and the recorded upper voltage unbalance level at different PV penetration levels for the different scenarios. It can be noted that in scenario 2, the injection of reactive power from PV inverters and STATCOM to suppress the voltage rise has reduced the voltage unbalance level at high PV penetration levels; however, the power losses increased significantly. For example, at 75% PV penetration level, the total energy losses rise by 45% to decrease the voltage unbalance from 3.12 to 2.29. In contrast to scenario 2, the proposed optimisation scheme manages to reduce the voltage unbalance level to 1.98 at 75% PV penetration level and minimise the total energy

losses by 25%. This indicates that the absence of coordination among various voltage regulation devices can potentially reduce the severity of voltage unbalance but with the cost of increasing the network losses, especially at high PV penetration levels.

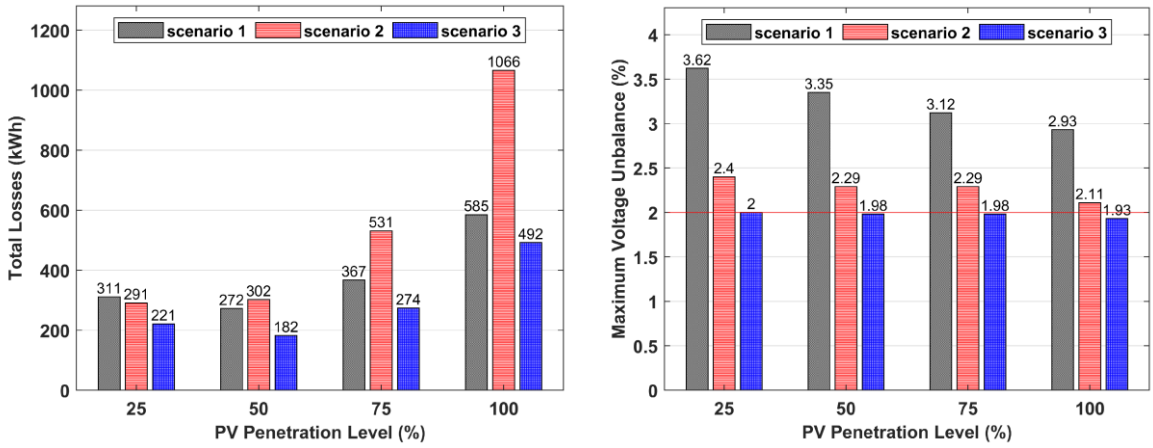

Figure 6.8. Comparison of total energy losses and maximum voltage unbalance

Finally, the proposed control is tested under a different load profile to resemble a diverse situation of the power distribution system where the peak of loads and PVs generation is not synchronised. The new three-phase load profile used in this case study is presented in Figure 6.9, which is based on real-world data in Oman provided by Mazoon Electricity Company (MZEC). It can be seen from Figure 6.10 that at a low PV penetration level (20%), the peak voltage unbalances recorded throughout the day were 3.59 for scenario 1, and 3.31 and 2.09 for scenario 2 and 3, respectively. These values are the same for the different PV penetration levels because they occurred at peak load (18:30), where the PV production is zero. Therefore, the PVs generated power for this type of load profile does not influence the maximum voltage unbalance level, but significantly impacts the overall energy losses. For example, at 100% penetration level, the energy losses per day are increased from 901 kWh to 1303 kWh when adopting the local control of voltage regulation devices, and after adopting the proposed control scheme, the energy losses are reduced to 769 kWh. Therefore, by implementing the proposed coordination scheme, the voltage unbalance is maintained at the standard bounds regardless of PV generation. This concludes that the

proposed coordination scheme can maintain the operational constraints limit in an unbalanced power distribution system under various load and PV generation profiles.

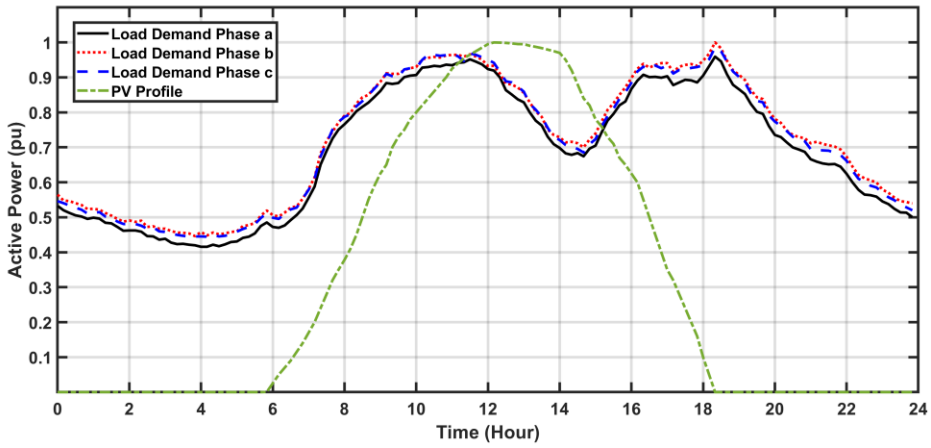

Figure 6.9. Different three-phase load profiles

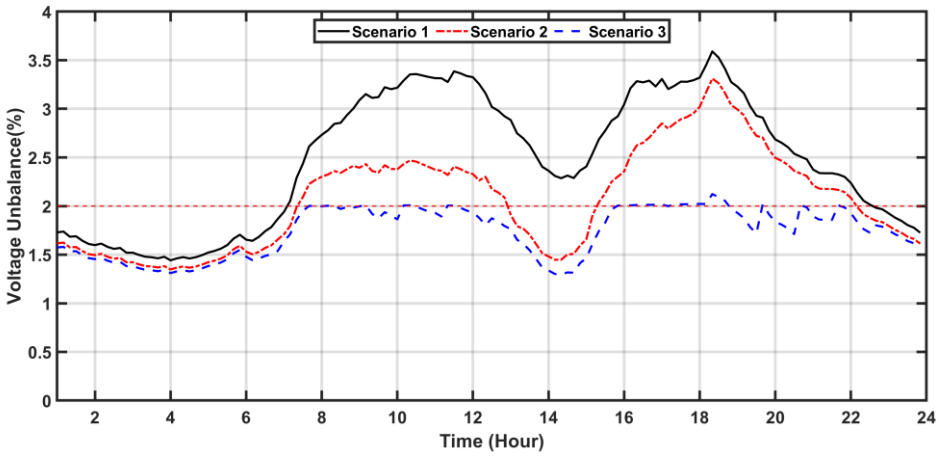

Figure 6.10. Comparison of maximum voltage unbalance recorded during a day

6.5.2 IEEE-123-Bus Test System

To further verify the scalability of the proposed optimisation model on large-scale power distribution systems, a modified IEEE123-bus test system is adopted, as presented in Figure 6.11. In this test system, the voltage unbalance is relatively low compared with the IEEE37-bus test system. For the purpose of the study, some loads were added into phase ‘a’ to increase the percentage of voltage unbalance. All the four voltage regulators are replaced with two OLTC connected between bus 1 and 2 and between bus 65 and 73. All shunt capacitors are replaced with one three-phase STATCOM connected at bus 103. The

locations of the PV systems and EVs are identified on the test system by square and triangle, respectively. All the assumptions and parameters of voltage control used previously are adopted here, considering the same load, PV and EVs profile (Figure 4.7 and Figure 4.8).

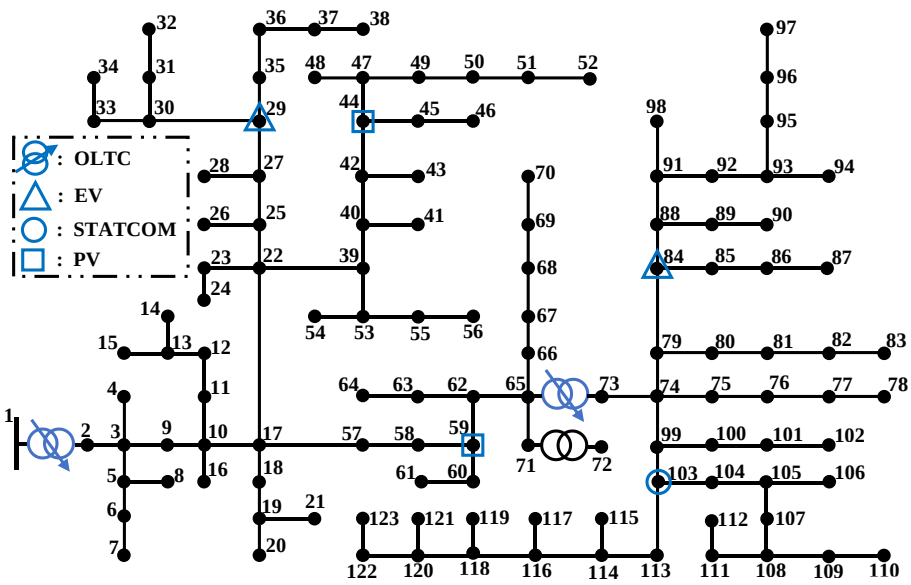

Figure 6.11. The modified IEEE 123-bus test feeder

In this case study, the network was tested under a 30% PV penetration level. Without incorporating voltage regulator devices, it can be observed from Figure 6.12 and Figure 6.13 that the voltage unbalance for almost half of the network nodes start violating the limit between 8:30 and 14:30. Even with incorporating voltage regulator devices that are controlled locally, more than 15 buses violated the standard limit of voltage unbalance. This makes mitigating the voltage unbalance in such a network challenging. To estimate the overall voltage unbalance of the whole system, the system voltage unbalance ($VU\%_{sys.}$) is introduced as follows:

$$VU\%_{sys.} = \sum_{i=1}^{N=123} \sum_{t=0}^{24} (VU\%_i^t)^2 \tag{6.19}$$

where $VU\%_i^t$ is the voltage unbalance factor at time t and at bus i, which can be calculated using equation (3.37).

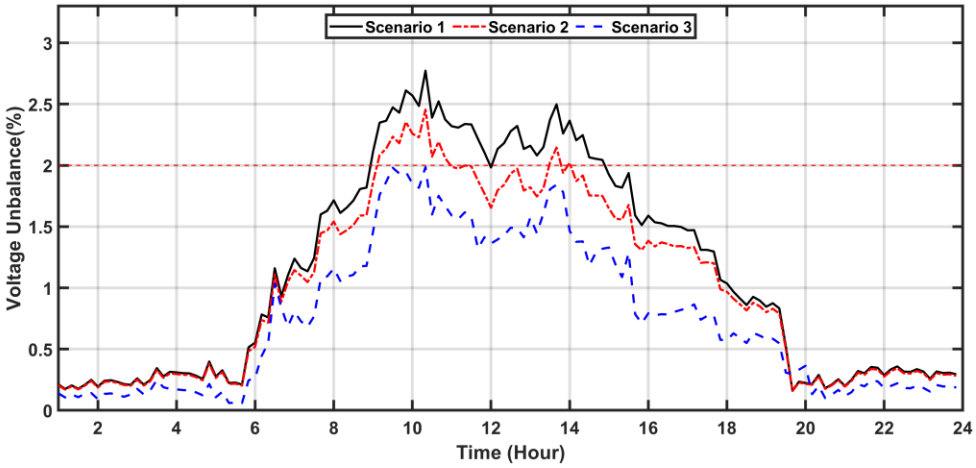

Figure 6.12. Comparison of maximum voltage unbalance recorded during the day

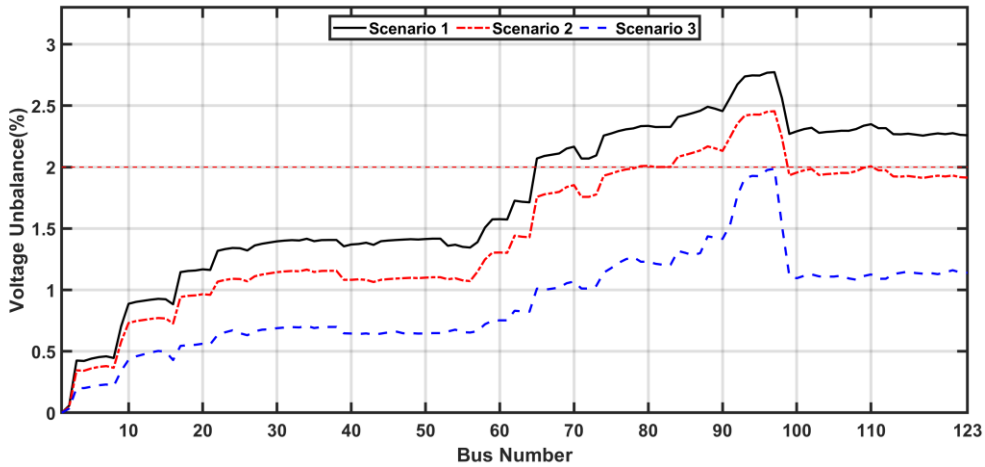

Figure 6.13. Comparison of maximum voltage unbalance recorded at each bus

Table 6.1 and Table 6.2 show the reduction rate of energy losses and the overall system voltage unbalance compared with the base case under 30% and 60% of PV penetration level. Compared with Scenario 1, the voltage unbalance factor for the whole system is reduced by 30.31% and 75.01% in Scenario 2 and Scenario 3, respectively, at 30% penetration level, and by 41% and 80% at 60% PV penetration level. This shows that adopting the proposed optimisation control can significantly improve voltage unbalance and can be twice as effective as local control. On the contrary, in Scenario 2, the network power losses increased in both penetration levels, whereas in Scenario 3, the power losses were reduced by more than 30%. This indicates that voltage unbalance can produce high power losses; however, minimising it does not always minimise power losses if effective

coordination control is missing. It should be pointed out that for all the performed case studies, the corresponding daily average OLTC tap is at most half of the equivalent daily maximum average number of tap changes, verifying the potential of the proposed optimisation model to maintain the operation of OLTC at minimum.

Table 6.1. Comparison of energy losses and $VU\%_{sys}$ reduction rate under 30% PV penetration level

Scenario	Energy Losses (kWh)	Reduction rate of losses (%)	VUF_{sys}	Reduction rate of VUF_{sys} (%)
1	265.78	---	1.4923	---
2	267.76	-0.74	1.0400	30.31
3	181.50	31.71	0.3730	75.01

Table 6.2. Comparison of energy losses and $VU\%_{sys}$ reduction rate under 60% PV penetration level

Scenario	Energy Losses (kWh)	Reduction rate of losses (%)	VUF_{sys}	Reduction rate of VUF_{sys} (%)
1	223.45	---	1.3973	---
2	238.54	-6.75	0.8168	41.54
3	138.81	37.88	0.2777	80.13

6.5.3 Different Optimisation Methods

To evaluate the accuracy and robustness of the developed AHPSO, some well-known optimisation techniques based on other PSO versions are used to solve the proposed optimisation problem. Since the proposed optimisation problem's nature is complex, analytical optimisation methods may not be reliable alternatives. Thus, three other versions of PSO, called pure standard PSO with constriction factor, hybrid PSO and Genetic Algorithm (PSO-GA) [123], and PSO based on Natural Selection (PSO-NS) [125], are considered for verifying the performance of the AHPSO method. A 100 trial runs based on various random initial values are conducted on both test systems, considering 20% of PV

penetration level and the resulting average and Standard Deviation (SD) of fitness value are reported. Table 6.3 and Table 6.4 show a comparison between the objective function values achieved by the different applied heuristic methods on the IEEE-37 test system and the IEEE-123 test system, respectively. The %RSD is the Rational Standard Deviation of the samples and is computed by dividing the standard deviation by the average value. It is employed to check the robustness of optimisation solution methods, where the lower percentage values indicate the solution method is more robust. The %RSD value (i.e., Table 6.3) shows that the proposed AHPSO standard deviation is 0.545% of the average value, which is pretty small compared with other methods. In other words, the optimisation value is tightly clustered around the mean, which means that the optimisation solution will be almost the same at each solution process. On the other hand, if the percentage were large, this would indicate that the objective function value is more spread out.

As observed from Table 6.3, the %RSD of the samples of the AHPSO (0.545%) is lower than other methods (2.831% for pure PSO, 1.307% for PSO-NS, and 1.086% for PSO-GA). Although the %RSD is relatively low for other methods, it can still compromise the network performance efficiency. For example, if we consider a large-scale network with optimised minimum power losses of 6MW, the PSO-GA method can bring an additional of 65.17kW power losses because of its %RSD=1.086%. This demonstrates the higher robustness of the AHPSO with respect to the changes in random initial values compared with the other three heuristic methods. It can also be noted for Table 6.4 that the average value (24.197) obtained by the AHPSO method on the IEEE-37 test system is very close to the best value (24.166) that was recorded during the whole trial, which also shows the superiority of the proposed method. Moreover, even at a large network scale, where the number of searching space and variables increase, the proposed optimisation solution method performs much better than other methods.

Table 6.3. Comparison of objective values for different optimisation methods on the IEEE-37 test system

	PSO	PSO-NS	PSO-GA	Proposed AHPSO
Best	27.751	27.751	27.751	**27.751**
Worst	31.356	29.307	29.110	**28.562**
Average	28.333	27.975	27.901	**27.828**
SD	0.802	0.365	0.303	**0.152**
%RSD	2.831	1.307	1.086	**0.545**

Table 6.4. Comparison of objective values for different optimisation methods on the IEEE-123 test system

	PSO	PSO-NS	PSO-GA	Proposed AHPSO
Best	24.166	24.166	24.166	**24.166**
Worst	26.214	25.010	25.154	**24.490**
Average	24.358	24.270	24.240	**24.197**
SD	0.268	0.158	0.143	**0.062**
%RSD	1.102	0.649	0.589	**0.258**

6.6 Summary

New coordination strategies are necessary to combat the challenges associated with the growing number of RET connections in an unbalanced power distribution system. This chapter has proposed an advanced coordination scheme between OLTC, STATCOM, PVs, and EVs to effectively maintain the network operational constraints within the standard limit while minimising the overall power losses. A new advanced hybrid particle swarm optimisation (AHPSO) was also developed to solve the optimisation problem, and its robustness was verified. Various case studies considering typical PV power generation and load demand data demonstrated the proposed approach's strength and scalability to alleviate voltage unbalance, limit the OLTC actions and reduce power losses under various PV penetration levels.

The investigation presented throughout this chapter emphasise the challenges and the opportunities of unbalanced voltage regulation in modern power distribution integrated with increased PVs and EVs. The autonomous-based control shows a lack of detecting the network voltage unbalance problem and sometimes can deteriorate its level. Moreover, in the extreme RETs penetration level, the autonomous-based control of reactive power compensator has caused network power losses to increase significantly. On the other hand, implementing a centralised-based control scheme has provided a monitoring and controlling platform and has presented the most potential benefits from an economical operation and voltage regulation perspective. Therefore, adopting such a scheme with an improved optimisation technique can further help the power distribution system operators to deliver efficient, secure, and reliable electric power to the end-users.

It should be pointed out that the cost analysis of adopting the proposed coordination scheme was not the focus of this research study. A cost-benefit assessment was not conducted for the developed approach basically because currently, some of the devices involved in centralised-based control, such as static transfer switches, are not commercially available in the market. Moreover, the cost-benefit resulting from minimising the voltage unbalance cannot accurately be quantified because of its long-term impact. However, as the need for centralised-based control devices rises and becomes available in the market, their prices will drop considerably. Moreover, as a result of providing a better power quality in the network and power losses reduction, the proposed centralised controls may become more cost-effective by also considering the investment that has already been adopted on the widespread two-way communication infrastructure and smart meters.

Chapter 7: Conclusions and Future Work

The expansion of grid-tied PV systems and EVs attached with their high propensity to provoke undesirable behaviours such as high voltage unbalance level calls for advanced management strategies for power distribution systems. Therefore, this thesis presented a comprehensive investigation of PVs and EVs connection on modern power distribution systems and proposed advanced approaches to leverage their connection, mitigate, and manage their adverse impacts. The chapter presents the conclusions of the research work followed by an outlining of possible future work opportunities.

7.1 Conclusions

The present power distribution systems are experiencing a transition toward an environmentally friendly connection of components due to growing concerns about climate change effects and seeking alternative energy sources. However, the increased integration and sudden influx of electrically coupled RETs, including PV systems and EVs, has introduced a number of operational challenges to the power distribution systems. Mainly, they can deteriorate the voltage balance, voltage rise and assets overloading, which is becoming increasingly common in renewable-rich distribution networks. To address these issues, this thesis presented investigations of the solutions to mitigate the detrimental impact of PV and EV connections to power distribution systems by developing novel frameworks and futuristic strategies that can support the transition of power distribution system paradigms. However, several technical obstacles need to be addressed before such schemes can be readily integrated into the actual power distribution system. These obstacles correspond to the limitations in load flow calculations and optimisation techniques tools that are involved in real-time monitoring and control of power distribution systems.

Therefore, this thesis first developed an alternative load flow calculation method (referred to as TPCIM) that is more suitable for the application of real-time control and management of a modern power distribution system that requires rapid and accurate analysis for decision making. Then, a new robust three-phase modelling of various modern power system components, including EV loads, SVC and STATCOM was developed, and their influence connection was investigated. The investigation shows the potential capability of the reactive power control of the PV inverters in reducing the severity of voltage unbalances, but they need a novel control strategy to keep the voltage unbalance level below the elevating levels. Therefore, an advanced step-based reactive power control of PV inverter was proposed to leverage the PVs system connection by allowing them to regulate the unbalanced voltage at the same time preserving the PV inverter from deteriorating. However, the proposed control has a limiting influence on the voltage at remote nodes and can cause additional power losses due to high PV penetration levels. To tackle these limitations, the thesis finally proposed a comprehensive coordination scheme between RETs and various voltage regulation devices. The coordination scheme provides the optimal setpoint of these devices to mainly minimise the total active power losses in the system while complying with operating and control variable constraints, such as voltage unbalance level and frequent operation of OLTC. As part of the coordination scheme, a new advanced hybrid particle swarm optimisation (AHPSO) was also developed to solve the proposed optimisation problem with improved accuracy and convergence.

The investigation presented throughout this thesis highlights that the random and uncoordinated connection between PVs and EVs can sometimes negatively impact the operation of the power distribution system. The PVs and EVs connection can heighten the unbalanced voltage level and operation strain to other voltage control devices (e.g., voltage regulator and capacitor bank). Moreover, at extreme PV penetration level, the autonomous

control of reactive power compensator has caused network power losses to increase significantly. All these sequences can threaten the efficient, economical and reliable operation of modern power distribution systems. Furthermore, the thesis findings provide an insight into the potential of RETs in voltage management, which could be beneficial to power distribution system operators and policymakers. For example, it has been found that extending the power factor operation range of PV inverter can provide adequate unbalanced voltage regulation. In addition, voltages rise at buses are not only the constraining factor for PV expansion but also increased network power losses can be what constraints PVs utilisation. Finally, the investigation illustrated the impact of inter-phase coupling between distribution lines on voltage regulation and revealed the necessity of considering an accurate unbalanced load flow calculation. For instance, due to unbalanced line coupling, the injection of power or connection of EVs in one phase can also affect the voltage magnitude of the other two phases, which cannot be counted while considering traditional balanced load flow calculation. Therefore, these findings provide an understanding of the challenges confronting the operation of the modern power distribution system and the necessity of implementing a centralised-based control scheme.

To this end, the research work presented in this thesis significantly contributes to the knowledge in the field of modern power distribution system modelling and voltage management. Firstly, a fast and accurate three-phase power-flow calculation tool was developed, which represents the kernel of the real-time management and control of power distribution systems. This also has led to developing robust models of some modern power components to suit the developed unbalanced load flow calculation, namely, STATCOM, SVC and EVs. Such an advanced load flow calculation method is helpful to accurately quantify the impact of RETs connections and assess the different approaches to address the power quality problem in unbalanced power distribution systems. This kind of assessment

could help the power distribution system operators to identify the best approaches to address the unbalanced voltage regulation problem, such as determining the best location of EVs charging stations and PV systems connection. Consequently, this has resulted in proposing a new control scheme of PV inverter that contributes to unbalanced voltage regulation while reducing the operation strain of the inverters. This could be an alternative approach for unbalanced voltage regulation requiring minimum investment, fast response and allowing more PVs system integration.

Furthermore, due to the improved computing time and reduced number of iterations, the developed load flow calculation becomes more suitable for real-time management and control applications, requiring a rapid computation time. Therefore, the application of developed unbalanced load flow calculation yielded to propose a comprehensive coordination scheme that tackles the unbalanced voltage regulation issue in modern power distribution systems integrated with a high level of RETs. The developed coordination scheme aims to facilitate a large number of RET connections and, at the same time leading to an effective and economic operation of the systems by mitigating voltage unbalance problems, minimising the OLTC actions, and overall network energy losses. This approach will potentially attract interest to the renewable-rich power distribution system operators, which makes PV systems and EVs a promising solution to ensure environmental sustainability and decrease reliance on fossil fuels. Finally, an advanced PSO (AHPSO) method that incorporates two state of the art versions of PSO was proposed to solve the multi-objective optimisation problems involved in the proposed coordination scheme. Such advanced optimisation technique demonstrates robustness in terms of accuracy, either for small or large power distribution systems, which could be considered a powerful alternative optimisation technique for optimising complex power system structures coupled with various controllable devices.

7.2 Future Work

The research work presented in this thesis includes various aspects related to the need for an effective modelling and control methodology to meet the active distribution network transition challenge robustly. These aspects focus on the unbalanced voltage regulation of modern power distribution systems integrated with three-phase PV inverters and semi-fast EV charging stations. However, there are other opportunities that can be investigated with continuous advancement in the modern power distribution system. The possible future research areas are listed as follows:

- The cost-benefit analysis from adopting a centralised control scheme could be performed. Deployment of a centralised control scheme requires metering and communication infrastructure, which might need a substantial investment. However, it would be interesting to study cost-benefit from voltage unbalance and power losses reduction perspective. Higher voltage unbalance levels can derate electrical equipment, affect their lifetime and increase the associated power losses, which need to be accurately qualified. Moreover, the daily power losses can be significantly minimised by utilising centralised-based control, and the saving cost-benefit can be enormous as the penetration level of PV increases. Therefore, a comprehensive cost-benefit analysis could provide technical feasibility to the proposed control scheme in future work.
- Using energy storage systems in voltage regulation could be an interesting field study to expand the scope of the research work. An energy storage system can be added in a specific location to store excessive PVs generated power and allow more PVs penetration levels. It can be an alternative approach to the reactive power management of PV inverters to reduce the severity of voltage unbalance, especially during the day-night when there is no PV power generation. Moreover, the coordination scheme employed in this research can be improved to incorporate energy storage systems and

investigate their significance with the presence of EVs and PVs on the power distribution system after being accurately modelled and economically justified.

- The connection of a three-phase PV system and semi-fast EV charging stations are only considered in this thesis; however, a single-phase PV system and other types of charging stations can also be available on the power distribution system. Although their integration might have a relatively small impact on the operation, their widespread might be a problem that needs to be investigated. Moreover, new power electronic-based devices have been recently proposed as an alternative to traditional power equipment such as solid state transformer. These new devices might need to be modelled for unbalanced load flow calculation and real-time application.
- This thesis considers only the steady-state characteristic behaviour of PVs and EVs for unbalanced voltage regulation studies since the unbalanced voltage is a steady-state parameter of the network and is estimated at 10 minutes intervals. Besides that, the PV power generations and loads profile captured at a step of 10-minute were used for the case studies. Therefore, PVs and EVs behaviour, such as the impact of the fast-moving cloud, was not investigated in this thesis and could be an area of interest for future research work.
- The optimal location of RETs infrastructure and voltage regulation device can also be considered as other key factors of minimising the severity of voltage unbalances problems and increasing the uptaking of renewable energy sources. Therefore, the developed unbalanced load flow calculation and optimisation technique could be used to identify and investigate the optimal location of EV charging stations and PV systems connections in future work.

References

[1] W. H. Kersting, *Distribution System Modeling and Analysis, Fourth Edition*. CRC Press, 2017.

[2] A. Rodriguez-Calvo, R. Cossent, and P. Frías, "Integration of PV and EVs in unbalanced residential LV networks and implications for the smart grid and advanced metering infrastructure deployment," *Int. J. Electr. Power Energy Syst.*, vol. 91, pp. 121–134, 2017.

[3] M. A. A. Al-Jaafreh and G. Mokryani, "Planning and operation of LV distribution networks: A comprehensive review," *IET Energy Syst. Integr.*, vol. 1, no. 3, pp. 133–146, 2019.

[4] IRENA (2019), "Future of Solar Photovoltaic: Deployment, investment, technology, grid integration and socio-economic aspects (A Global Energy Transformation: paper)," International Renewable Energy Agency, Abu Dhabi.

[5] "ITF Transport Outlook 2017," OECD, Paris, Jan. 2017.

[6] K. Bell and S. Gill, "Delivering a highly distributed electricity system: Technical, regulatory and policy challenges," *Energy Policy*, vol. 113, pp. 765–777, 2018.

[7] N. Mahmud and A. Zahedi, "Review of control strategies for voltage regulation of the smart distribution network with high penetration of renewable distributed generation," *Renew. Sustain. Energy Rev.*, vol. 64, pp. 582–595, 2016.

[8] A. Tavakoli, S. Saha, M. T. Arif, M. E. Haque, N. Mendis, and A. M. T. Oo, "Impacts of grid integration of solar PV and electric vehicle on grid stability, power quality and energy economics: a review," *IET Energy Syst. Integr.*, vol. 2, no. 3, pp. 243–260, 2019.

[9] A. M. M. Nour, A. Y. Hatata, A. A. Helal, and M. M. El-Saadawi, "Review on voltage-violation mitigation techniques of distribution networks with distributed rooftop PV systems," *IET Gener. Transm. Distrib.*, vol. 14, no. 3, pp. 349 – 361, 2020.

[10] W. Murray, M. Adonis, and A. Raji, "Voltage control in future electrical distribution networks," *Renew. Sustain. Energy Rev.*, vol. 146, p. 111100, 2021.

[11] D. C. Kullay Reddy, S. S. Narayana, and V. Ganesh, "Towards an enhancement of power quality in the distribution system with the integration of BESS and FACTS device," *Int. J. Ambient Energy*, pp. 1–9, 2019.

[12] S. A. A. Kazmi, M. K. Shahzad, A. Z. Khan, and D. R. Shin, "Smart distribution networks: A review of modern distribution concepts from a planning perspective," *Energies*, vol. 10, no. 4, p. 501, 2017.

[13] O. Gandhi, D. S. Kumar, C. D. Rodríguez-Gallegos, and D. Srinivasan, "Review of power system impacts at high PV penetration Part I: Factors limiting PV penetration," *Sol. Energy*, vol. 210, pp. 181–201, 2020.

[14] D. S. Kumar, O. Gandhi, C. D. Rodríguez-Gallegos, and D. Srinivasan, "Review of power system impacts at high PV penetration Part II: Potential solutions and the way forward," *Sol. Energy*, vol. 210, pp. 202–221, 2020.

[15] E. Mohagheghi, M. Alramlawi, A. Gabash, and P. Li, "A survey of real-time optimal power flow," *Energies*, vol. 11, no. 11, p. 3142, 2018.

[16] A. Ehsan and Q. Yang, "State-of-the-art techniques for modelling of uncertainties in

active distribution network planning: A review," *Appl. Energy*, vol. 239, pp. 1509–1523, 2019.

[17] N. Daratha, B. Das, and J. Sharma, "Coordination between OLTC and SVC for voltage regulation in unbalanced distribution system distributed generation," *IEEE Trans. Power Syst.*, vol. 29, no. 1, pp. 289–299, 2013.

[18] F. Zhao, T. Zhao, Y. Ju, K. Ma, and X. Zhou, "Research on three-phase optimal power flow for distribution networks based on constant Hessian matrix," *IET Gener. Transm. Distrib.*, vol. 12, no. 1, pp. 241–246, 2018.

[19] M. Nour, J. P. Chaves-Ávila, G. Magdy, and Á. Sánchez-Miralles, "Review of positive and negative impacts of electric vehicles charging on electric power systems," *Energies*, vol. 13, no. 18, p. 4675, 2020.

[20] T.-H. Chen, C.-H. Yang, and N.-C. Yang, "Examination of the definitions of voltage unbalance," *Int. J. Electr. Power Energy Syst.*, vol. 49, pp. 380–385, 2013.

[21] C. Mateo *et al.*, "European representative electricity distribution networks," *Int. J. Electr. Power Energy Syst.*, vol. 99, pp. 273–280, 2018.

[22] C. on C. Change, "Net Zero: The UK's Contribution to Stopping Global Warming." Committee on Climate Change London, 2019.

[23] S. Bruno, S. Lamonaca, G. Rotondo, U. Stecchi, and M. La Scala, "Unbalanced three-phase optimal power flow for smart grids," *IEEE Trans. Ind. Electron.*, vol. 58, no. 10, pp. 4504–4513, 2011.

[24] F. Shahnia, A. Ghosh, G. Ledwich, and F. Zare, "Voltage unbalance improvement in low voltage residential feeders with rooftop PVs using custom power devices," *Int. J. Electr. Power Energy Syst.*, vol. 55, pp. 362–377, 2014.

[25] N. Hashemipour *et al.*, "Multi-objective optimisation method for coordinating battery storage systems, photovoltaic inverters and tap changers," *IET Renew. Power Gener.*, vol. 14, no. 3, pp. 475–483, 2020.

[26] M. M. Rahman, A. Arefi, G. M. Shafiullah, and S. Hettiwatte, "A new approach to voltage management in unbalanced low voltage networks using demand response and OLTC considering consumer preference," *Int. J. Electr. Power Energy Syst.*, vol. 99, pp. 11–27, 2018.

[27] A. M. Howlader, S. Sadoyama, L. R. Roose, and Y. Chen, "Active power control to mitigate voltage and frequency deviations for the smart grid using smart PV inverters," *Appl. Energy*, vol. 258, p. 114000, 2020.

[28] M. Zeraati, M. E. H. Golshan, and J. M. Guerrero, "Voltage Quality Improvement in Low Voltage Distribution Networks Using Reactive Power Capability of Single-Phase PV Inverters," *IEEE Trans. Smart Grid*, vol. 10, no. 5, pp. 5057–5065, 2019.

[29] G. Dileep, "A survey on smart grid technologies and applications," *Renew. Energy*, vol. 146, pp. 2589–2625, 2020.

[30] L. A. Wolsey and G. L. Nemhauser, *Integer and combinatorial optimization*, vol. 55. John Wiley & Sons, 1999.

[31] C. Li, V. R. Disfani, H. V. Haghi, and J. Kleissl, "Coordination of OLTC and smart inverters for optimal voltage regulation of unbalanced distribution networks," *Electr. Power Syst. Res.*, vol. 187, p. 106498, 2020.

[32] M. M. Haque and P. Wolfs, "A review of high PV penetrations in LV distribution networks: Present status, impacts and mitigation measures," *Renew. Sustain. Energy Rev.*, vol. 62, pp. 1195–1208, 2016.

[33] S. Deb, K. Tammi, K. Kalita, and P. Mahanta, “Impact of electric vehicle charging station load on distribution network,” *Energies*, vol. 11, no. 1, p. 178, 2018.

[34] A. Kharrazi, V. Sreeram, and Y. Mishra, “Assessment techniques of the impact of grid-tied rooftop photovoltaic generation on the power quality of low voltage distribution network-A review,” *Renew. Sustain. Energy Rev.*, vol. 120, p. 109643, 2020.

[35] C. H. Dharmakeerthi, N. Mithulananthan, and T. K. Saha, “Impact of electric vehicle fast charging on power system voltage stability,” *Int. J. Electr. Power Energy Syst.*, vol. 57, pp. 241–249, 2014.

[36] M. Karimi, H. Mokhlis, K. Naidu, S. Uddin, and A. H. A. Bakar, “Photovoltaic penetration issues and impacts in distribution network–A review,” *Renew. Sustain. Energy Rev.*, vol. 53, pp. 594–605, 2016.

[37] J. Pahasa and I. Ngamroo, “PHEVs bidirectional charging/discharging and SoC control for microgrid frequency stabilization using multiple MPC,” *IEEE Trans. Smart Grid*, vol. 6, no. 2, pp. 526–533, 2014.

[38] H. F. Farahani, “Improving voltage unbalance of low-voltage distribution networks using plug-in electric vehicles,” *J. Clean. Prod.*, vol. 148, pp. 336–346, 2017.

[39] F. Shahnia, A. Ghosh, G. Ledwich, and F. Zare, “Predicting voltage unbalance impacts of plug-in electric vehicles penetration in residential low-voltage distribution networks,” *Electr. Power Components Syst.*, vol. 41, no. 16, pp. 1594–1616, 2013.

[40] T. Chen *et al.*, “A review on electric vehicle charging infrastructure development in the uk,” *J. Mod. Power Syst. Clean Energy*, vol. 8, no. 2, pp. 193–205, 2020.

[41] M. R. Islam, H. Lu, M. J. Hossain, and L. Li, “Mitigating unbalance using distributed network reconfiguration techniques in distributed power generation grids with services for electric vehicles: A review,” *J. Clean. Prod.*, p. 117932, 2019.

[42] F. Shahnia, R. Majumder, A. Ghosh, G. Ledwich, and F. Zare, “Voltage imbalance analysis in residential low voltage distribution networks with rooftop PVs,” *Electr. Power Syst. Res.*, vol. 81, no. 9, pp. 1805–1814, 2011.

[43] L. Wang, R. Yan, and T. K. Saha, “Voltage regulation challenges with unbalanced PV integration in low voltage distribution systems and the corresponding solution,” *Appl. Energy*, vol. 256, p. 113927, 2019.

[44] K. Ma, L. Fang, and W. Kong, “Review of distribution network phase unbalance: Scale, causes, consequences, solutions, and future research directions,” *CSEE J. Power Energy Syst.*, vol. 6, no. 3, pp. 479–488, 2020.

[45] K. Ma, R. Li, and F. Li, “Utility-scale estimation of additional reinforcement cost from three-phase imbalance considering thermal constraints,” *IEEE Trans. Power Syst.*, vol. 32, no. 5, pp. 3912–3923, 2016.

[46] W. Kong, K. Ma, and F. Li, “Probabilistic impact assessment of phase power imbalance in the LV networks with increasing penetrations of low carbon technologies,” *Electr. Power Syst. Res.*, vol. 202, p. 107607, 2022.

[47] M. T. Bina and A. Kashefi, “Three-phase unbalance of distribution systems: Complementary analysis and experimental case study,” *Int. J. Electr. Power Energy Syst.*, vol. 33, no. 4, pp. 817–826, 2011.

[48] J. Faiz, H. Ebrahimpour, and P. Pillay, “Influence of unbalanced voltage supply on efficiency of three phase squirrel cage induction motor and economic analysis,” *Energy Convers. Manag.*, vol. 47, no. 3, pp. 289–302, 2006.

[49] I. S. Association, “141-1993. IEEE Recommended Practice for Electric Power

Distribution for Industrial Plants (ANSI).” IEEE Press, 1994.

[50] M. Campbell and G. Arce, “Effect of motor voltage unbalance on motor vibration: Test and evaluation,” *IEEE Trans. Ind. Appl.*, vol. 54, no. 1, pp. 905–911, 2017.

[51] Z. Liu and J. V Milanović, “Probabilistic estimation of voltage unbalance in MV distribution networks with unbalanced load,” *IEEE Trans. Power Deliv.*, vol. 30, no. 2, pp. 693–703, 2014.

[52] T. Gönen, *Electric power distribution system engineering*, vol. 2. CRC press Boca Raton, 2008.

[53] M. E. Khodayar, M. R. Feizi, and A. Vafamehr, “Solar photovoltaic generation: Benefits and operation challenges in distribution networks,” *Electr. J.*, vol. 32, no. 4, pp. 50–57, 2019.

[54] S. Hashemi and J. Østergaard, “Methods and strategies for overvoltage prevention in low voltage distribution systems with PV,” *IET Renew. Power Gener.*, vol. 11, no. 2, pp. 205–214, 2017.

[55] P. Chaudhary and M. Rizwan, “Voltage regulation mitigation techniques in distribution system with high PV penetration: A review,” *Renew. Sustain. Energy Rev.*, vol. 82, pp. 3279–3287, 2018.

[56] S. M. Ismael, S. H. E. A. Aleem, A. Y. Abdelaziz, and A. F. Zobaa, “State-of-the-art of hosting capacity in modern power systems with distributed generation,” *Renew. energy*, vol. 130, pp. 1002–1020, 2018.

[57] K. Wang, S. Skiena, and T. G. Robertazzi, “Phase balancing algorithms,” *Electr. Power Syst. Res.*, vol. 96, pp. 218–224, Mar. 2013.

[58] D. Pudjianto *et al.*, “Smart control for minimizing distribution network reinforcement cost due to electrification,” *Energy Policy*, vol. 52, pp. 76–84, 2013.

[59] L. Fang, K. Ma, and X. Zhang, “A statistical approach to guide phase swapping for data-scarce low voltage networks,” *IEEE Trans. Power Syst.*, vol. 35, no. 1, pp. 751–761, 2019.

[60] S. S. M. Reshikeshan, S. L. Matthiesen, M. S. Illindala, A. A. Renjit, and R. Roychowdhury, “Autonomous voltage regulation by distributed PV inverters with minimal inter-node interference,” *IEEE Trans. Ind. Appl.*, vol. 57, no. 3, pp. 2058–2066, 2021.

[61] M. Zeraati, M. E. H. Golshan, and J. M. Guerrero, “Distributed Control of Battery Energy Storage Systems for Voltage Regulation in Distribution Networks With High PV Penetration,” *IEEE Trans. Smart Grid*, vol. 9, no. 4, pp. 3582–3593, 2018.

[62] Y. Naderi, S. H. Hosseini, S. G. Zadeh, B. Mohammadi-Ivatloo, J. C. Vasquez, and J. M. Guerrero, “An overview of power quality enhancement techniques applied to distributed generation in electrical distribution networks,” *Renew. Sustain. Energy Rev.*, vol. 93, pp. 201–214, 2018.

[63] S. Xu *et al.*, “Application Examples of STATCOM,” *Flex. AC Transm. Syst. FACTS*, pp. 511–584, 2020.

[64] D. G. Photovoltaics and E. Storage, “IEEE standard for interconnection and interoperability of distributed energy resources with associated electric power systems interfaces,” *IEEE Std*, pp. 1547–2018, 2018.

[65] R. Tonkoski, L. A. C. Lopes, and T. H. M. El-Fouly, “Coordinated Active Power Curtailment of Grid Connected PV Inverters for Overvoltage Prevention,” *IEEE Trans. Sustain. Energy*, vol. 2, no. 2, pp. 139–147, 2011.

[66] S. Paudyal, B. P. Bhattarai, R. Tonkoski, S. Dahal, and O. Ceylan, “Comparative Study of Active Power Curtailment Methods of PVs for Preventing Overvoltage on Distribution Feeders,” in *2018 IEEE Power & Energy Society General Meeting (PESGM)*, 2018, pp. 1–5.

[67] P. Jahangiri and D. C. Aliprantis, “Distributed Volt/VAr Control by PV Inverters,” *IEEE Trans. Power Syst.*, vol. 28, no. 3, pp. 3429–3439, 2013.

[68] M. J. E. Alam, K. M. Muttaqi, and D. Sutanto, “A Multi-Mode Control Strategy for VAr Support by Solar PV Inverters in Distribution Networks,” *IEEE Trans. Power Syst.*, vol. 30, no. 3, pp. 1316–1326, 2015.

[69] H. Li, C. Wen, K.-H. Chao, and L.-L. Li, “Research on Inverter Integrated Reactive Power Control Strategy in the Grid-Connected PV Systems,” *Energies*, vol. 10, no. 7, p. 912, 2017.

[70] A. Momeneh, M. Castilla, J. Miret, P. Martí, and M. Velasco, “Comparative study of reactive power control methods for photovoltaic inverters in low-voltage grids,” *IET Renew. Power Gener.*, vol. 10, no. 3, pp. 310–318, 2016.

[71] D. Chathurangi, U. Jayatunga, S. Perera, A. P. Agalgaonkar, and T. Siyambalapitiya, “Comparative evaluation of solar PV hosting capacity enhancement using Volt-VAr and Volt-Watt control strategies,” *Renew. Energy*, vol. 117, pp. 1063–1075, 2021.

[72] R. M. Kamel, “New inverter control for balancing standalone micro-grid phase voltages: A review on MG power quality improvement,” *Renew. Sustain. Energy Rev.*, vol. 63, pp. 520–532, 2016.

[73] J. M. S. Callegari, M. P. Silva, R. C. de Barros, E. M. S. Brito, A. F. Cupertino, and H. A. Pereira, “Lifetime evaluation of three-phase multifunctional PV inverters with reactive power compensation,” *Electr. Power Syst. Res.*, vol. 175, p. 105873, 2019.

[74] A. El-Naggar and I. Erlich, “Control approach of three-phase grid connected PV inverters for voltage unbalance mitigation in low-voltage distribution grids,” *IET Renew. Power Gener.*, vol. 10, no. 10, pp. 1577–1586, 2016.

[75] D. V Bozalakov, J. Laveyne, J. Desmet, and L. Vandevelde, “Overvoltage and voltage unbalance mitigation in areas with high penetration of renewable energy resources by using the modified three-phase damping control strategy,” *Electr. Power Syst. Res.*, vol. 168, pp. 283–294, 2019.

[76] F. Olivier, P. Aristidou, D. Ernst, and T. Van Cutsem, “Active Management of Low-Voltage Networks for Mitigating Overvoltages Due to Photovoltaic Units,” *IEEE Trans. Smart Grid*, vol. 7, no. 2, pp. 926–936, 2016.

[77] T. T. Mai, A. N. M. M. Haque, P. P. Vergara, P. H. Nguyen, and G. Pemen, “Adaptive coordination of sequential droop control for PV inverters to mitigate voltage rise in PV-Rich LV distribution networks,” *Electr. Power Syst. Res.*, p. 106931, 2020.

[78] N. Safitri, F. Shahnia, and M. A. S. Masoum, “Coordination of single-phase rooftop PVs in unbalanced three-phase residential feeders for voltage profiles improvement,” *Aust. J. Electr. Electron. Eng.*, vol. 13, no. 2, pp. 77–90, 2016.

[79] K. Turitsyn, P. Sulc, S. Backhaus, and M. Chertkov, “Options for control of reactive power by distributed photovoltaic generators,” *Proc. IEEE*, vol. 99, no. 6, pp. 1063–1073, 2011.

[80] L. Wang, R. Yan, F. Bai, T. K. Saha, and K. Wang, “A Distributed inter-phase coordination algorithm for voltage control with unbalanced PV integration in LV systems,” *IEEE Trans. Sustain. Energy*, vol. 11, no. 4, pp. 2687–2697, 2020.

[81] C. Li, V. R. Disfani, Z. K. Pecenak, S. Mohajeryami, and J. Kleissl, “Optimal OLTC

voltage control scheme to enable high solar penetrations," *Electr. Power Syst. Res.*, vol. 160, pp. 318–326, 2018.

[82] V. V. V. S. N. Murty and A. K. Sharma, "Optimal coordinate control of OLTC, DG, D-STATCOM, and reconfiguration in distribution system for voltage control and loss minimization," *Int. Trans. Electr. Energy Syst.*, vol. 29, no. 3, p. e2752, 2019.

[83] F. Meng, B. Chowdhury, and M. S. Hossan, "Optimal integration of DER and SST in active distribution networks," *Int. J. Electr. Power Energy Syst.*, vol. 104, pp. 626–634, 2019.

[84] K. Alboaouh and S. Mohagheghi, "Voltage, var and watt optimization for a distribution system with high PV penetration: A probabilistic study," *Electr. Power Syst. Res.*, vol. 180, p. 106159, 2020.

[85] N. Efkarpidis, T. De Rybel, and J. Driesen, "Optimization control scheme utilizing small-scale distributed generators and OLTC distribution transformers," *Sustain. Energy, Grids Networks*, vol. 8, pp. 74–84, 2016.

[86] W. G. C. Bandara, G. Godaliyadda, M. P. B. Ekanayake, and J. B. Ekanayake, "Coordinated photovoltaic re-phasing: A novel method to maximize renewable energy integration in low voltage networks by mitigating network unbalances," *Appl. Energy*, vol. 280, p. 116022, 2020.

[87] F. Shahnia, P. J. Wolfs, and A. Ghosh, "Voltage unbalance reduction in low voltage feeders by dynamic switching of residential customers among three phases," *IEEE Trans. Smart Grid*, vol. 5, no. 3, pp. 1318–1327, 2014.

[88] A. Ameli, A. Ahmadifar, M.-H. Shariatkhah, M. Vakilian, and M.-R. Haghifam, "A dynamic method for feeder reconfiguration and capacitor switching in smart distribution systems," *Int. J. Electr. Power Energy Syst.*, vol. 85, pp. 200–211, 2017.

[89] N. Gupta, A. Swarnkar, and K. R. Niazi, "A novel strategy for phase balancing in three-phase four-wire distribution systems," in *2011 IEEE Power and Energy Society General Meeting*, 2011, pp. 1–7.

[90] N. Jabalameli and A. Ghosh, "Online Centralized Coordination of Charging and Phase Switching of PEVs in Unbalanced LV Networks With High PV Penetrations," *IEEE Syst. J.*, vol. 15, no. 1, pp. 1015–1025, 2021.

[91] M. R. Islam, H. Lu, J. Hossain, and L. Li, "Multiobjective Optimization Technique for Mitigating Unbalance and Improving Voltage Considering Higher Penetration of Electric Vehicles and Distributed Generation," *IEEE Syst. J.*, vol. 14, no. 3, pp. 3676–3686, 2020.

[92] U. Ghatak and V. Mukherjee, "An improved load flow technique based on load current injection for modern distribution system," *Int. J. Electr. Power Energy Syst.*, vol. 84, pp. 168–181, 2017.

[93] W. H. Kresting and D. L. Mendive, "An application of ladder network theory to the solution of three phase radial load flow problem," in *IEEE PES winter meeting*, 1976, pp. 76044–76048.

[94] D. Shirmohammadi, H. W. Hong, A. Semlyen, and G. X. Luo, "A compensation-based power flow method for weakly meshed distribution and transmission networks," *IEEE Trans. power Syst.*, vol. 3, no. 2, pp. 753–762, 1988.

[95] C. S. Cheng and D. Shirmohammadi, "A three-phase power flow method for real-time distribution system analysis," *IEEE Trans. Power Syst.*, vol. 10, no. 2, pp. 671–679, 1995.

[96] I. Kocar, J. Mahseredjian, U. Karaagac, G. Soykan, and O. Saad, "Multiphase load-

flow solution for large-scale distribution systems using MANA," *IEEE Trans. Power Deliv.*, vol. 29, no. 2, pp. 908–915, 2013.

[97] L. R. de Araujo, D. R. R. Penido, S. C. Júnior, J. L. R. Pereira, and P. A. N. Garcia, "Comparisons between the three-phase current injection method and the forward/backward sweep method," *Int. J. Electr. Power Energy Syst.*, vol. 32, no. 7, pp. 825–833, 2010.

[98] W. Alabri and D. Jayaweera, "Unbalanced Three-Phase Power Flow Calculation in a Smart Distribution System using Power and Current Injection Hybrid Method," *8th Saudi Arab. Smart Grid Conf. (SASG 2018)*, pp. 1–7, 2018.

[99] H. Saadat, "Power System Analysis,(2nd)," *McGraw-Hill High. Educ.*, 2009.

[100] B. Sereeter, K. Vuik, and C. Witteveen, "Newton Power Flow Methods for Unbalanced Three-Phase Distribution Networks," *Energies*, vol. 10, no. 10, p. 1658, 2017.

[101] H. W. Dommel, W. F. Tinney, and W. L. Powell, "Further developments in Newton's method for power system applications," 1970.

[102] P. A. N. Garcia, J. L. R. Pereira, S. Carneiro, V. M. da Costa, and N. Martins, "Three-phase power flow calculations using the current injection method," *IEEE Trans. Power Syst.*, vol. 15, no. 2, pp. 508–514, 2000.

[103] P. A. N. Garcia, J. L. R. Pereira, and S. Carneiro, "Voltage control devices models for distribution power flow analysis," *IEEE Trans. Power Syst.*, vol. 16, no. 4, pp. 586–594, 2001.

[104] M. J. E. Alam, K. M. Muttaqi, and D. Sutanto, "A three-phase power flow approach for integrated 3-wire MV and 4-wire multigrounded LV networks with rooftop solar PV," *IEEE Trans. Power Syst.*, vol. 28, no. 2, pp. 1728–1737, 2013.

[105] V. M. da Costa, N. Martins, and J. L. R. Pereira, "Developments in the Newton Raphson power flow formulation based on current injections," *IEEE Trans. power Syst.*, vol. 14, no. 4, pp. 1320–1326, 1999.

[106] P. A. N. Garcia, J. L. R. Pereira, S. Carneiro, M. P. Vinagre, and F. V Gomes, "Improvements in the representation of PV buses on three-phase distribution power flow," *IEEE Trans. Power Deliv.*, vol. 19, no. 2, pp. 894–896, 2004.

[107] S. Kamel, M. Abdel-Akher, and F. Jurado, "Improved NR current injection load flow using power mismatch representation of PV bus," *Int. J. Electr. Power Energy Syst.*, vol. 53, pp. 64–68, 2013.

[108] C. R. Fuerte-Esquivel and E. Acha, "Unified power flow controller: a critical comparison of Newton–Raphson UPFC algorithms in power flow studies," *IEE Proceedings-Generation, Transm. Distrib.*, vol. 144, no. 5, pp. 437–444, 1997.

[109] E. Acha, C. R. Fuerte-Esquivel, H. Ambriz-Perez, and C. Angeles-Camacho, *FACTS: modelling and simulation in power networks*. John Wiley & Sons, 2004.

[110] X.-P. Zhang, C. Rehtanz, and B. Pal, *Flexible AC transmission systems: modelling and control*. Springer Science & Business Media, 2012.

[111] T. V Trujillo, C. R. Fuerte-Esquivel, and J. H. T. Hernandez, "Advanced three-phase static VAr compensator models for power flow analysis," *IEE Proceedings-Generation, Transm. Distrib.*, vol. 150, no. 1, pp. 119–127, 2003.

[112] S. Kamel and F. Jurado, "Modeling of STATCOM in load flow formulation," in *Static Compensators (STATCOMs) in Power Systems*, Springer, 2015, pp. 405–435.

[113] F. Rabea, S. Kamel, F. Jurado, and O. Abdel-Rahim, "Implementation of a simplified

SVC model into Newton-Raphson load flow algorithm," in *Innovative Trends in Computer Engineering (ITCE), 2018 International Conference on*, 2018, pp. 374–379.

[114] H. Abdi, S. D. Beigvand, and M. La Scala, "A review of optimal power flow studies applied to smart grids and microgrids," *Renew. Sustain. Energy Rev.*, vol. 71, pp. 742–766, 2017.

[115] M. Ebeed, S. Kamel, and F. Jurado, "Optimal Power Flow Using Recent Optimization Techniques," *Class. Recent Asp. Power Syst. Optim.*, pp. 157–183, Jan. 2018.

[116] B. Khan and P. Singh, "Optimal power flow techniques under characterization of conventional and renewable energy sources: A comprehensive analysis," *J. Eng.*, vol. 2017, 2017.

[117] X. J. Zeng, H. F. Zhai, M. X. Wang, M. Yang, and M. Q. Wang, "A system optimization method for mitigating three-phase imbalance in distribution network," *Int. J. Electr. Power Energy Syst.*, vol. 113, pp. 618–633, 2019.

[118] A. Nakiganda, S. Dehghan, and P. Aristidou, "Comparison of AC Optimal Power Flow Methods in Low-Voltage Distribution Networks," in *2021 IEEE PES Innovative Smart Grid Technologies Europe (ISGT Europe)*, 2021, pp. 1–5.

[119] Y. Del Valle, G. K. Venayagamoorthy, S. Mohagheghi, J.-C. Hernandez, and R. G. Harley, "Particle swarm optimization: basic concepts, variants and applications in power systems," *IEEE Trans. Evol. Comput.*, vol. 12, no. 2, pp. 171–195, 2008.

[120] V. Roberge, M. Tarbouchi, and F. Okou, "Optimal power flow based on parallel metaheuristics for graphics processing units," *Electr. Power Syst. Res.*, vol. 140, pp. 344–353, 2016.

[121] K. K. Mehmood, S. U. Khan, S.-J. Lee, Z. M. Haider, M. K. Rafique, and C.-H. Kim, "A real-time optimal coordination scheme for the voltage regulation of a distribution network including an OLTC, capacitor banks, and multiple distributed energy resources," *Int. J. Electr. Power Energy Syst.*, vol. 94, pp. 1–14, 2018.

[122] A. H. Elsheikh and M. Abd Elaziz, "Review on applications of particle swarm optimization in solar energy systems," *Int. J. Environ. Sci. Technol.*, vol. 16, no. 2, pp. 1159–1170, 2019.

[123] C.-F. Juang, "A hybrid of genetic algorithm and particle swarm optimization for recurrent network design," *IEEE Trans. Syst. Man, Cybern. Part B*, vol. 34, no. 2, pp. 997–1006, 2004.

[124] I. Ziari, G. Ledwich, A. Ghosh, and G. Platt, "Optimal distribution network reinforcement considering load growth, line loss, and reliability," *IEEE Trans. Power Syst.*, vol. 28, no. 2, pp. 587–597, 2012.

[125] S. Naka, T. Genji, T. Yura, and Y. Fukuyama, "A hybrid particle swarm optimization for distribution state estimation," *IEEE Trans. Power Syst.*, vol. 18, no. 1, pp. 60–68, 2003.

[126] R. Ranjan, B. Venkatesh, A. Chaturvedi, and D. Das, "Power flow solution of three-phase unbalanced radial distribution network," *Electr. Power Components Syst.*, vol. 32, no. 4, pp. 421–433, 2004.

[127] J. Arrillaga and C. P. Arnold, "Computer analysis of power systems," *Analysis*, vol. 9, no. 7.8, pp. 7–9, 1990.

[128] M. Bazrafshan and N. Gatsis, "Comprehensive modeling of three-phase distribution systems via the bus admittance matrix," *IEEE Trans. Power Syst.*, vol. 33, no. 2, pp. 2015–2029, 2017.

[129] G. Vulasala and S. Sirigiri, “A Three Phase Power Flow Method for Unbalanced Radial Distribution systems with Inclusion of Voltage Regulator and Transformer Modeling,” *i-Manager’s J. Electr. Eng.*, vol. 3, no. 2, p. 26, 2009.

[130] K. Lindén and I. Segerqvist, “Modelling of load devices and studying load/system characteristics,” *Licent. thesis*, vol. 99, p. 100, 1992.

[131] W. H. Kersting, “Radial distribution test feeders,” *IEEE Trans. Power Syst.*, vol. 6, no. 3, pp. 975–985, 1991.

[132] W. Alabri and D. Jayaweera, “Unbalanced Modelling of STATCOM and SVC in Hybrid Load Flow Method,” in *2019 IEEE PES Innovative Smart Grid Technologies Europe (ISGT-Europe)*, 2019, pp. 1–5.

[133] W. Alabri and D. Jayaweera, “Impact of Semi-fast Charging Stations on Unbalanced Power Distribution Systems Integrated with PV Systems,” in *2021 IEEE PES Innovative Smart Grid Technologies Europe (ISGT-Europe)*, 2021, pp. 1–5.

[134] S. R. Sinsel, R. L. Riemke, and V. H. Hoffmann, “Challenges and solution technologies for the integration of variable renewable energy sources—a review,” *Renew. energy*, vol. 145, pp. 2271–2285, 2020.

[135] G. S. Chawda, A. G. Shaik, O. P. Mahela, S. Padmanaban, and J. B. Holm-Nielsen, “Comprehensive review of distributed FACTS control algorithms for power quality enhancement in utility grid with renewable energy penetration,” *IEEE Access*, vol. 8, pp. 107614–107634, 2020.

[136] M. Ayala-Chauvin, B. S. Kavrakov, J. Buele, and J. Varela-Aldás, “Static Reactive Power Compensator Design, Based on Three-Phase Voltage Converter,” *Energies*, vol. 14, no. 8, p. 2198, 2021.

[137] N. G. Hingorani, L. Gyugyi, and M. El-Hawary, *Understanding FACTS: concepts and technology of flexible AC transmission systems*, vol. 1. IEEE press New York, 2000.

[138] J. M. Ramirez, J. M. Gonzalez-Lopez, J. C. Rosas-Caro, R. Tapia-Olvera, J. M. Lozano, and A. Valderrabano-Gonzalez, “Study of STATCOM in abc Framework,” in *Static Compensators (STATCOMs) in Power Systems*, Springer, 2015, pp. 371–403.

[139] B. Uzum, A. Onen, H. M. Hasanien, and S. M. Muyeen, “Rooftop Solar PV Penetration Impacts on Distribution Network and Further Growth Factors—A Comprehensive Review,” *Electronics*, vol. 10, no. 1, p. 55, 2021.

[140] W. Alabri and D. Jayaweera, “Voltage regulation in unbalanced power distribution systems with residential PV systems,” *Int. J. Electr. Power Energy Syst.*, vol. 131, p. 107036, Oct. 2021.

[141] H. Shareef, M. M. Islam, and A. Mohamed, “A review of the stage-of-the-art charging technologies, placement methodologies, and impacts of electric vehicles,” *Renew. Sustain. Energy Rev.*, vol. 64, pp. 403–420, 2016.

[142] J. Dixon and K. Bell, “Electric vehicles: battery capacity, charger power, access to charging and the impacts on distribution networks,” *ETransportation*, vol. 4, p. 100059, 2020.

[143] B. K. Jha, A. Kumar, D. K. Dheer, D. Singh, and R. K. Misra, “A modified current injection load flow method under different load model of EV for distribution system,” *Int. Trans. Electr. Energy Syst.*, vol. 30, no. 4, p. e12284, 2020.

[144] F. Milano and O. Hersent, “Optimal load management with inclusion of electric vehicles and distributed energy resources,” *IEEE Trans. Smart Grid*, vol. 5, no. 2, pp.

662–672, 2014.

[145] A. Shukla, K. Verma, and R. Kumar, “Voltage-dependent modelling of fast charging electric vehicle load considering battery characteristics,” *IET Electr. Syst. Transp.*, vol. 8, no. 4, pp. 221–230, 2018.

[146] M. A. Azzouz, M. F. Shaaban, and E. F. El-Saadany, “Real-time optimal voltage regulation for distribution networks incorporating high penetration of PEVs,” *IEEE Trans. Power Syst.*, vol. 30, no. 6, pp. 3234–3245, 2015.

[147] HCT GreenNest Eco House, “AC Electric,” 2019. https://dataloggers.livetozero.com/hct/index.html (accessed Jul. 12, 2019).

[148] T. Olowu, A. Sundararajan, M. Moghaddami, and A. Sarwat, “Future challenges and mitigation methods for high photovoltaic penetration: A survey,” *Energies*, vol. 11, no. 7, p. 1782, 2018.

[149] A. Hoke, R. Butler, J. Hambrick, and B. Kroposki, “Steady-state analysis of maximum photovoltaic penetration levels on typical distribution feeders,” *IEEE Trans. Sustain. Energy*, vol. 4, no. 2, pp. 350–357, 2012.

[150] H. Fallahzadeh-Abarghouei, S. Hasanvand, A. Nikoobakht, and M. Doostizadeh, “Decentralized and hierarchical voltage management of renewable energy resources in distribution smart grid,” *Int. J. Electr. Power Energy Syst.*, vol. 100, pp. 117–128, 2018.

[151] Y. Ch, S. K. Goswami, and D. Chatterjee, “Effect of network reconfiguration on power quality of distribution system,” *Int. J. Electr. Power Energy Syst.*, vol. 83, pp. 87–95, 2016.

[152] X. Su, M. A. S. Masoum, and P. Wolfs, “Comprehensive optimal photovoltaic inverter control strategy in unbalanced three-phase four-wire low voltage distribution networks,” *IET Gener. Transm. Distrib.*, vol. 8, no. 11, pp. 1848–1859, 2014.

[153] I. S. Board, *IEEE Standard for Interconnecting Distributed Resources with Electric Power Systems: 1547-2003*. IEEE, 2003.

[154] M. N. I. Sarkar, L. G. Meegahapola, and M. Datta, “Reactive power management in renewable rich power grids: A review of grid-codes, renewable generators, support devices, control strategies and optimization algorithms,” *IEEE Access*, vol. 6, pp. 41458–41489, 2018.

[155] A. Ali, D. Raisz, and K. Mahmoud, “Optimal oversizing of utility-owned renewable DG inverter for voltage rise prevention in MV distribution systems,” *Int. J. Electr. Power Energy Syst.*, vol. 105, pp. 500–513, 2019.

[156] S. A. Solar Technology, “Description of the Operating Parameters - SUNNY TRIPOWER 60 / SUNNY HIGHPOWER PEAK1.” [Online]. Available: http://www.windandsun.co.uk/media/995570/SMA-Sunny-Highpower-PEAK1-Description-of-the-Operating-Parameters.pdf

[157] Z. Cheng, Z. Li, J. Liang, J. Si, L. Dong, and J. Gao, “Distributed coordination control strategy for multiple residential solar PV systems in distribution networks,” *Int. J. Electr. Power Energy Syst.*, vol. 117, p. 105660, 2020.

[158] M. Kolhe and M. Rasul, “3-Phase grid-connected building integrated photovoltaic system with reactive power control capability,” *Renew. Energy*, vol. 154, pp. 1065–1075, 2020.

[159] J. P. Bonaldo, F. L. Tofoli, R. V. A. Monteiro, and H. K. Morales-Paredes, “Comparative analysis of techniques for the limitation of compensation currents in multifunctional grid-tied inverters,” *Int. J. Electr. Power Energy Syst.*, vol. 126, p.

106574.

[160] L. Hassaine, E. OLias, J. Quintero, and V. Salas, “Overview of power inverter topologies and control structures for grid connected photovoltaic systems,” *Renew. Sustain. Energy Rev.*, vol. 30, pp. 796–807, 2014.

[161] L. Hassaine and M. R. Bengourina, “Design and digital implementation of power control strategy for grid connected photovoltaic inverter,” *Int. J. Power Electron. Drive Syst.*, vol. 10, no. 3, p. 1564, 2019.

[162] T.-F. Wu, C.-H. Chang, L.-C. Lin, G.-R. Yu, and Y.-R. Chang, “A D-$\Sigma $ Digital Control for Three-Phase Inverter to Achieve Active and Reactive Power Injection,” *IEEE Trans. Ind. Electron.*, vol. 61, no. 8, pp. 3879–3890, 2013.

[163] W. Alabri and D. Jayaweera, “Optimal coordination of unbalanced power distribution systems with integrated photovoltaic systems and semi-fast electric vehicles charging stations,” *IET Gener. Transm. Distrib.*, pp. 1–17, 2022.

[164] X. Yuan *et al.*, “Multi-objective optimal power flow based on improved strength Pareto evolutionary algorithm,” *Energy*, vol. 122, pp. 70–82, 2017.

[165] P. P. Biswas, P. N. Suganthan, R. Mallipeddi, and G. A. J. Amaratunga, “Optimal power flow solutions using differential evolution algorithm integrated with effective constraint handling techniques,” *Eng. Appl. Artif. Intell.*, vol. 68, pp. 81–100, 2018.

[166] C. A. C. Coello, G. B. Lamont, and D. A. Van Veldhuizen, *Evolutionary algorithms for solving multi-objective problems*, vol. 5. Springer, 2007.

[167] Y. Z. Y. Ghazali, “Managing on-load tap changer life cycle in tenaga nasional berhad (TNB) distribution power transformers,” *CIRED-Open Access Proc. J.*, vol. 2017, no. 1, pp. 303–307, 2017.

[168] A. Heidari-Akhijahani, A. Safdarian, and M. Lehtonen, “Unbalance mitigation by optimal placement of static transfer switches in low voltage distribution feeders,” *IET Gener. Transm. Distrib.*, vol. 14, no. 20, pp. 4612–4621, 2020.

Appendices

Appendix A: Admittance Matrix for the Transformers

This appendix provides elements of the transformer admittance matrix for various transformer arrangements [127].

Table A. 1. Transformer admittance matrix elements for different transformers [127]

Transformer connection	**Self-admittance matrices**		**Mutual admittance matrices**	
	Y_{pp}	Y_{ss}	Y_{ps}	Y_{sp}
YNyn0	Y_I	Y_I	$-Y_I$	$-Y_I$
Yy0	Y_{II}	Y_{II}	$-Y_{II}$	$-Y_{II}$
YNd1	Y_I	Y_{II}	Y_{III}	Y_{III}^T
Yd1	Y_{II}	Y_{II}	Y_{III}	Y_{III}^T
Dyn1	Y_{II}	Y_I	Y_{III}	Y_{III}^T
Dyn11	Y_{II}	Y_I	Y_{III}^T	Y_{III}
Dd0	Y_{II}	Y_{II}	$-Y_{II}$	$-Y_{II}$

where submatrices given in the Table A.1, are as follows:

$$Y_I = \begin{bmatrix} y_t & 0 & 0 \\ 0 & y_t & 0 \\ 0 & 0 & y_t \end{bmatrix} \tag{A.1}$$

$$Y_{II} = \left(\frac{1}{3}\right) . \begin{bmatrix} 2y_t & -y_t & -y_t \\ -y_t & 2y_t & -y_t \\ -y_t & -y_t & 2y_t \end{bmatrix} \tag{A.2}$$

$$Y_{II} = \left(\frac{1}{\sqrt{3}}\right) . \begin{bmatrix} -y_t & y_t & 0 \\ 0 & -y_t & y_t \\ y_t & 0 & -y_t \end{bmatrix} \tag{A.3}$$

where y_t is the transformer leakage admittance. If the transformer has an off-nominal tap ratio α:β, where α and β are located on the primary and secondary sides respectively, then the elements of the transformer admittance matrix need to be updated as follows:

- Divide Y_{pp} by α^2 and Y_{ss} by β^2
- Divide Y_{ps} and Y_{sp} by $\alpha\beta$

Appendix B: The 5-bus Test Network Data

This appendix provides the information of the 5-bus test network, which was utilised to validate the proposed STATCOM and SVC model developed in chapter 4 [109]. All the data are in pu on a 100 MVA base.

Table B. 1. Generation data of the 5-bus test network

	Voltage Magnitude (pu)			**Active power (pu)**		
Bus No.	Phase A	Phase B	Phase C	Phase A	Phase B	Phase C
1 -Slack	1.06	1.06	1.06	-	-	-
2	1	1	1	0.4	0.4	0.4

Table B. 2. Load data of the 5-bus test network

	Active power (pu)			**Reactive power (pu)**		
Bus No.	Phase A	Phase B	Phase C	Phase A	Phase B	Phase C
2	0.2	0.1739	0.23	0.1	0.08695	0.115
3	0.5175	0.45	0.3913	0.1725	0.15	0.1304
4	0.3478	0.46	0.4	0.0435	0.0575	0.05
5	0.6	0.5217	0.69	0.1	0.087	0.115

Table B. 3. Line data of the 5-bus test network

From	**To**	**(R+jX) in pu**			**B in pu**		
1	**2**	0.0333+j0.1000	0.0133+j0.0400	0.0133+j0.0400	0.1000	0.0400	0.0400
		0.0133+j0.0400	0.0333+j0.1000	0.0133+j0.0400	0.0400	0.1000	0.0400
		0.0133+j0.0400	0.0133+j0.0400	0.0333+j0.1000	0.0400	0.0400	0.1000
1	**3**	0.1333+j0.4000	0.0533+j0.1600	0.0533+j0.1600	0.0833	0.0333	0.0333
		0.0533+j0.1600	0.1333+j0.4000	0.0533+j0.1600	0.0333	0.0833	0.0333
		0.0533+j0.1600	0.0533+j0.1600	0.1333+j0.4000	0.0333	0.0333	0.0833
2	**3**	0.1000+j0.3000	0.0400+j0.1200	0.0400+j0.1200	0.0667	0.0267	0.0267
		0.0400+j0.1200	0.1000+j0.3000	0.0400+j0.1200	0.0267	0.0667	0.0267
	4	0.0400+j0.1200	0.0400+j0.1200	0.1000+j0.3000	0.0267	0.0267	0.0667
2	**5**	0.0667+j0.2000	0.0267+j0.0800	0.0267+j0.0800	0.0500	0.0200	0.0200
		0.0267+j0.0800	0.0667+j0.2000	0.0267+j0.0800	0.0200	0.0500	0.0200
		0.0267+j0.0800	0.0267+j0.0800	0.0667+j0.2000	0.0200	0.0200	0.0500
3	**4**	0.0167+j0.0500	0.0067+j0.0200	0.0067+j0.0200	0.0333	0.0133	0.0133
		0.0067+j0.0200	0.0167+j0.0500	0.0067+j0.0200	0.0133	0.0333	0.0133
		0.0067+j0.0200	0.0067+j0.0200	0.0167+j0.0500	0.0133	0.0133	0.0333
4	**5**	0.1333+j0.4000	0.0533+j0.1600	0.0533+j0.1600	0.0833	0.0333	0.0333
		0.0533+j0.1600	0.1333+j0.4000	0.0533+j0.1600	0.0333	0.0833	0.0333
		0.0533+j0.1600	0.0533+j0.1600	0.1333+j0.4000	0.0333	0.0333	0.0833